Tomas Bata University in Zlín
Faculty of Technology

Doctoral Thesis

The study of functional ingredients from corn silk

Author: **MAgr. Li Peng**

Degree programme: P2901 Chemistry and Food Technology

Degree course: 2901V013 Food Technology

Supervisor: Prof. Ing. Lubomír Lapčík, Ph.D.

Zl ń, November, 2020

Key words: *corn silk, thermal properties, radical scavenging, maturity stage, flavonoids, steroids, polysaccharides, kinetic models*

ABSTRACT

The thesis studies the physicochemical and biochemical properties of the bioactive functional substances from the extracts of corn silk including flavonoids, polysaccharides and steroids, which are widely applied in the areas of food production, pharmacy, veterinary, animal feed and healthcare.

There are three main parts of the research containing 1, corn silk flavonoids, polysaccharides and steroids extraction, determination (related to the technologies of UV-VIS, HPLC, NMR, FTIR and Fluorescence excitation−emission mapping) and extraction methods optimization. 2, corn silk physicochemical property analysis including thermal analysis (related to the technology of TG/DTA), microstructure research (related to the technology of SEM). 3, corn silk flavonoids, polysaccharides and steroids biochemical property analysis including anti-radical (related to the free-radicals of DPPH, ABTS and technology of EPR), anti-oxident capability (to the ferricion and copper ion), vitro enzyme inhibition activity including the enzymes of α-glucosidase and α-amylase (anti-diabetes), thrombin (anti-coagulation), angiotensin converting enzyme(ACE) (anti-hypertension) and xanthine oxidase(XOD) (anti-gout).

The whole research is based on the three different maturity stages of corn slik for the different content and proportion of flavonoids, polysaccharides and steroids in each maturity stage, which are silking stage (CS - S), milky stage (CS - M) and mature stage (CS - MS).

CONTENTS

ACKNOWLEDGEMENTS

INTRODUCTION

Corn has a widespread application as a domastic animals feed, food additives and material of alcohol through fermentated or unfermentated technology (Ivanišová et al., 2017; Michalová & Tancinová, 2017). Corn silk (CS) is the dried thrum and stigma of Zea mays L. (corn) , cheap, high yielding and usually considered as a by-product to be abandoned, burned or used as fodder (Zhang, 1998). It is one of the Chinese traditional medicine recorded in many classics. According to the Southern Yunnan Material Medicine and Chinese Medicine Dictionary, corn silk is non-poisonous, also diuretic, cholagogic and resolutive. Corn silk could be used to cure many kinds of diseases clinically, such as diabetes, nephritis and hypertension etc (Jin, 1980). In addition, in terms of the results from the worldwide scientists, corn silk also has the effects of anti-fatigue (Hu et al., 2010), anti-depression (Mahmoudi & Ehteshami, 2010), anti-free radical, anti-cancer (Ebrahimzadeh, Pourmorad, & Hafezi, 2008; Z. A. Maksimović & Kovačević, 2003) and anti-radiation (Bai et al., 2010). Native American Indians usually use corn silk to cure urinary tract infection, malaria and heart disease (Hasanudin et al., 2012). In many countries, corn silk is applied to sell in markets as tea and weight-losing products for its good effect of cooling blood, purging heat and removing the damp and heat in human body.

The previous researches have successfully applied the fermentated corn fodder to improve the nutrition quality of chicken meat (Angelovicová & Semivanová, 2013; Macanga et al., 2017; Štenclová et al., 2016). In addition, corn was also used to improve the sensory quality of crackers (Kuchtová, Minarovicová, Kohajdová, & Karovicová, 2016). The corn fermentated alcohol has a broad usage in food and chemistry industry, veterinary, pharmaceutical and manufacturing industry for its nutritional value and anti-oxidant properties (Krejzová et al., 2017; Süli, Hamarová, & Sobeková, 2017).

Corn silk contains many sorts of nutritional and functional ingredients, including sterols, polysaccharides, alkaloids, flavones, cryptoxanthins, polyphenols, organic acids, vitamins and allantoins etc. (Li & Lapcik, 2018) In this thesis, it will mainly research about corn silk flavonoids, polysaccharides and steroids based on the three different maturity stages which are silking stage (CSS), milky stage (CSM) and mature stage (CSMS).

1. CURRENT STATUS OF THE ISSUES

1.1 The Technology Of Corn Silk Bioactive Ingredients Extraction (CSBIE)

1.1.1 CS Polysaccharides (CSP) Extraction

The traditional technology of CSP extraction includes hot water, enzyme, ultrasonic-assisted and microwave-assisted extraction (C., M., & K., 2016; Yin, You, & Jiang, 2011; L. Zhang & Wang, 2017; Zhu & Liu, 2013). However, Chen et al. combined enzymolysis and ultrasonic assisted technology, made the extractive condition milder, the costs and energy-consumption lower and the operational process simpler. The optimal enzymolysis-ultrasonic assisted extractive condition is cellulose content was 7.5% for 150min at 55°C and liquid-solid ratio is 31.8 for 34.2min at 66.3°C, respectively. In these conditions, the yield of CSP increased from 4.56% to 7.10 (compared with hot water extraction) and the CSP conformation changed into a more anti-oxidative and anti-cancer activity (Chen et al., 2014). While, both Maran et al. and Chen et al. applied Box-Behnken design (BBD) response surface methodology to statistic, analyze and optimize extractive conditions. BBD is an independent, rotatable quadratic design without embedded factorial or fractional factorial points where the variable combinations are at the midpoints of the edges of the variable space and at the center (Prakash Maran, Sivakumar, Sridhar, & Prince Immanuel, 2013), thus, BBD is more effective and simpler to arrange and interpret experiments then optimize the extractive conditions (Zhao et al., 2011). The quadratic equation is as follows:

$$Y = \beta_0 + \sum_{j=1}^{k} \beta_j X_j + \sum_{j=1}^{k} \beta_{jj} X_j^2 + \sum_{i}^{k} \sum_{<j=2}^{k} \beta_{ij} X_i X_j + e_i$$

Where Y is the response; X_i and X_j are variables (i and j range from 1 to k); β_0 is the model intercept coefficient; β_j, β_{jj} and β_{ij} are interaction coefficients of linear, quadrantic and the second-order terms, respectively; k is the number of independent parameters and e_i is the error (Prakash Maran, Manikandan, Thirugnanasambandham, Vigna Nivetha, & Dinesh, 2013).

1.1.2 CS Flavonoids (CSF) Extraction

The total flavonoids extractive technology includes hot water, alkaline water or alkaline dilute alcohol, organic solvent extraction. Additionally, microwave, ultrasonic extraction, supercritical fluid extraction, enzyme, aqueous two-phase, semi bionic extraction, membrane separation, thermal fluid extraction and high pressure liquid extraction (Jing et al., 2016; Ko, Kwon, & Chung, 2016; Shan, Xie, Zhu, & Peng, 2012; Wang et al., 2016; Wei, Yang, Chiu, & Hong, 2013; Weiz, Braun, Lopez, de Mar á, & Breccia, 2016; Xie et al., 2017; R. Yang, Geng, Lu, & Fan, 2017; Y. Zhang, Shan, & Gao, 2011; Zhou, Xiao, Li, & Cai, 2011). Peng et al. applied 80°C hot water extraction, the parity of CSF was 10.45% (Peng, Zhang, & Zhou, 2016); Liu et al. applied 50°C 95% ethanol to extract CSF, the

highest total CSF content is 69.4±5.1 µg RE/ g DCS (RE= rutin equivalents; DCS= dry mass of corn silk) (J. Liu, Wang et al., 2011); Liu et al. used supercritical fluid to extract CSF and used BBD response surface methodology to analyze and optimize the extractive conditions. The maximal yield of CSF was approximately 4.24mg/g, the optimal conditions were 50.88℃, 41.80MPa, 2.488ml/g water content in ethanol co-solvent, 120 min extractive time, 0.4mm particle sizes and 20% aqueous ethanol as the co-solvent (J. Liu et al., 2011).

1.1.3 CS Phenolic (CSP) Extraction

Plant polyphenol extraction technology includes solvent extraction, ultrasonic and microwave assisted extraction, supercritical fluid extraction, ion precipitation extraction, adsorption separation (Bakirtzi, Triantafyllidou, & Makris, 2016; Bhattacharya, Srivastav, & Mishra, 2014; Firdaous et al., 2017; Périno, Pierson, Ruiz, Cravotto, & Chemat, 2016; Prasad, 2016; Złotek, Mikulska, Nagajek, & Świeca, 2016). Liu et al. applied 50℃ ethanol to extract CSP the highest total phenolic content was 164.1±9.7 µg GAE/ g DCS (GAE=gallic acid equivalents; DCS=dry mass of CS) (J. Liu et al., 2011).

1.2 The Relation Between CSBIE Content And CS Type, Maturity

CSBIE content is also related to the type and maturity of CS. Sarepona et al. tested the total phenolic (TPC), total flavonoids (TFC) and total anthocyanin (TAC) of 5 purple waxy corns, 3 white waxy corns and 2 super sweet corns in silking stage, milky stage and maturity stage showed TPC and TAC were highest at the milking stage, TFC were highest at the silking stage, TPC and TFC were highest in super sweet corn and white corn at the silking stage (Sarepoua, Tangwongchai, Suriharn, & Lertrat, 2015). In the study of Rahman, immature silks contain higher content of polyphenol and flavonoid (Rahman & Wan Rosli, 2014a).

1.3 The Anti-Oxidative Activity Of CS Extracts

Many kinds of CS bioacitive composition, particularly, phenolics, polysaccharides, flavonoids, tannins and anthocyanins are all anti-oxidative, which can scavenge oxygen free-radical and inhibit peroxidation (Z. Maksimović, Malenčić, & Kovačević, 2005a; Mohsen & Ammar, 2009). Liu et al. found two kinds of CSF glycoside isoorientin-2''-o- α-L-rhamnoside and 3'-methoxymaysin particularly isoorientin-2''-o- α-L-rhamnoside showed significant total anti-oxidant activity, DPPH radical scavenging activity, reducing power and iron-chelating capacity compared with other corn silk flavone glycoside (J. Liu et al., 2011). Zilie et al. compared the antioxidant activity between 4 corn silks (yellow, green, pink, and purple colored silks) and 6 medicinal herbs (Mentha Diperita,

Melissa officinalis, Ginkgo biloba, Thymus serpyllum, Salvia officinalis and green tea), the result showed corn silk contained more phenolic and flavonoid compounds and had stronger antioxidant activity (Žilić, Janković, Basić, Vančetović, & Maksimović, 2016). Maksimovic et al. evaluated 15 corn silks aqueous acetone extracts antioxidant activity illustrated that polyphenol content is the dominated standard to estimate the anti-oxidant capacity (Z. Maksimović, Malenčić, & Kovačević, 2005b). Rahman et al. found the water, ethanol and ethyl acetate extracts from immature CS had a stronger anti-oxidant capacity than the mature CS (Rahman & Wan Rosli, 2014a). Chen et al. studied, Enzymalysis-ultrasonic assisted CSP extracts had higher anti-oxidant and anti-cancer activities than extracted by hot water (Chen et al., 2014). Vranjes et al. studied the effects of bearberry, parsley and CS extracts on antioxidant capacity in mice kidneys showed parsley and corn silk extracts could be a new therapeutic approach for oxidation- induced kidney diseases (Vranješ et al., 2016). Chen et al. studied 3 chemical modified CSP (sulfated, acetylated and carboxymethylated derivatives) revealed the carboxylmethylated polysaccharide had higher solubility, narrower molecular weight distribution, lower intrinsic viscosity, a hyper branched conformation, significantly higher anti-oxidant abilities than the natural polysaccharides and other derivatives could be a novel nutraceutical agent for human consumption (Chen et al., 2013).

1.4 CS Extracts Anti - Diabetic Effects

CS has been long used as an anti - diabetic traditional herb in China and America (Hasanudin, Hashim, & Mustafa, 2012). The aqueous extracts of CS include polysaccharides, flavonoids and phenols are all able to reduce the glucose level (Sabiu, O'Neill, & Ashafa, 2016). Besides, Chen et al. also found chemical modified CSP (carboxylmethylated polysaccarides) had better α-amylase inhibitory abilities (Chen et al., 2013). While Zho compared the anti-diabrbetic effects of CSP between normal and hyperglycemia rats demonstrated CSP had no hypoglycemia activity to normal rats but remarkable a hypoglycemic effect to hyperglycemia rats (Zhao, Yin, Yu, Liu, & Chen, 2012).

1.5 The Anti - Cancer Capacity Of CS

CS is very suitable to cure and prevent the oxidant-induced and inflammation-induced cancer since the extracts of CS has prominent anti-oxidant, free-radical and anti-inflammation capacity (Hasanudin et al., 2012; Rafsanjany et al., 2015). Yang et al. studied anti-hepatoma activity of CSP in H22 tumor-bearing mice, demonstrated CPS could inhibit hepatocarcinoma tumor growth, extend the survival time of H22 tumor-bearing mice, increase the body weight and peripheral white blood cells (WBC) count, also enhanced the serum cytokines production such as IL-2, IL-6 and TNF-α without toxicological effects. So CS could be used as an auxiliary anti-cancer drug to reduce or limit the grievously

effected chemotherapy (J. Yang, Li, Xue, Wang, & Liu, 2014). Choi et al. also researched the neuroprotective effects of CSF glycoside on oxidative stress (H_2O_2)-induced apoptotic cell death of human neuroblastoma SK-N-MC cells showed CS pretreatment reduced the cytotoxic effect of H_2O_2 on SK-N-MC cells, the lactate dehydrogenase release, the intracellular reactive oxygen species level and inhibited the cleavage of poly ADP-ribose polymerase. Also, the DNA damage and H_2O_2-induced apoptotic cell death were significantly attenuated. Besides, CS pretreatment (5-50 μg/ml) for 2h significantly and dose-dependently increased the mRNA levels of antioxidant enzymes (CAT, GPx-1, SOD-1, SOD-2 and HO-1) in H_2O_2 (200μM)-insulted cells (Choi, Kim, Choi, & Park, 2014). Lee studied CS flavonoid anti-cancer activity on androgen-independent human prostate cancer cell (PC-3) demonstrated CS dose-dependently reduced the PC-3 cell viability with an 87% reduction at 200 μg/ml. Also, CS treatment significantly induced apoptotic cell death, DNA fragmentation, depolarization of mitochondrial membrane potential and reduction in Bcl-2 and pro-caspase-3 expression levels. Additionally, CS could also enhance the PC-3 cell death by application with 5-FU etoposide, cisplatin or camptothecin (Lee et al., 2014). Liu et al. found CS flavonoids had nitrite-scavenging ability, it could be also used to prevent nitrite-induced cancer and chronic diseases (J. Liu et al., 2011).

OBJECTIVES OF THE THESIS

Through the research of corn silk flavonoids, polysaccharides and steroids extraction, determination (related to the technologies of UV-VIS, HPLC, NMR, FTIR and Fluorescence excitation−emission mapping) and extraction methods optimization, the basic chemical structure, content of corn silk bioactive substances can be confirmed and the optimal method of bioactive substances extraction can be built. According to the research of corn silk physicochemical property analysis including thermal analysis (related to the technology of TG/DTA), microstructure research (related to the technology of SEM), the microstructure and thermal property of corn silk powder/fiber can be known. In accordance with the research of corn silk flavonoids, polysaccharides and steroids biochemical property analysis including anti-radical (related to the free-radicals of DPPH, ABTS and technology of EPR), anti-oxident capability (related to the ferricion and copper ion), Vitro enzyme inhibition activity including the enzymes of α-glucosidase and α-amylase (anti-diabetes), thrombin (anti-coagulation), angiotensin converting enzyme (ACE) (anti - hypertension) and xanthine oxidase (XOD) (anti-gout), the pharmaceutical and healthcare function of corn silk extracts can be learnt for the further research of curing diseases such as diabetes, aging, hypertension, heart disease and gout. Also based on the research of different maturity stages of corn silk, the best picking time of corn silk for pharmaceutical and nutritional use can be certain.

MATERIALS AND METHODS

15

1. CS SAMPLE PROCESSING

Corn silk samples were collected from the corn kernels type dent produced in a field in Southern Moravia agricultural region (Uherské Hradiště County, Czech Republic). Fresh corn silk fibers were first 14 days dryied on air in the shade and then final drying was done in a thermostatic hot air drying oven (Hot air sterillizator Stericell 55 Standard, BMT Medical Technology, Czech Republic), pulverized in a table top blender (Philips HR2170/40, The Netherlands) and sifted through an 80mesh sieve (Analysette 3, Fritsch, Germany) to obtain the final product powder samples. There were collected three types of corn silk materials, dependent on the growth stage. The first one was silking stage (assigned as CS-S), the second one was the milky stage (assigned as CS-M), the third one was mature stage (assigned as CS-MS) (Rahman & Wan Rosli, 2014b; Sarepoua et al., 2015).

2. CS SAMPLE PHYSICOCHEMICAL PROPERTY ANALYSIS

2.1 SEM analysis of the CS powder samples

Scanning electron microscope (SEM) is an observation method between transmission electron microscope and optical microscope. It uses a focused narrow high-energy electron beam to scan the sample, through the interaction between the beam and the substance, to stimulate a variety of physical information, to collect, magnify and image the information to achieve the purpose of characterizing the micro-morphology of the substance. The resolution of the new scanning electron microscope can reach upto 1 nm; the magnification can be continuously adjusted to 300,000 times or more; and the depth of field is large, the field of view is large and the imaging stereoscopic effect is good. In addition, the combination of scanning electron microscope and other analytical instruments can observe the micro-topography and analyze the composition of the material micro-area. Scanning electron microscopy is widely used in the research of geotechnical materials, graphite, ceramics and nano materials. Therefore, scanning electron microscopy plays an important role in the field of scientific research.

In this study, the microscopic shape and size of the CS powder and fiber samples were measured by the scanning electron microscopy (SEM), the images were captured by a Hitachi 6600 FEG microscope (Japan) operating in the secondary electron mode with an accelerating voltage of 1 keV. (Will, 2020)

2.2 TG/DTA analysis of the CS powder samples

Thermogravimetric analysis (TG) is a method of measuring the relationship between the mass of a substance and temperature or time under program - controlled temperature. By analyzing the thermogravimetric curve, we can know the composition, thermal stability, thermal decomposition of the sample and the intermediate products that it may produce and the products that are related to the quality.

Differential thermal analysis (DTA) is a stable substance (reference substance) that does not undergo any chemical reaction and physical change at a certain experimental temperature and the same amount of unknown substance is compared with the same environment at a moderate rate of temperature change. Compared with the temperature of the standard in the same environment, the change in temperature should increase or decrease temporarily. The decrease is represented by endothermic reaction, and the increase is represented by exothermic reaction. (Mukasyan, 2017)

In this study, thermogravimetry (TG) and differential thermal analysis (DTA) experiments were performed on simultaneous DTA−TG apparatus (Shimadzu DTG 60, Japan). Measurements were performed at heat flow rate of 5 ℃/min in the static nitrogen atmosphere (gas flow of 50 ml/min) at the temperature range

from 30 ℃ to 550 ℃. The apparat was calibrated using Indium as a standard (Q. Liu, Lv, Yang, He, & Ling, 2005; Wu, Pan, Deng, & Pan, 2008).

3. CS FUNCTIONAL INGREDIENTS EXTRACTION, CONTENT DETERMINATION AND EXTRACTION METHODS OPTIMIZATION

3.1 UV-VIS

Ultraviolet-visible spectrophotometry is a method for measuring the absorbance of substances in the wavelength range of 190 to 760 nm for identification, impurity inspection and quantitative determination. When light passes through the solution of the tested substance, the degree of absorption varies along with the wavelength of the light. Therefore, by measuring the absorbance of the substance at different wavelengths, and plotting the relationship between the absorbance and the wavelength to obtain the absorption spectrum of the measured substance. From the absorption spectrum, the maximum absorption wavelength λmax and the minimum absorption wavelength λmin can be determined. The absorption spectrum of a substance has characteristics related to its structure. Therefore, the substance can be identified by comparing the spectrum of the sample with the reference spectrum or the reference spectrum in a specific wavelength range, or by determining the maximum absorption wavelength, or by measuring the absorption ratio at two specific wavelengths. When it is used for quantification, the absorbance of a sample solution of a certain concentration is measured at the maximum absorption wavelength, and compared with the absorbance of a control solution of a certain concentration, the concentration of the sample solution is calculated by the absorption coefficient method (Kafle, 2020).

In this study, UV/VIS spectrophotometer used was Lambda 25 (Perkin Elmer, MA, USA). Measurements were performed in the wavelength range from 200 to 700 nm in 1 cm quartz cells (Marques et al., 2013).

3.2 Fluorescence Excitation−Emission Mapping

Objects store light with shorter wavelengths of light and then slowly emit light of longer wavelengths. This light is called fluorescence. If the energy-wavelength diagram of fluorescence is made, then this diagram is the fluorescence spectrum. Fluorescence spectra can only be obtained by spectral detection.

The high-intensity laser can elevate a considerable number of molecules in the absorbing matter to excited quantum states in the fluorescence spectroscopy. Therefore, the sensitivity of the fluorescence spectrum is greatly improved. The fluorescence spectrum using a laser as a light source is suitable for the detection of ultra-low concentration samples. For example, the single pulse detection limit of fluorescein sodium with a tunable dye laser pumped by a nitrogen molecular laser has reached 10^{-10} molar / liter, which is better than that of a common light source. The highest sensitivity obtained is improved by an order of magnitude.

Fluorescence spectrum includes two kinds, excitation spectrum and emission spectrum. The excitation spectrum is the change of the fluorescence intensity at a

wavelength measured by the fluorescent substance under the excitation light of different wavelengths, that is, the relative efficiency of the excitation light at different wavelengths; the emission spectrum is the action of excitation light at a fixed wavelength. The distribution of the lower fluorescence intensity at different wavelengths, which is the relative intensity of light components of different wavelengths in fluorescence.

In this study, fluorescence excitation−emission maps of the different maturity stages corn silk extracts were measured on a FLS980 fluorescence spectrometer (Edinburgh Instruments, UK). Each experiment was repeated 10 times (Dankowska, 2016).

3.3 CS flavonoids extraction and content determination

3.3.1 Materials

All reagents and chemicals used in this research such as rutin, ethanol, sodium nitrite, aluminium nitrate and sodium hydroxide were purchased from Sigma - Aldrich (USA) in an analytical reagents purity grade. As a solvent distilled water was used. Distilled water conductivity was about 0.6 μS/cm).

3.3.2 Rutin standard curve

Disolve 20 mg lutin into 70v.% ethanol to 50 ml (0.4 mg/ml lutin solution); separately were brought 0, 1, 2, 4, 6, 8, 10 ml 0.4 mg/ml lutin standard solutions into 50 ml volumetric flasks, added 70% ethanol 12 ml, then added 2 ml 5w.% $NaNO_2$, shaked up and placed for 10 min to react. Then into the solutions were added 2 ml 10w.% $Al(NO3)_3$, shaked up and placed for 10min to react, then diluted with 20 ml 10w.% NaOH to the scale of volumetric flask, placed for 5min. Each experiment was repeated 5 times. There was used 510 nm UV spectrometry to measure the absorbance of the solutions. Obtained absorbance vs. concentration dependency data were used to build up the standard curve. The numerical linear regression analysis was performed to obtain standard curve lineasr regression parameters. Each experiment was repeated 3 times (Peng et al., 2016).

3.3.3 Determination of the CS flavonoids content

Use the 1/10 solid-liquid ratio of cornsilk powder and 70v.% ethanol to extract the flavonoids in temperatures of 40 °C and 80 °C for 20, 30, 40, 50, 60 minutes extraction time intervals. Then the flavonoids extract solutions were centrifuged on Hettich EBA 21 centrifuge (Germany) at 3000 rpm for 10 min to get the supernatant. Then there was used the same methodology as lutin standard curve to measure the flavonoids absorbance and there was used the lutin standard curve to count the given content of flavonoids. Each experiment was repeated 5 times (Peng et al., 2016).

3.4 CS polysaccharides extraction and content determination

3.4.1 Materials

All reagents and chemicals used in this research such as glucose, diethyl ether phenol, sulfuric acid (H_2SO_4), ethanol, anhydrous ethanol, acetone were purchased from Sigma - Aldrich (USA) in an analytical reagents purity grade. As a solvent distilled water was used. Distilled water conductivity was about 0.6 μS/cm).

3.4.2 Glucose standard curve

Precisely weigh 100.5mg glucose which was dried to constant weight. Dilute the glucose with distilled water to 100ml to get the standard glucose solution. Take standard solution 0, 2, 4, 6, 8, 10, 12ml and dilute them with distilled water to 100ml. Suck up the above solutions 0.3ml into 10ml test tubes, then add 6% phenol solution 0.6ml, then instantly add 3ml concentrated sulfuric acid, shake up. Then place them into 40°C water bath for 30min，then put them into refrigerator and cool down for 10min. Then use UV spectrometry to measure their absorbance in 490nm. Use absorbance （A） as Y axil, mass concentration (C) (μg/ml) as X axil to get the regression equation (Hossain et al., 2014).

3.4.3 Determination of the CS polysaccharides content

Use diethyl ether to degrease the CS powder sample in room temperature for 12 hours, then use 36°C constant temperature drying box to dry to the degreased corn silk powder, then weigh 50g degreased power into round-bottom flask and add 750ml distilled water, then put the round-bottom flask into 100°C water bath for 2 hours. Then centrifuge the sample in the speed of 10000 r/min for 10min to get the supernatant and sediment, then use the sediment to repeat the above hot water extraction and centrifugation process and merge twice centrifugal supernatant, then vacuum concentrate，then add 70% ethanol into concentrated solution to precipitate，then use anhydrous ethanol, acetone and ether to ordinally wash the sediment, then dry the sediment with 50°C hot air, then get the corn silk polysaccharides. Use the same method as the standard glucose curve to measure the UV absorbance, then use the standard glucose curve to calculate the content of polysaccharides. Each experiment was repeated 5 times (Hossain et al., 2014).

3.5 CS steroids extraction and content determination

3.5.1 Materials

All reagents and chemicals used in this research such as β- sitosterol, ethanol, phosphoric acid, sulfuric acid and ferric chloride were purchased from Sigma-Aldrich (USA) in an analytical reagents purity grade. As a solvent distilled water was used. Distilled water conductivity was about 0.6 μS/cm).

3.5.2 β - sitosterol standard curve

Precisely weigh 10 mg β – sitosterol into 10 ml volumetric flask, use absolute ethyl alcohol dilute to scale. Fetch 1ml above solution into 10ml volumetric flask, use absolute ethyl alcohol to dilute to scale as the standard sample solution. Precisely move the standard sample solution 0, 1, 2, 3, 4, 5 ml into 50 ml conical flask, separately add 5, 4, 3, 2, 1, 0 ml absolute ethyl alcohol, then slowly pour the pulfate – phosphate - ferric reagent 5 ml long the cup wall into every conical flask separately, shake up, cool down in room temperature for 20 min. Then was measured the 530 nm absorbance by UV spectrometry. Each experiment was repeated 5 ×. Obtained absorbance vs. concentration dependency data were used to build up the standard curve. The numerical linear regression analysis was performed to obtain standard curve lineasr regression parameters. Each experiment was repeated 3 × (Hossain et al., 2014).

3.5.3 Determination of the CS steroids content

Weigh 5 samples 3 g corn silk powder, add 70 % ethanol (material: liquid = 1 : 20), then use 200 W ultrasonic extract for 15 min, 30 min, 45 min, 60 min, 75 min for the silking, milky and mature stages. Then was used 119 W microwave extraction apparatus for 8 min, followed by addition of pulfate-phosphate- ferric reagent to process for 20 min (the same procedure as for standard curve determination), then measure the 530 nm absorbance by UV spectrometry. Then use the standard curve to calculate the content of steroids from the CS samples. Each experiment was repeated 5 × (Hossain et al., 2014).

4. BIOCHEMICAL PROPERTY ANALYSIS OF CS EXTRACTS

4.1 Radical scavenging effect of CS extracts determination

Free radical reaction, also known as free radical reaction, is a variety of chemical reactions involving free radicals. The outer layer of the radical electron shell has an unpaired electron, which has a strong affinity for adding a second electron, so it can act as a strong oxidant. The more important one in the atmosphere is the OH-radical, which can react with various trace gases. In the chemical reaction formed by photochemical smog, there are many free radical reactions, which play an important role in the initiation, transmission and termination processes in the chain reaction. Many free radicals are intermediate products, such as hydrogen peroxide radicals (HO2-), alkoxy radicals (RO-), peroxyalkyl radicals (RO2-), acyl radicals (RCO-), etc. (Reddy, 2020)

4.1.1 Materials

All reagents and chemicals used in this research such as DPPH, ABTS, potassium persulfate ($K_2S_2O_8$), ethanol, methanol, copper chloride, hydrogen peroxide (H_2O_2), 5,5-dimethyl-1-pyrroline N-oxide (DMPO), sodium phosphate buffer, potassium ferricyanide [$K_3Fe(CN)_6$], trichloroacetic acid, ferric chloride ($FeCl_3$), neokuproiny, ammonium acetate (CH_3COONH_4) were purchased from Sigma-Aldrich (USA) in an analytical reagents purity grade. As a solvent distilled water was used. Distilled water conductivity was about 0.6 μS/cm).

4.1.2 EPR spin - trapping measurement of the CS extracts

The thermal decomposition of copper chloride ($CuCl_2$) in H_2O_2 at 333 K was used as reactive radicals to test the radical scavenging capability (RSC) of cornsilk extracts, the EPR spin-trapping technique was used 5,5-dimethyl-1-pyrroline N-oxide as a spin trap. Chloride radical anions (Cl•) generated upon thermal decomposition of $CuCl_2$ represent reactive species with high reduction potential, capable to react with organic compounds, the paramagnetic species in H_2O_2 solvent were added to the double bond of DMPO spin trapping agent to produce the corresponding spin adducts. All EPR measurements were operated in a 4-mm flat quartz cell in a Bruker TE102 (ER 4102 ST) cavity, using the EMX EPR spectrometer (Bruker, Germany) working in the X-band. The ER 4111 VT temperature unit (Bruker, Germany) was used for temperature regulation. The reaction mixture contained 100 μL H_2O_2 extracts (pure H_2O_2 as reference), 100 μL H_2O_2, 25 μL of 0.2 M DMPO dissolved in H_2O_2 and 25 μL of 0.01 M $CuCl_2$ (H_2O_2). The time course of EPR spectra of the DMPO spin adducts was recorded in 66-s intervals for 22 min at 333 K (each spectrum represents an accumulation of three scans). The integral EPR intensity (double integral) found after 22 min of thermal treatment for the sample solution was compared with the reference

measurement. The difference between the integral EPR intensities of the reference and the samples in 22nd min characterises the amount of radicals scavenged by the various components present in the sample acting as radical scavengers. The RSC values were calculated as a percentage of scavenged radicals relative to the reference sample (H_2O_2). These values were recalculated to trolox equivalent antioxidant capacity (TEAC) using calibration curve measured analogously for trolox solutions in $CuCl_2/DMPO/H_2O_2$ systems, then the obtained radical scavenging characteristics of investigated samples were evaluated in 1 mol of trolox/1 g of extract (Yamasaki & Grace, 1998).

4.1.3 DPPH radical scavenging activity measurement

Separately put 1 mL CS-S, CS-M, CS-MS corn silk extracts into 3 mL 1.44×10^{-4} mol/L DPPH radical, use same concentration vitamin C and lutin as comparison groups, 4 mL 1.44×10^{-4} mol/L DPPH without scavenger as the control group to determine the 516 nm absorbance in different reaction time. Determine the dynamic relation between absorbance and time along with the reaction between the different scavengers and DPPH radical and use absorbance as the Y - axis, time as X - axis to draw the dynamic relation curves, the inhibition level of DPPH was calculated by the following equition:

$$Inhibition = [(A_0 - A_1)/A_0] \times 100\%$$

where A_0 is the 516 nm absorbance of the control group at the initial time (0 min), A_1 is the 516 nm absorbance of the scavenger sample at the ending time (Masek, Chrzescijanska, Latos, Zaborski, & Podsedek, 2017).

4.1.4 ABTS radical scavenging activity measurement

Mix 17,2 mg ABTS, 3,3 mg $K_2S_2O_8$ and 5 ml H_2O as oxidation starter, radicals are formed and oxidized after 24 hours and then kept in freezer (-6 ℃), then add 60 ml of water to 1 ml of oxidized solution of ABTS as the solution of ABTS to test the CS extracts radical scavenging activity. Then mix 2.5ml ABTS solution with 0.5ml CS-S, CS-M, CS-MS CS extracts solution respectively (each maturity stage CS sample was extracted for 60 min and 90 min), use VC (the same concentration as the mean concentration of all of the CS extracts samples) as comparison, water as reference and determine the 734 nm absorbance in different time. Determine the dynamic relation between absorbance and time along with the reaction between the different scavengers and ABTS radical and use absorbance as the Y - axis, time as X - axis to draw the dynamic relation curves, the inhibition level of ABTS was calculated by the following equition:

$$Inhibition = [(A_0 - A_1)/A_0] \times 100\%$$

where A_0 is the 734 nm absorbance of the control group at the initial time (0 min), A_1 is the 734 nm absorbance of the scavenger sample at the ending time (Masek et al., 2017).

4.1.5 Ferricion reducing anti-oxidant power

Separately put 1 mL CS-S, CS-M, CS-MS CS extracts solutions into 2.5 mL, 0.2 M, pH 6.6 phosphate buffer and 2.5 mL, 1% $K_3Fe(CN)_6$. Then incubate the mixture at 50°C for 20 minutes. Then terminate the reaction by adding 2.5 mL, 10% trichloroacetic acid. Then mix the upper layer of 2.5 mL solution with 2.5 mL distilled water and 0.5 mL, 0.1% $FeCl_3$, then measure the 700 nm absorbance of the reaction mixture against a blank sample. The increased absorbance of the reaction mixture represents the reducing power (Masek et al., 2017).

4.1.6 Copper ion reductive capability

The base of this assay is Cu(II) to Cu(I) reduction. 0.25 mL, 0.01 M $CuCl_2$ was mixed with 0.25 mL, 7.5×10^{-3} M neokuproiny ethanol solution and 0.25 mL, 1 M CH_3COONH_4 buffer solution. Then add CS-S, CS-M, CS-MS CS extracts solution 0.25 mL respectively, then volume the mixture to 2 mL by distilled water and maintain at the room temperature for 30 minutes. Then measure the 450 nm absorbance against the blank sample (0.25 mL water). The increased absorbance represents the copper ion reductive capability (Masek et al., 2017).

4.2 CS extracts bioactive ingredients, functional groups and molecuar chemical structures analysis and determination

4.2.1 Materials

All reagents and chemicals used in this research such as methanol, glacial acetic acid, acetonitrile were purchased from Sigma-Aldrich (USA) in an analytical reagents purity grade. As a solvent distilled water was used. Distilled water conductivity was about 0.6 μS/cm).

4.2.2 NMR analysis

Nuclear Magnetic Resonance (NMR) is nuclear magnetic resonance. It is a nucleus whose magnetic moment is not zero. Under the action of external magnetic field, the spin energy level undergoes Zeeman splitting, and it resonates to absorb the radio frequency radiation of a certain frequency. Nuclear magnetic resonance spectroscopy is a branch of spectroscopy, whose resonance frequency is in the radio frequency band, and the corresponding transition is the transition of nuclear spin on the nuclear Zeeman level.

In this study, the methanolic CS-S, CS-M, CS-MS CS extracts were put into 5 mm NMR (Bruker, Germany) tubes and measured on a 600 MHz NMR spectrometer equipped with a VNMRS console and PFG Dual Broadband DBG600-5F probe (Varian/Agilent). After initial tuning, matching, locking, and shimming, the 90-degree pulse was calibrated and transmitter offset was set to residual water signal frequency. The tnnoesy pulse sequence was used with 1 s relaxation delay (including 0.99 s water presaturation), 100 ms mixing time (with water presaturation) and 4 s acquisition time (Larina, 2019).

4.2.3 FTIR analysis

FTIR is mainly composed of Michelson interferometer and computer, the infrared light emitted by the infrared light source S is collimated into a parallel infrared light beam and enters the interference system. After being adjusted by the interferometer, a beam of interference light is obtained. The interference light passes through the sample Sa, obtains the interference signal containing the spectral information, and reaches the detector D, which converts the interference signal into an electrical signal. The interference signal here is a function of time, that is, the interference graph drawn by the interference signal, the abscissa of which is the moving time or moving distance of the moving mirror. This interferogram is sent to a computer through an A / D converter, and the computer performs a fast Fourier transform calculation to obtain an infrared spectrogram with the wave number as the abscissa. Then send it to the plotter through the D / A converter and draw a standard infrared absorption spectrum that people are very familiar with.

In this study, the FTIR spectra were recorded on a FTIR spectrometer (Thermo Electron Scientific Instruments Corporation, USA) in the region of $4000 - 400 \text{ cm}^{-1}$ (Mohamed, Jaafar, Ismail, Othman, & Rahman, 2017).

4.2.4 HPLC analysis

High performance liquid chromatography (HPLC) is also known as "high pressure liquid chromatography", "high speed liquid chromatography", "high resolution liquid chromatography", "modern column chromatography" and so on. High performance liquid chromatography is an important branch of chromatography. It uses a liquid as the mobile phase and uses a high-pressure infusion system to pump a single solvent with different polarities or a mixed solvent with different ratios and buffers into the mobile phase equipped with a stationary phase. In the chromatographic column, after each component in the column is separated, it enters the detector for detection, thereby realizing the analysis of the sample. This method has become an important application of separation and analysis technology in the fields of chemistry, medicine, industry, agronomy, commodity inspection and legal inspection.

In this study, absolute methanol extracted corn silk flavonoids (extraction temperatures were 60℃, 70℃ and 80℃) were filtrate by 0.2μm filter membrane, stored in 4℃, then analyzed by UHPLC Dionex Ultimate 3000, UV / VIS detector, DAD (Thermo Fisher Scientific, USA), conditions of HPLC are Phenomenex Kinetex C18 chromatographic column (150mm x 4.6 mm; 5 μm); mobile phase A : 99/1: water / glacial acetic acid 99.8%; mobile phase B: 67/32/1: water / acetonitrile / glacial acetic acid 99.8%; flow rate: 1ml/min; determine wavelength: 275nm; column temperature: 30℃；injection volume: 10μl；external standard method; processing time: 45min; mobile phase gradient: gradient elution: 0 - 10 min 10 - 20% B,10 - 16 min 20 - 40% B, 16 - 20 min 40 - 50% B, 25 - 25 min 50 - 70% B, 25-30 min 70% B, 30 - 40 min 70 -10% B, 40 - 45 min 10% B. (Lozano-Sánchez, Borrás-Linares, Sass-Kiss, & Segura-Carretero, 2018)

4.3 Vitro Enzyme Inhibition Test

The vitro enzyme inhibition test refers to the simulation of the external animal and plant environment in vitro, which is based on the enzyme inhibitor and the enzyme reaction kinetics. It has a wide range of uses in biochemistry, pharmaceuticals and medicine. (Deng et al., 2019)

4.3.1 Materials

All reagents and chemicals used in this research such as 10% fetal bovine serum, dimethyl sulfoxide (DMSO), 5% thiazolyl blue tetrazolium bromide (MTT), phosphate buffer (PBS), Tris-HCl, hydrochloric acid (HCl), Sodium carbonate (Na_2CO_3) boric acid buffer, P – nitroglucoside (pNPG) thrombin, fibrin, angiotensin converting enzyme, hippuryl histidine leucine, α- glucosidase, α-amylase, xanthine, xanthine oxidase (XOD), uric acid and captopril were purchased from Sigma-Aldrich (USA) in an analytical reagents purity grade. As a solvent distilled water was used. Distilled water conductivity was about 0.6 μS/cm).

4.3.2 Thrombin inhibition activity test

Put 40 μL CS flavonoids, polysaccharides and steroids extracts into 140 μL 0.1% fibrinogen, place for 10 min, then add 10 μL thrombin solution, shake up, then place in 37°C for 2 min, then measure the 405 nm absorbance (A_{405}). Use 0.05M Tris - HCl (pH 7.2) buffer instead of thrombin as the blank group. The thrombin inhibition rate equation is as follows:

$$Y=(A_1-A_2)/(A_1-A_0)\times 100\%$$

where Y is the thrombin inhibition rate, A_1 is the A_{405} without inhibitor, A_2 is the A_{405} with inhibitor and A_0 is the A_{405} of the blank group (Whelihan, Kiankhooy, & Brummel-Ziedins, 2014).

4.3.3 ACE inhibition activity test

Put 10μL CS flavonoids, polysaccharides and steroids extracts into 30μL hippuryl histidine leucine as the substrate, then place the mixed solution 37°C thermostatic waterbath for 5 min, then add 20μL ACE in 37°C temperature for 30 min, then add 60μL 1mol/L HCl to terminate the reaction. Use 228nm absorbance (A_{228}) to calculate the ACE inhibition rate. Use captopril with pH 8.3 boric acid buffer plus CS extracts sample solutions as the blank group. The ACE inhibition rate equation is as follows:

$$Y=[(M-N)/M]X100\%$$

where Y is the ACE inhibition rate, M is the blank group A_{228}, N is the A_{228} of the CS sample extracts groups (Sawicki et al., 2019).

4.3.4 α- glucosidase inhibition activity test

Put 5μL α- glucosidase (10 unit/mL 0.1mol/L pH 6.8 PBS) solution and 10μL CS extracts samples into 620μL 0.1mol/L PBS, place the mixed solution in 37.5°C for 20 min, then add 10μL 10mmol/L pNPG as the substrate to initiate the reaction.

After 30 min reaction in 37.5℃, add 650μL 1mol/L Na_2CO_3 to terminate the reaction. Use 410_{nm} light to measure the absorbance (A_{410}). Use the above mixed solution without CS extracts as the blank group. The α- glucosidase inhibition rate calculation equation is as follows:

$$Y=[(A_0-A_1)/A_0]\times 100\%$$

where Y is the α- glucosidase inhibition rate, A_0 is the blank group A_{410} and A_1 is the CS extracts groups A_{410}. (Kato-Schwartz et al., 2020)

4.3.5 α- amylase inhibition activity test

Put 10μL α- amylase (1 unit/L) into 10μL CS extracts solutions, place for 15 min, then add 500μL 1% starch (PBS) solution to initiate the reaction. After 5 min reaction in 37.5℃, add 600μL DNS reagent to terminate the reaction. Then put the above reacted solution in boiling water bath for 15 min, then cool down to the room temperature. Use 540 nm light to measure the absorbance (A_{540}) and use the group without CS extracts as the blank. The α- amylase inhibition rate calculation equation is as follows:

$$Y=[(A_0-A_1)/A_0]\times 100\%$$

where Y is the α- amylase inhibition rate, A_0 is the blank group A_{540} and A_1 is the CS extracts groups A_{540}. (Kato-Schwartz et al., 2020)

4.3.6 XOD inhibition activity test

Mix 300μL CS extracts solutions, 210μL pH 7.5 PBS and 180μL 0.01unit/mL XOD solution (pH 7.5 PBS as the solvent) in 25℃ for 15 min, then add 360μL 1.5M/mL xanthine solution (pH 7.5 PBS as the solvent) to react in 25℃ for 30 min. Use the 150mL 1mol/L HCl as the terminator, measure the 290nm absorbance (A_{290}) to calculate the XOD inhibition rate. Use the group adding HCl before XOD as the blank. The XOD inhibition rate calculation equation is as follows:

$$Y=[(A_0-A_1)/A_0]\times 100\%$$

where Y is the XOD inhibition rate, A_0 is the blank group A_{290} and A_1 is the CS extracts groups A_{290}. (Li et al., 2018)

RESULT AND DISCUSSION

1. CS SAMPLE PHYSICOCHEMICAL PROPERTY ANALYSIS

1.1 SEM analysis of the CS powder samples

There are shown SEM images of the tested corn silk powders and fibers in Figure 1. They are characteristic with the rectangular shape of individual particles exhibiting complex microporous structure on the intersection. Such structures are typical for plants cellulose based materials.
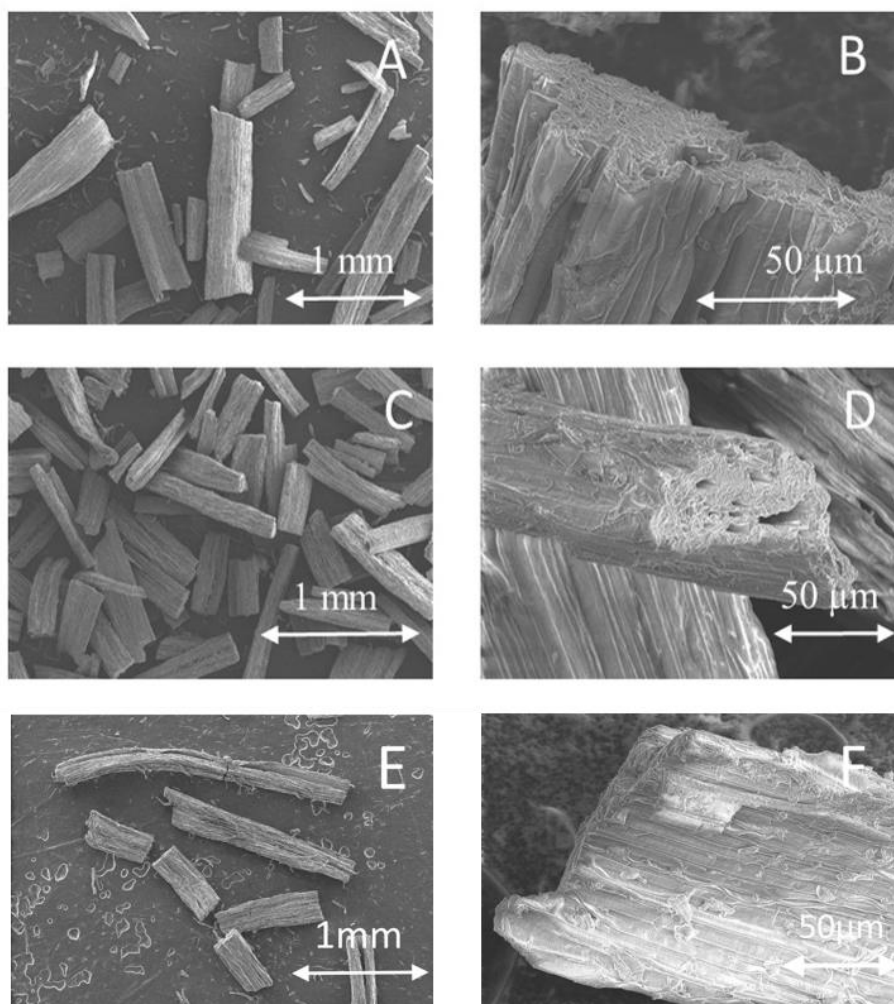
Figure 1. Studied corn silk SEM images: A, B – CS - S, C, D – CS - M, E, F – CS - MS.

1.2 TG/DTA analysis of the CS powder samples

The moisture content and thermoal analysis by TG and DTA of the samples were resulted as in Figure 2, which are the typical multistep decomposition process for all CS- S, CS- M and CS- MS samples as shown in Figure 2A. The first step decomposition of CS-S was in the temperature range from 30 to 120 ℃ with observed weight loss 8.3 % attributed to the moisture content. Total decomposition step was about 77.45 % in the temperature range of 30 to 550 ℃.

Similarly, for the sample CS-M and CS-MS, TG data exhibited the first step decomposition of 5.9 % and 10.04 % in the same temperature range as CS-S followed by the total weight loss of 65.5 % and 83.88% in the temperature range of 30 to 550 ℃，which indicated the CS-MS contains the most thermally labile substances compared with CS-S and CS-M.

There are two endothermic peaks in Figure 2B. The first one was located in the temperature of 54.3 ℃ for CS-S and CS-MS, 60.2 ℃ for CS-M attributed to the melting point of flavonoids (Miziara et al. 2017). The second one was observed at 397 ℃ (CS-MS), 415.1 ℃ (CS-M) and 419.7 ℃ (CS-S) attributed to the total thermal decomposition with the formation of a low quantity carbonaceous residues respectively. Observed exotheric process at 524 ℃ corresponds to the decomposition CS - MS sample.
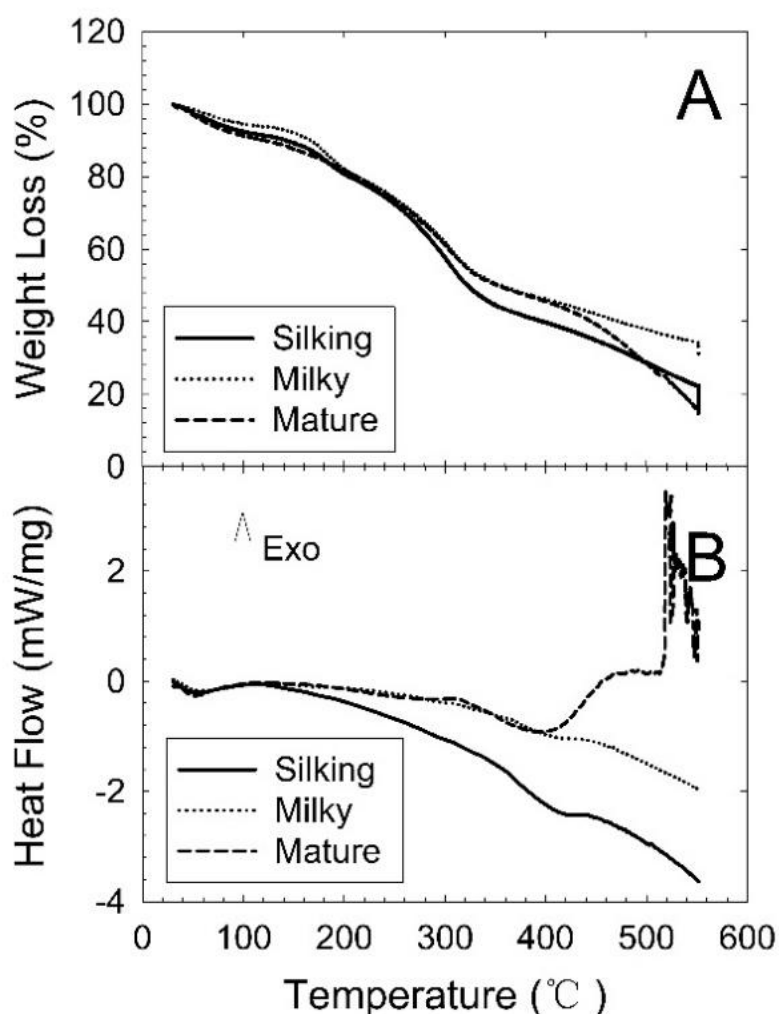
Figure 2. Thermal analysis of CS samples: A – Thermogravimetry (TG),
B – differential thermal analysis (DTA).

2. CS FUNCTIONAL INGREDIENTS EXTRACTION, CONTENT DETERMINATION AND EXTRACTION METHODS OPTIMIZATION

2.1 CS flavonoids extraction and content determination

2.1.1 Rutin standard curve

In Figure 3 there is shown a typical lutin standard curve as obtained according to the standard procedure described in detail in the materials and methodology section. Obtained regression parameters are given as the Figure 3 inset as well. Obtained data were of a high correlation as indicated by the correlation coefficient being 0.995.
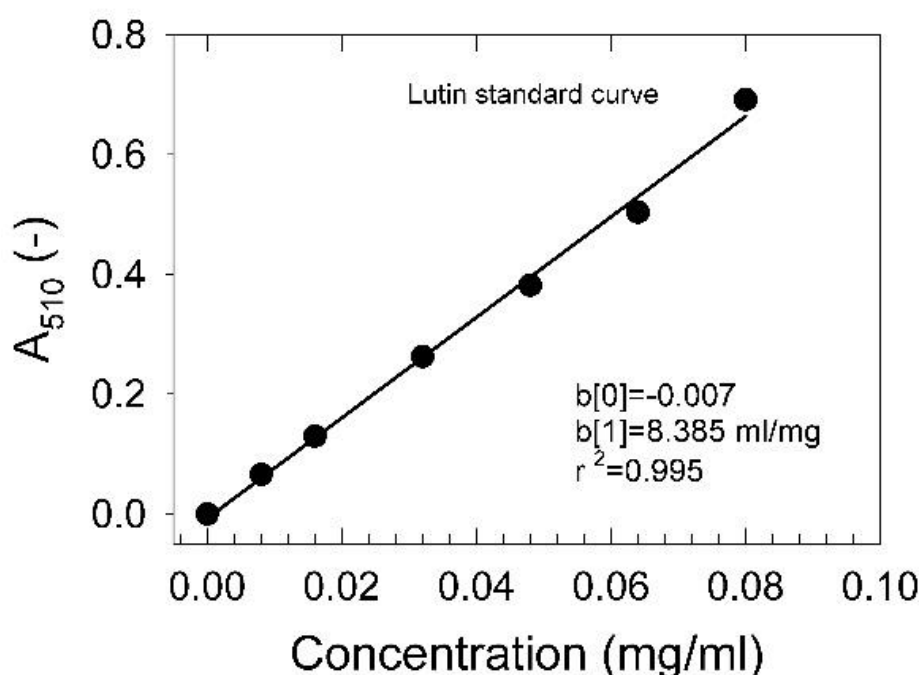
Figure 3. Lutin standard curve. Inset: Linear regression standard curve parameters.

2.1.2 Determination of the CS flavonoids content and extraction methods optimization

Effects of the extraction time and of the extraction temperature are summarized in Figure 4, where kinetics data of the extraction of CS-S, CS-M and CS-MS samples are plotted in flavonoids concentration vs. extraction time coordinates. Each extraction was performed at two different temperatures, the first one was of 40 ℃ and the second one at 80 ℃. All of the CS-S, CS-M and CS-MS dependencies were of a complex non-linear character, modeled as a third order polynomial dependency. However, in the case of CS-S, for both extraction temperatures the same characteristic sinusoidal pattern was found exhibiting the maximum extraction efficiency at 50 ℃. Observed concentrations were of about 6.5×10^{-3} mg/ml for CS-S extracted at 40 ℃, about 5×10^{-3} mg/ml for CS-M

extracted at 80 ℃, about 9.5×10^{-3} mg/ml for CS-MS extracted at 80 ℃ indicates that the extracted flavonoids substances are sensitive on thermal history and are undergoing thermal decomposition similarly as reported by Chaaban et al. (Chaaban et al., 2017). In the latter paper, the linear degradation pattern was found for rutin at 70 ℃ degradation temperature. With increasing degradation temperature up to 130 ℃ the exponential decay pattern was found. In the case of CS-M, the maximum extraction efficiency was found at 30 min extraction time being of 5.8×10^{-3} mg/ml at 40 ℃ extraction temperature. However, at higher temperature, the degradation of the flavonoids content was observed, and only the exponential decay pattern was found as indicated in Figure 4B. That is why, the maximum extraction was found at 20 min extraction time at 80 ℃ extraction temperature. It was found, that the highest extracted flavonoids content was $(7.2 \pm 0.3) \times 10^{-3}$ mg/ml for CS-M 80 ℃ sample and $(12.2 \pm 0.4) \times 10^{-3}$ mg/ml for CS - MS 80 ℃ sample. However, for the CS-S the highest content was found of $(6.8 \pm 2.1) \times 10^{-3}$ mg/ml for CS-S 40 ℃ sample. To characterize obtained extracts of flavonoids, the UV VIS as well as fluorescence spectra were measured as shown in Figures 5 to 8. Prior to the fluorescence mapping analysis of the studied corn silk extracts, the UV VIS spectra were recorded.

These were typical with three major absorption regions at 260nm and 360 nm (near ultraviolet region), and at visible light region of 490 nm. The absorption of electromagnetic radiation in the near ultraviolet region is typical for poly-unsaturated and aromatic compounds such as flavonoids. All of CS-S, CS-M and CS-MS exhibited similar UV VIS spectra except the visible range region, where a 480 nm shoulder peak occurred for CS-M sample.

Results of the fluorescence excitation-emission mapping of the studied extracts are shown in Figure 8. These are characteristic similarly as the UV VIS absorption spectra with the three distinct fluorescence emission regions at 320 nm, 450 nm and 680 nm. Emission region located at 450 nm was ascribed to the flavonoids compounds similarly as observed by Shan et al. (Shan et al. 2017), who found, that the flavonols characteristic excitation/emission spectral range is 365 – 390 nm/450 – 470 nm. The excitation/emission spectral range of 480 – 500 nm/510 – 520 nm was ascribed to flavanols.

There were found three distinct excitation wavelengths regions at about 275nm, 350 nm and 420 nm. Obtained results indicate, that the major difference among CS-S, CS-M and CS-MS is in the fluorescence emission centered at the 450 nm region, where the intensity of the fluorescence emission was highest for CS-S extracted at 80 ℃ for 50 minutes. Furthermore, there was found that the fluorescence emission intensity region located at 450 nm region was of higher intensity for CS-S in comparison to CS-M and CS-MS at 80 ℃ extraction temperature. Observed results were considered as statistically significant ($p \leq 0.05$). These results are in an excellent correspondence with the TG analysis, where the first step decomposition weight loss was found higher for CS-S in comparison to

CS-M and CS-MS. However, there was not found any major difference between fluorescence emission intensities located at 320 nm region for all studied materials.
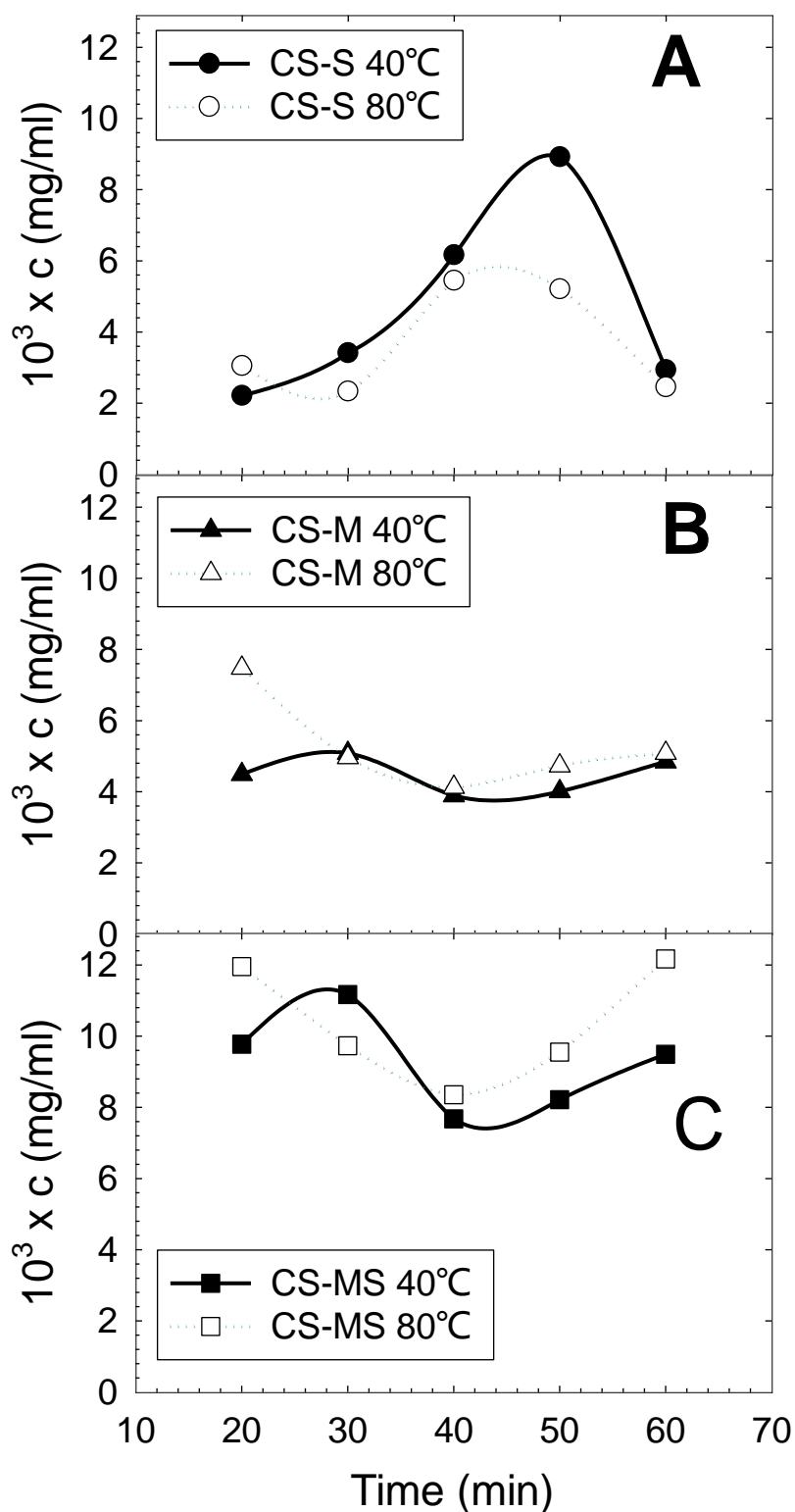
Figure 4. Flavonoids extraction kinetics: A – corn silk silking stage, B – corn silk milky stage, C – corn silk mature stage.
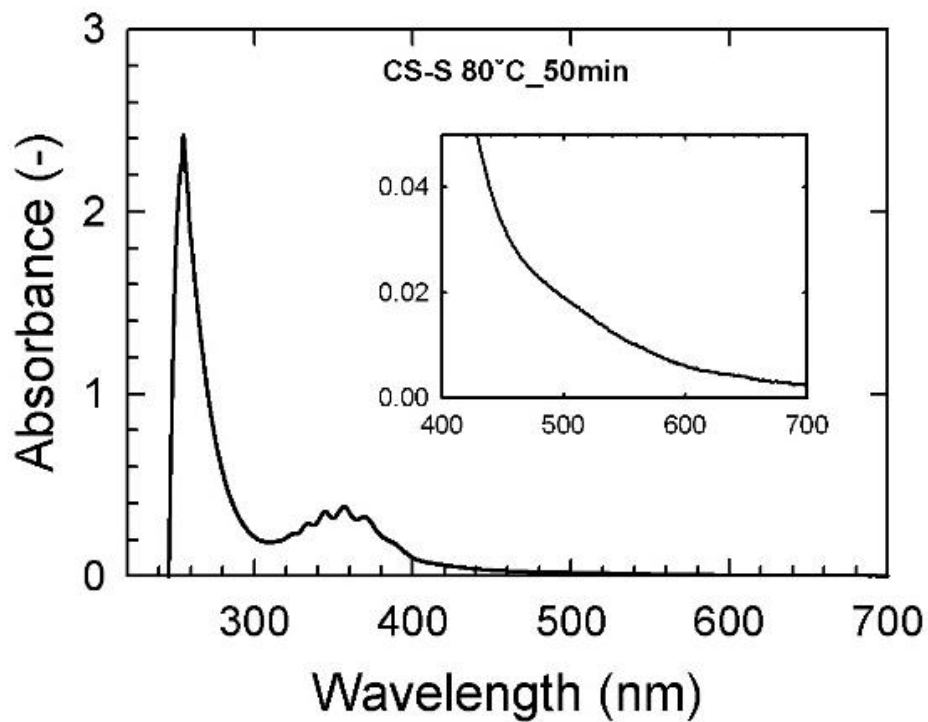
Figure 5. UV VIS spectrum of flavonoids of the CS-S sample extracted at 80℃ temperature after 50min extraction time. Inset: expanded 400 nm to 700 nm region.
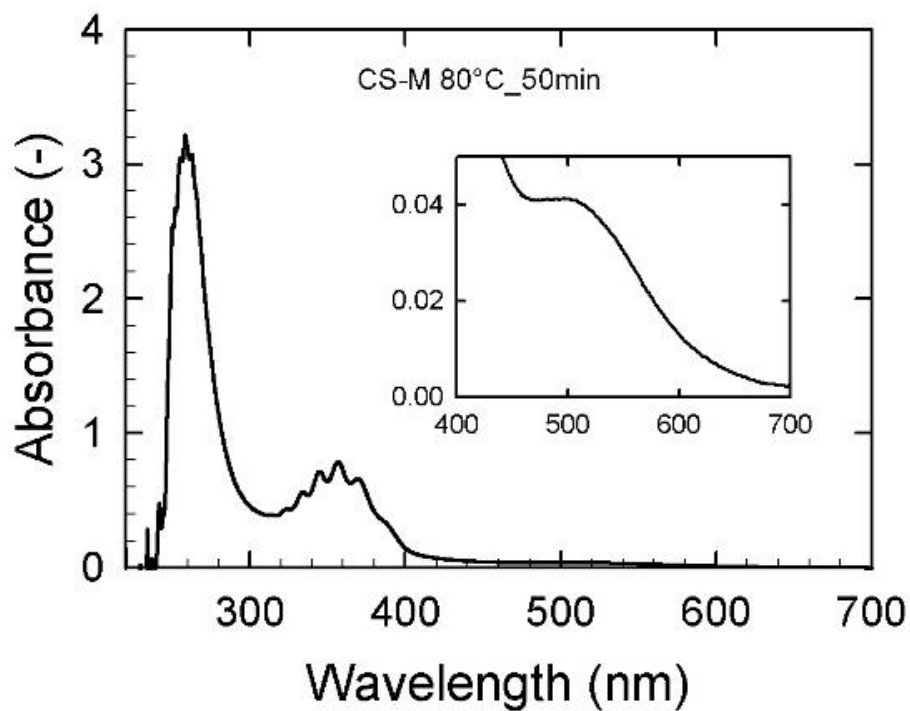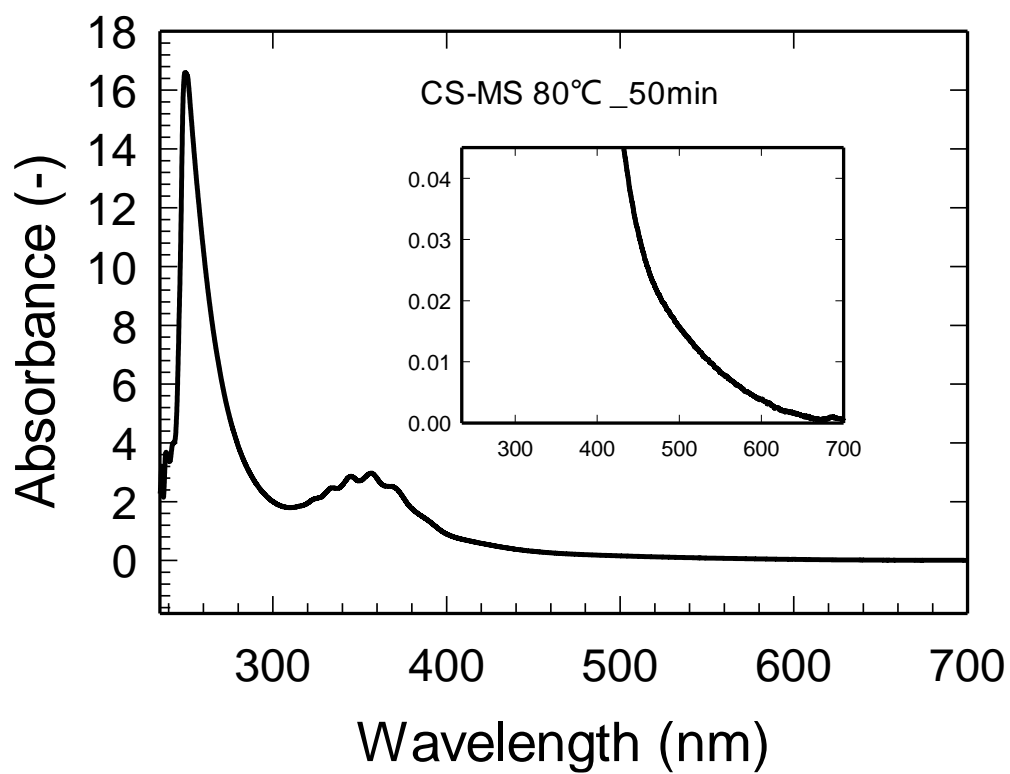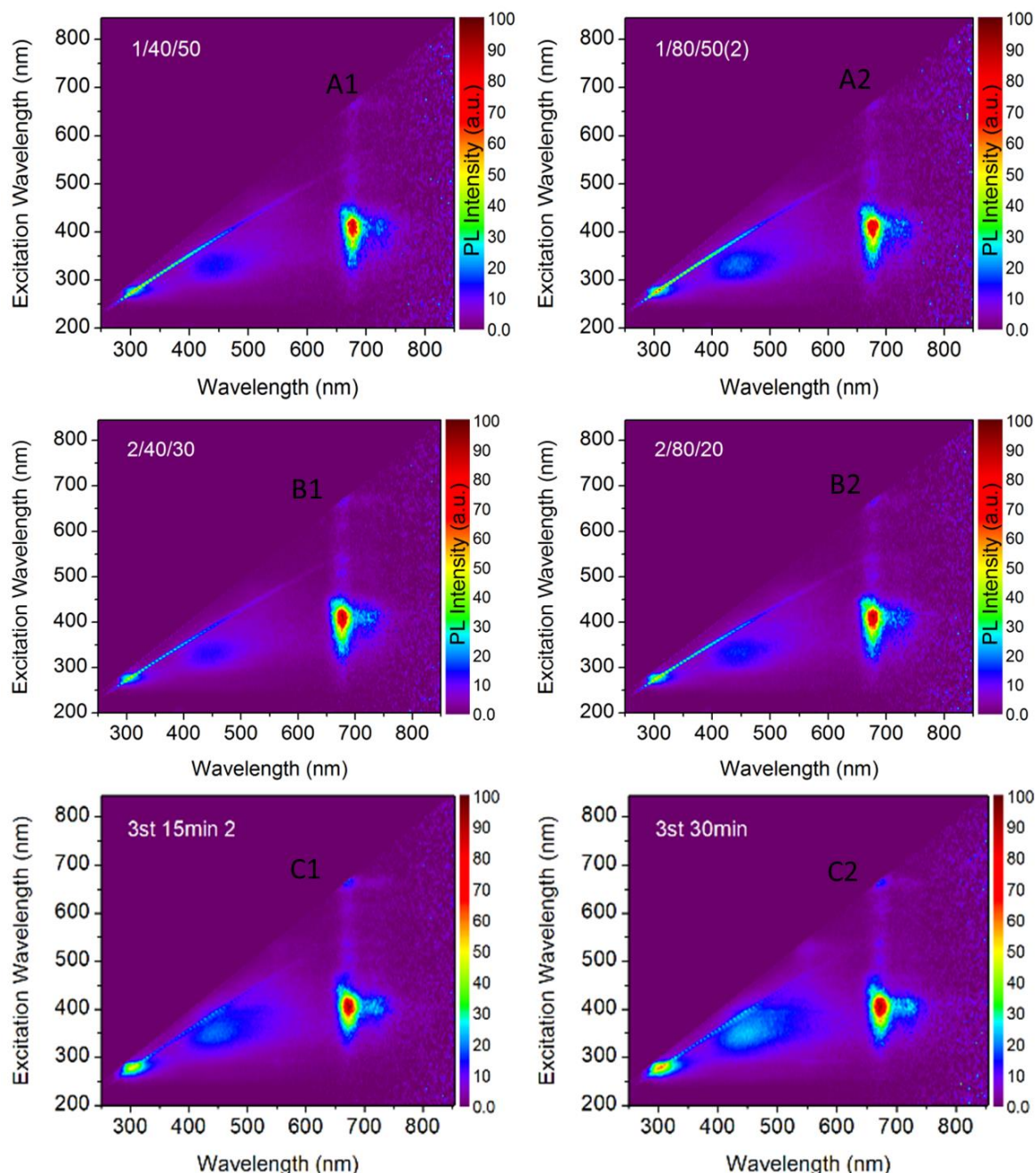

Figure 6. UV VIS spectrum of flavonoids of the CS-M sample extracted at 80℃ temperature after 50min extraction time. Inset: expanded 400 nm to 700 nm region.

Figure 7. UV VIS spectrum of flavonoids of the CS-MS sample extracted at 80℃ temperature after 50min extraction time. Inset: expanded 400 nm to 700 nm region.

Figure 8. Results of the fluorescence excitation-emission mapping of the studied corn silk flavonoids extracts. Inset legend A/B/C: A=CS - S sample, B=CS - M sample, C=CS - M sample

2.2 CS polysaccharides extraction and content determination

2.2.1 Glucose standard curve

In Figure 9 there is shown a typical lutin standard curve as obtained according to the standard procedure described in detail in the materials and methodology section. Obtained regression parameters are given as the Figure 9 inset as well. Obtained data were of a high correlation as indicated by the correlation coefficient being 0.995.
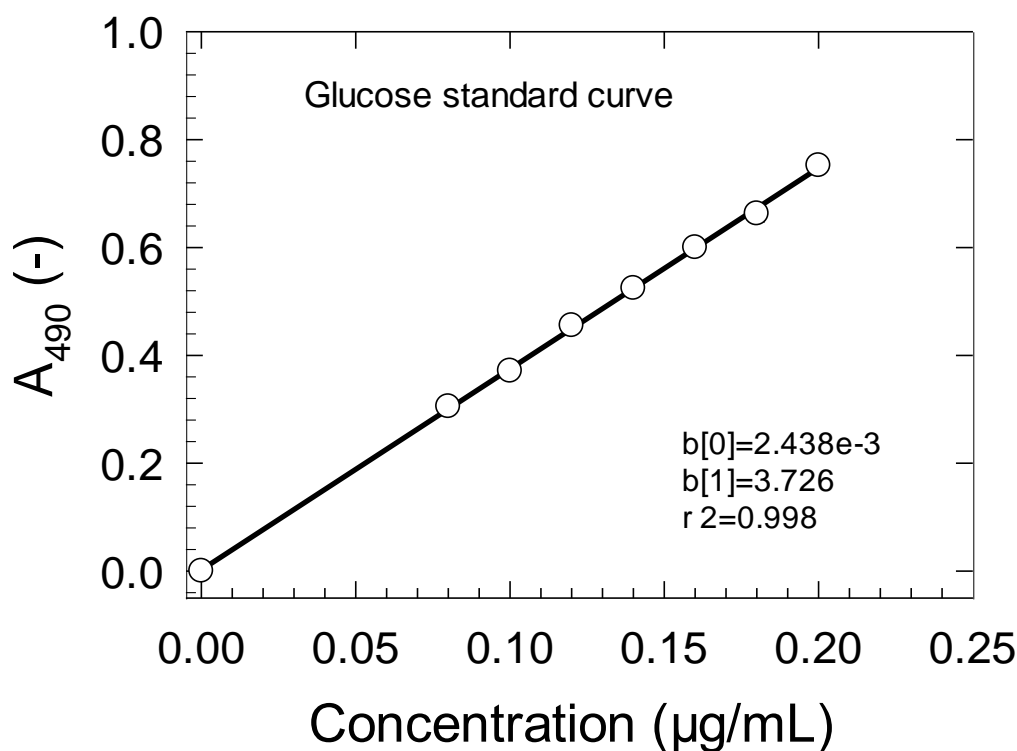
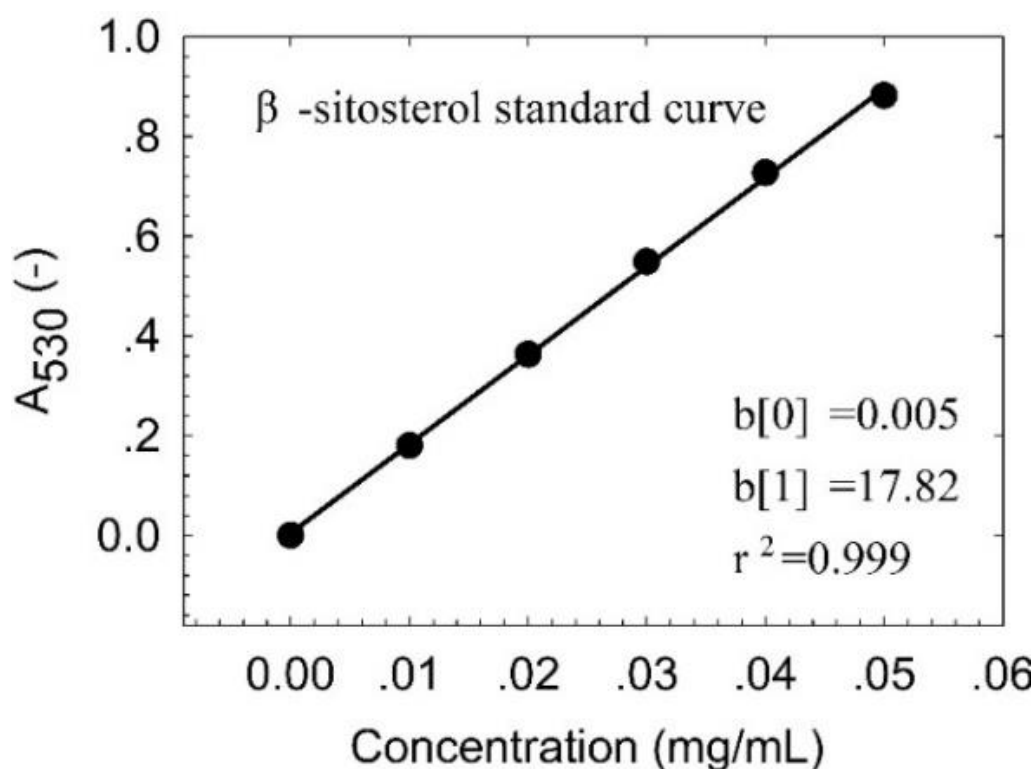*Figure 9. Glucose standard curve. Inset: Linear regression standard curve parameters.*

2.2.2 Determination of the CS polysaccharides content and extraction methods optimization

As can be seen in Figure 10, within the same extraction temperature of 100°C，the all of the CS-S, CS-M and CS-MS polysaccharides concentrations have the positive correlation with extraction time and all of the 3 maturity stages showed the similar trends of the kinetics, which is from 80 – 100 min, the polysaccharides content increase trends are sheer and from 100 – 120 min, the trends became subdued. The maximum polysaccharides extraction content for CS-S sample was 0.12 µg/ml in the 120 min as well as 0.16 µg/ml for CS-M and 0.33 µg/ml for CS-MS. It is notable that the CS-MS has a much higher polysaccharides yield than CS-S and CS-M. On the contrary, the CS-S has the lowest yield of polysaccharides.

Figure 11 shows, within the same extraction time 2 hours, all of the CS-S, CS-M and CS-MS polysaccharides concentrations have the positive correlation with the extraction temperature. CS-M and CS-MS have the similar trend of the temperature vs. polysaccharides concentration kinetics, which is 60 – 80 °C, the increasing was sheer and from 80 – 100 °C, the trend became subdued. The CS-S polysaccharides extraction kinetic showed a potential of increase even in the temperature higher than 100°C, however the totally trend of CS-S polysaccharides

yield increase from 60 – 100 °C was subdued compared with the trend of CS-M and CS-MS. It is remarkable that the CS-MS yield was much higher than the CS - S and CS-M, which is in accord with the result of Figure 10.

The CS-S, CS-M and CS-MS polysaccharides extracts 200 – 700 nm wavelength absorbance was also determined by UV VIS and they all showed the similar curves of the light absorbance. The apparent peaks are in the wavelength range of 470 – 490 nm, which is the typical absorption wavelength of polysaccharides.

Therefore, in accordance with the Figure 10 – Figure 14 results, the optimal extraction method of CS polysaccharides extraction conditions are 100 °C extraction temperature, 2 hours extraction time with the CS-MS sample.
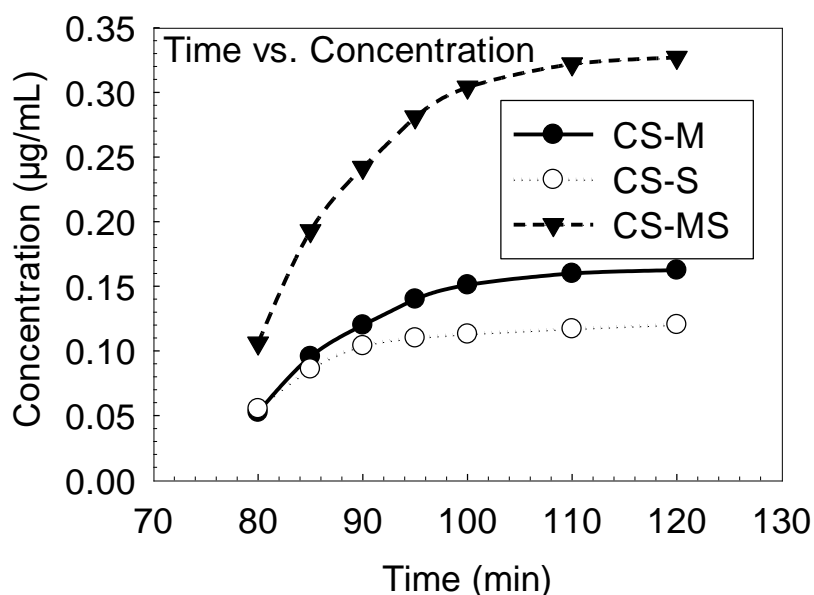
Figure 10. Within 100°C extraction temperature, the CS-S, CS-M and CS-MS polysaccharides extraction time vs. concentration kinetics
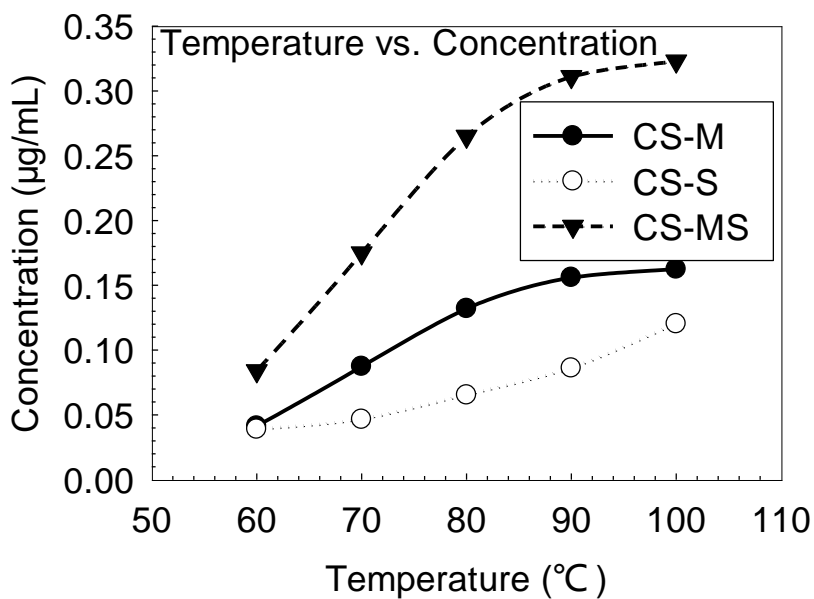
Figure 11. Within 2 hours extraction time, the CS-S, CS-M and CS-MS polysaccharides extraction temperature vs. concentration kinetics
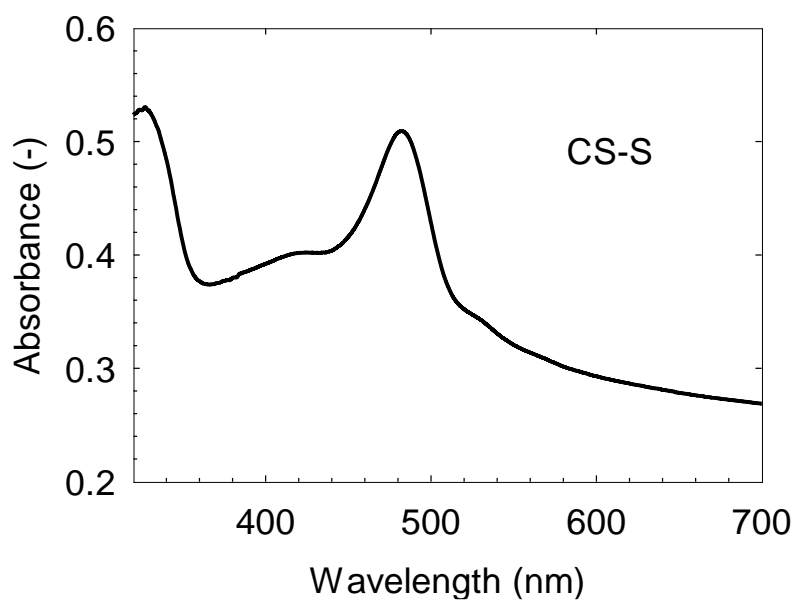
Figure 12. UV VIS spectrum of polysaccharides of the CS-S sample extracted at 100℃ temperature after 90min extraction time.
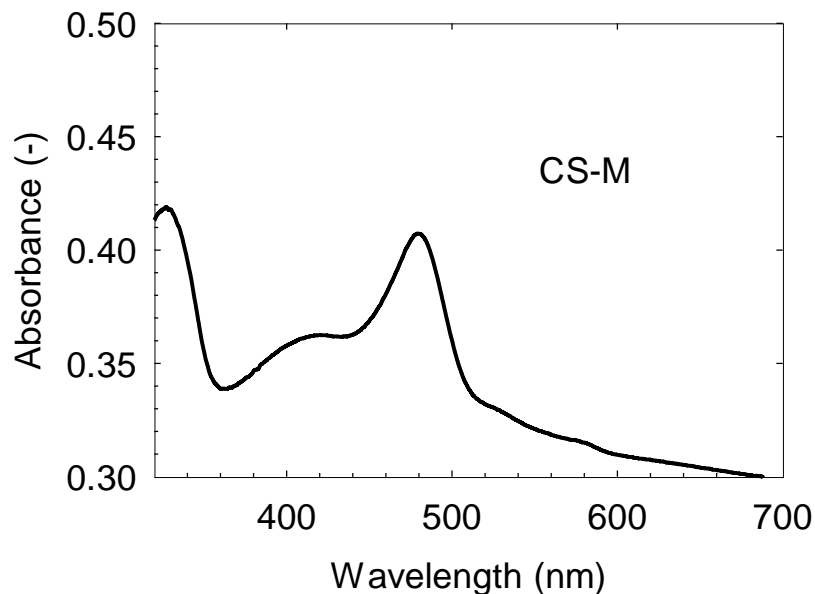
Figure 13. UV VIS spectrum of polysaccharides of the CS-M sample extracted at 100°C temperature after 90min extraction time.
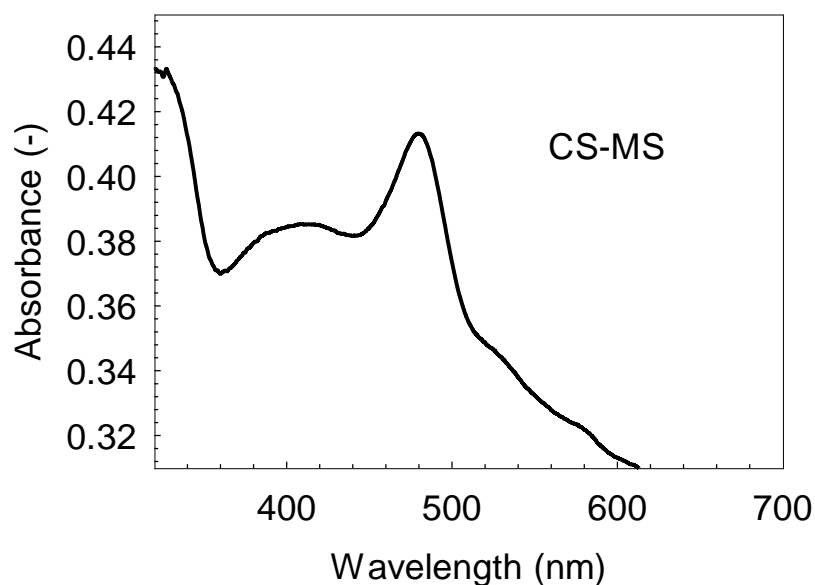
Figure 14. UV VIS spectrum of polysaccharides of the CS-MS sample extracted at 100°C temperature after 90min extraction time.

2.3 CS steroids extraction and content determination

2.3.1 β- sitosterol standard curve

The β- sitosterol standard curve is shown in Figure 15, the regression parameters and inset as well. The Obtained data were highly correlated as the correlation coefficient 0.999.

Figure 15. β- sitosterol standard curve. Inset: Linear regression standard curve parameters.

2.3.2 Determination of the CS steroids content and extraction methods optimization

Figure 16 shows the effects of the Ultrasonic time and different maturity stages by the steroids concentration vs. ultrasonic time correlations. All of the CS-S, CS - M and CS-MS were a non – linear character, modeled as a third order polynomial dependencies. However, all of those three stages extraction contrations had a direct proportionality trend with the increase of the ultrasonic processing time. All of the three stages samples had an obvious increasing range of the extraction concentration from ultrasonic extraction time 15 min to 60 min. From 60 min to 75 min, three samples showed a similar steady tendency which means from 60 min to 75 min the increase of the concentration is not conspicuous anymore. Therefore, the 75 min ultrasonic extraction time can be marked as the optimum extraction time to obtain maximum extracted content for all of the three stages. Obtained maximum concentrations were as follows: CS-S 0.09 mg/ml, CS-M 0.12 mg/ml, CS-MS 0.37 mg/ml. It is noteworthy, that the CS-MS had a much higher maximum extraction concentration as well as the increasing rate in comparison to CS-S and CS-M samples. This imply that the CS-MS has much higher content of steroids than CS-S and CS-M. Simultaneously, the ultrasonic assisted technique can be sonsidered to be much more effective to CS-MS sample extraction rather than for CS- S and CS-M. , which is in agreement with the results of UV-VIS and fluorescence excitation – emmision mapping illustrated in Figures 17 to 20.

The UV VIS and fluorescence spectra were resulted in Figures 17 to 20, which were the typical three major light absorption regions at near ultraviolet region of 350 nm and visible light region of 500 nm and 650 nm. The electromagnetic radiation absorption in the visible light region is typical for anthraquinone and phenanthrene compounds such as steroids. All of the CS-S, CS-M and CS-MS exhibited similar UV VIS spectra.

The fluorescence excitation-emmision mapping result of the CS extracts are illustrated in Figure 8. Similar as the UV VIS measurement, there were three distinct fluorescence enission regions at 300 nm, 430 nm and 680 nm respectively.

There were three distinct excitation wavelengths regions at about 275nm, 350 nm and 380 nm, which indicate the difference among CS-S, CS-M and CS-MS is in the fluorescence emission centered at the 300 nm and 430 nm regions. The highest intensity of the fluorescence emission at 300 nm was found for CS-MS extracted at 40 ℃ for 15 minutes in the ultrasonic extraction bath. Moreover, the fluorescence emmision intensity region at 430 nm region was the highest intensity for CS-MS as well. Observed results were considered as statistically significant ($p \leq 0.05$). However, there was no any major difference for all studied materials at the fluorescence emmision intensity of 670 nm region.
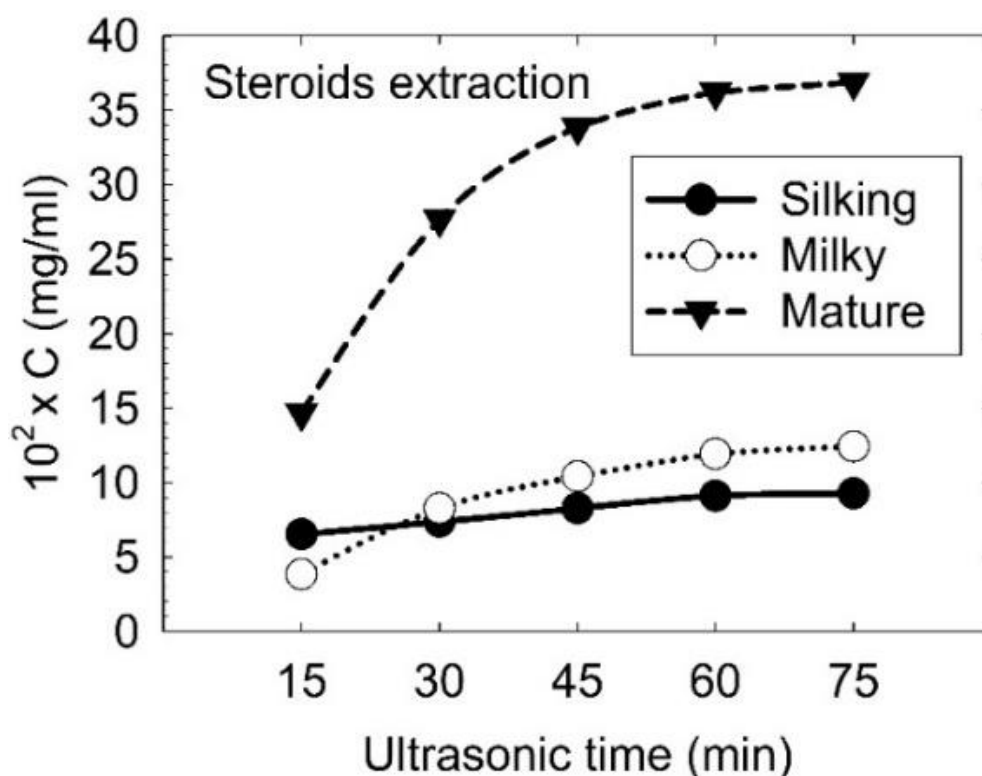
Figure 16. Ultrasonic assisted CS steroids extraction kinetics
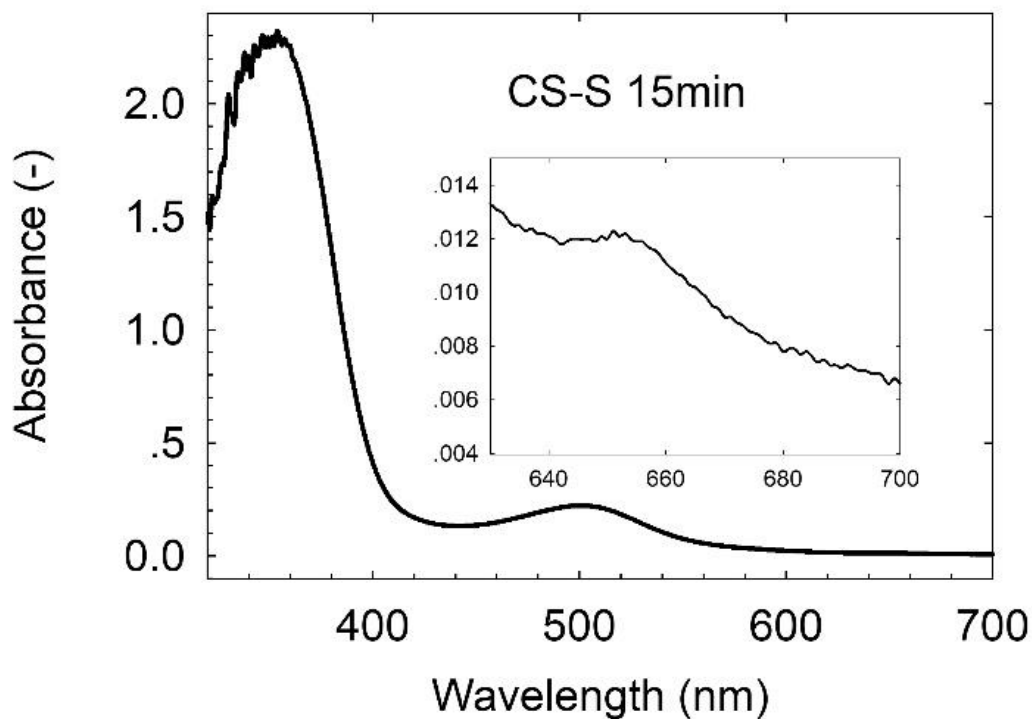
Figure 17. Result of the UV VIS spectrum for the CS-S sample extracted with ultrasonic-assistance for 15min. Inset: expanded 630 nm to 700 nm region.
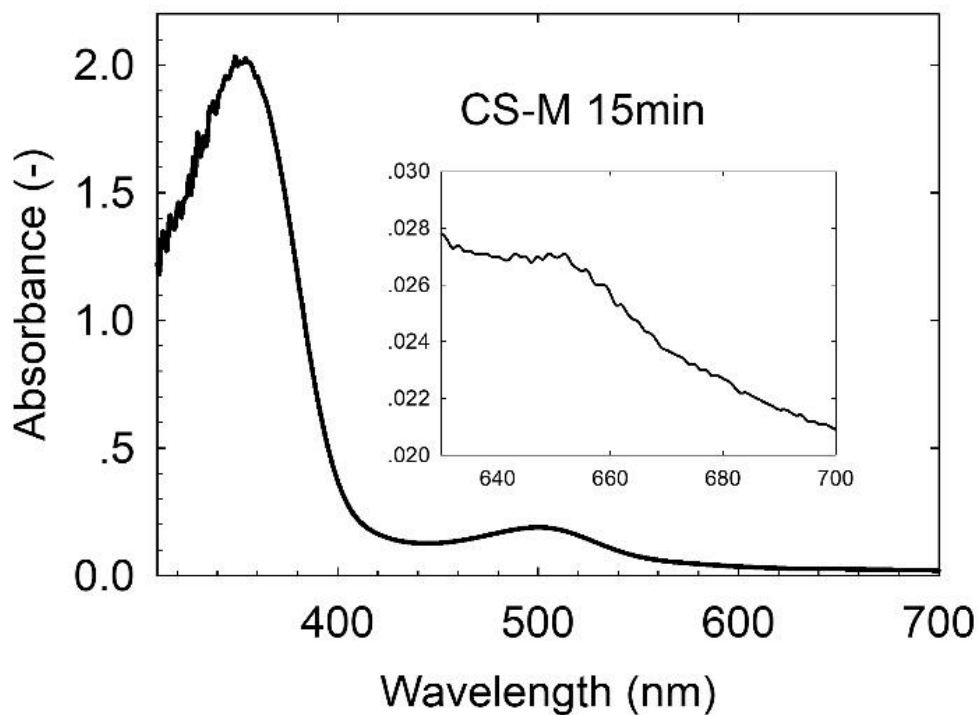
Figure 18. Result of the UV VIS spectrum for the CS-M sample extracted with ultrasonic-assistance for 15min. Inset: expanded 630 nm to 700 nm region.
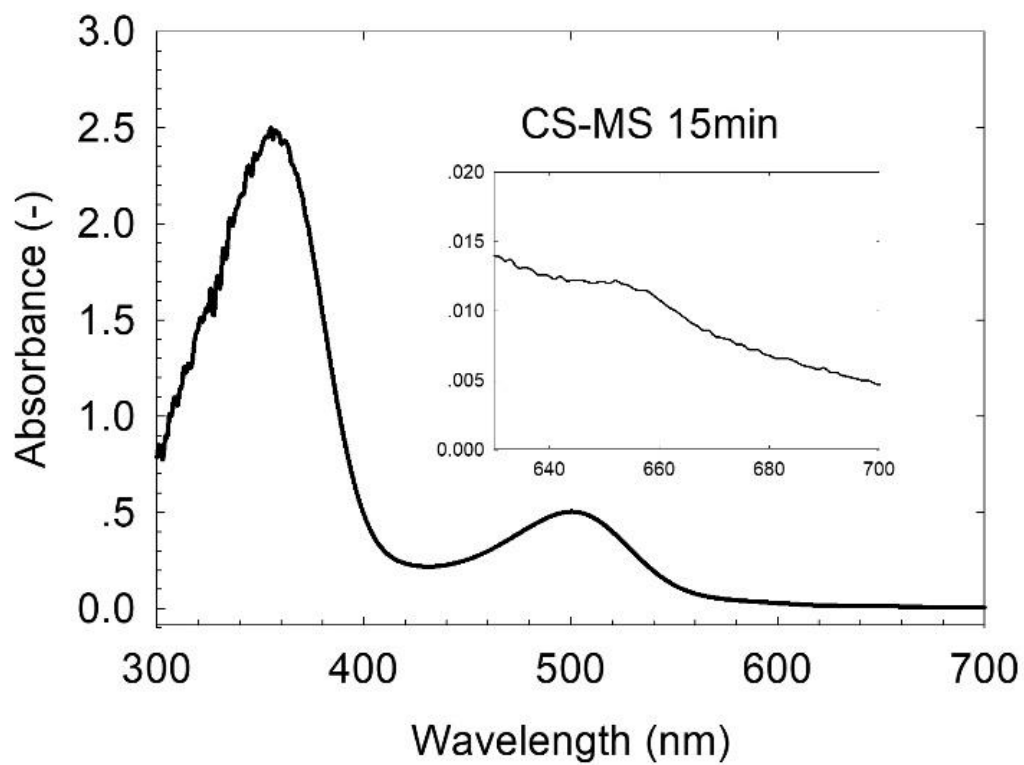
Figure 19. Result of the UV VIS spectrum for the CS-MS sample extracted with ultrasonic-assistance for 15min. Inset: expanded 630 nm to 700 nm region.
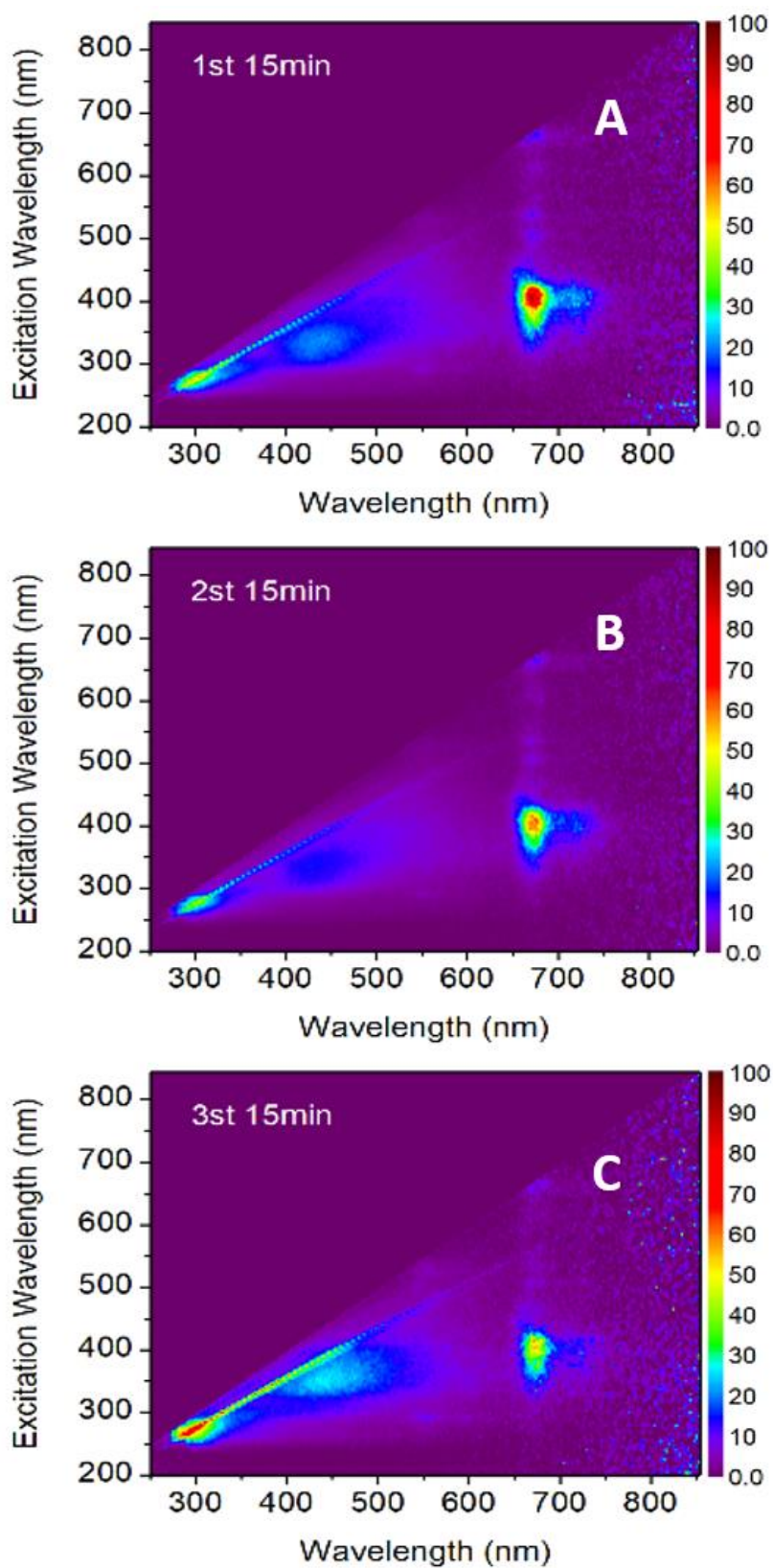
Figure 20. The fluorescence excitation − emmision mapping of the CS extracts. Inset legend: A − CS-S, B − CS-M, C – CS-MS. Extraction temperature (40 ℃ or 80 ℃), 15 min ultrasonic extraction time.

3. BIOCHEMICAL PROPERTY ANALYSIS OF CS EXTRACTS

3.1 Radical scavenging effect of CS extracts determination

3.1.1 EPR spin - trapping measurement of the CS extracts

As can be seen in Figure 21, the extracts of CS with 70% ethanol has much stronger radical scavenging capability than water extracts and both water and 70% ethanol extracts show the similar difference according to the maturity stages of CS, which is the CS-MS extracts have the strongest radical scavenging capability, then CS-S medium, CS-M the weakest. Compared with water, 70% ethanol is a more effective solvent to extract more radical scavengers from CS but also more influential to the DMPO radical since the reducibility of the ethanol itself. Therefore, the afterwards experiments applied the 70% ethanol as the solvent.
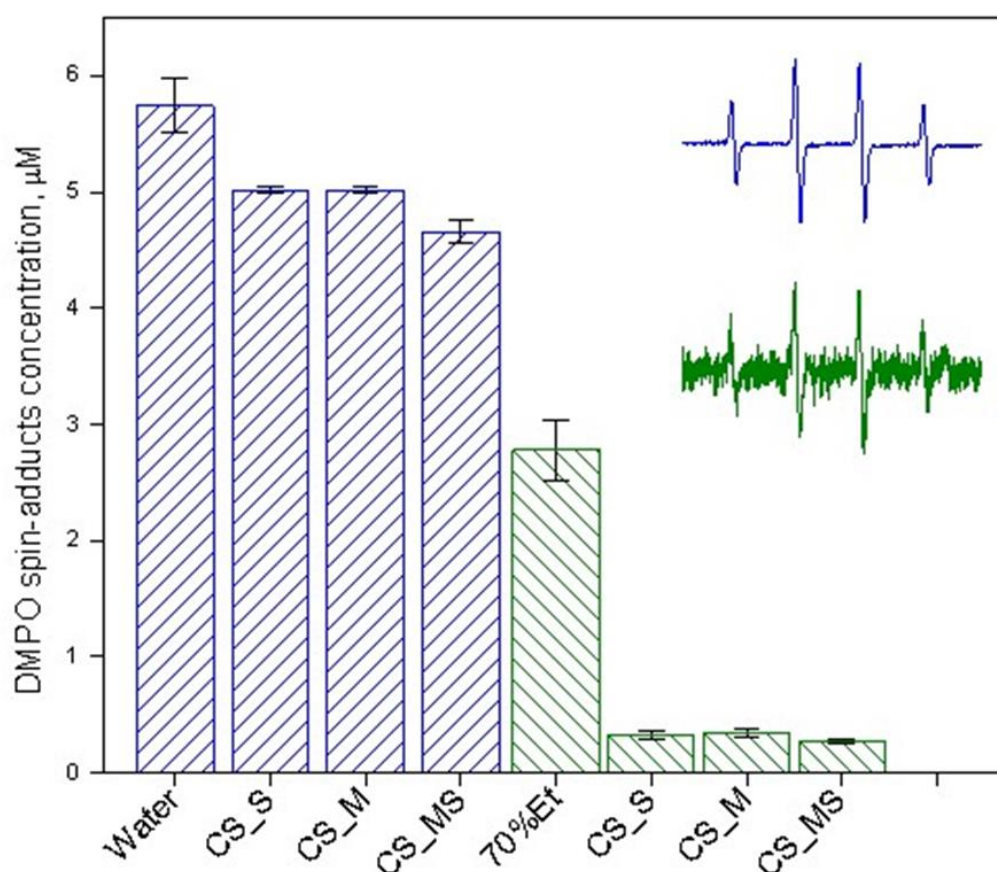
Figure 21. EPR test of cornsilk exrtacts with water and 70% ethanol solvent in CS-S, CS-M, CS-MS

3.1.2 DPPH radical scavenging activity measurement

Figure 22 - 24 illustrate the the effect of DPPH scavenging from the strongest to the lightest is vitamin C, rutin and CS extracts according to the time and A_{516}, all of vitamin C, rutin and CS extracts have the prominent scavenging effect from

0 to 5 min and from 5-60 min the effect became mitigatory gradually. The scavenging effect of vitamin C stopped after 5 min means vitamin C had consumed all of the DPPH radical in the mixed solution. The same pattern of CS extracts and rutin also can be seen in Figure 22 - 24, and table 1, along with the higher concentration of the anti-oxidant materials, comes the stronger effect of DPPH scavenging. Table 1 shows the DPPH radical scavenging capability of the CS-S, CS-M, CS-MS extracts and the corresponding same concentration VC and rutin. CS-S extracts had a higher capability of DPPH radical scavenging than the CS-M but almost the same. Comparatively, CS-MS extracts had a much higher capability of DPPH radical scavenging than CS-S and CS-M. The result is also matched the result of EPR measurement.
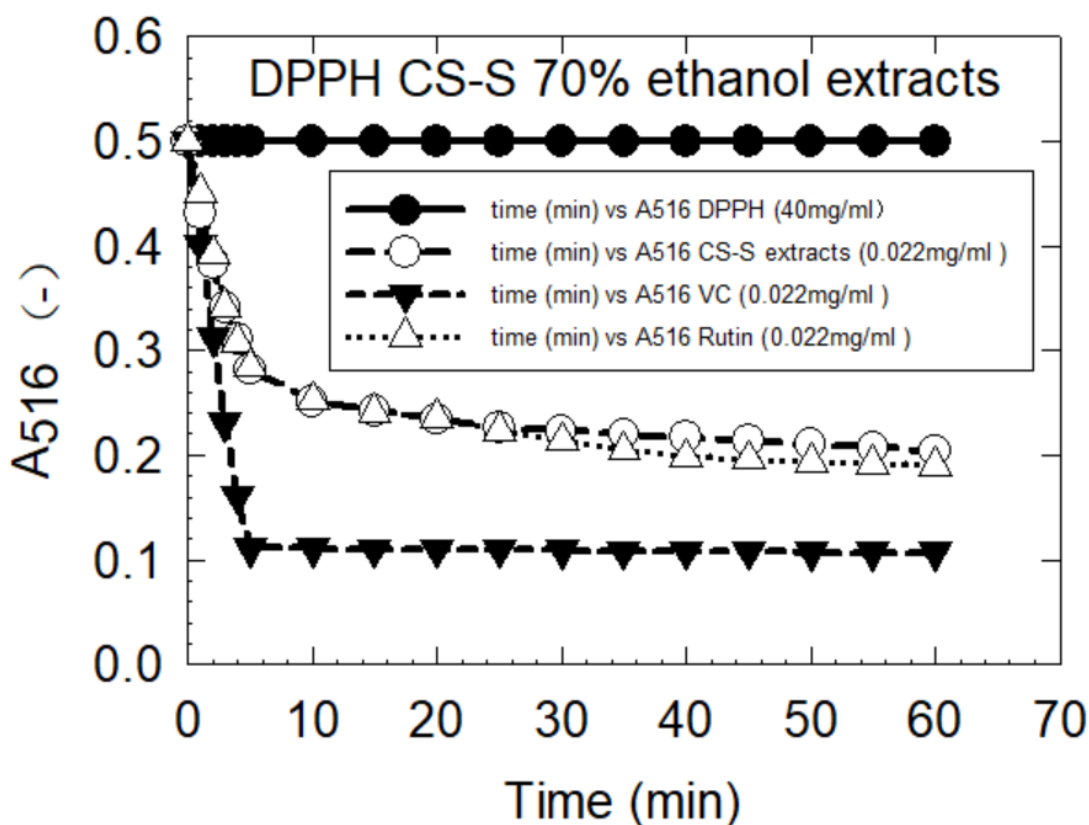
Figure 22. DPPH CS-S 70% ethanol extracts scavenging kinetics
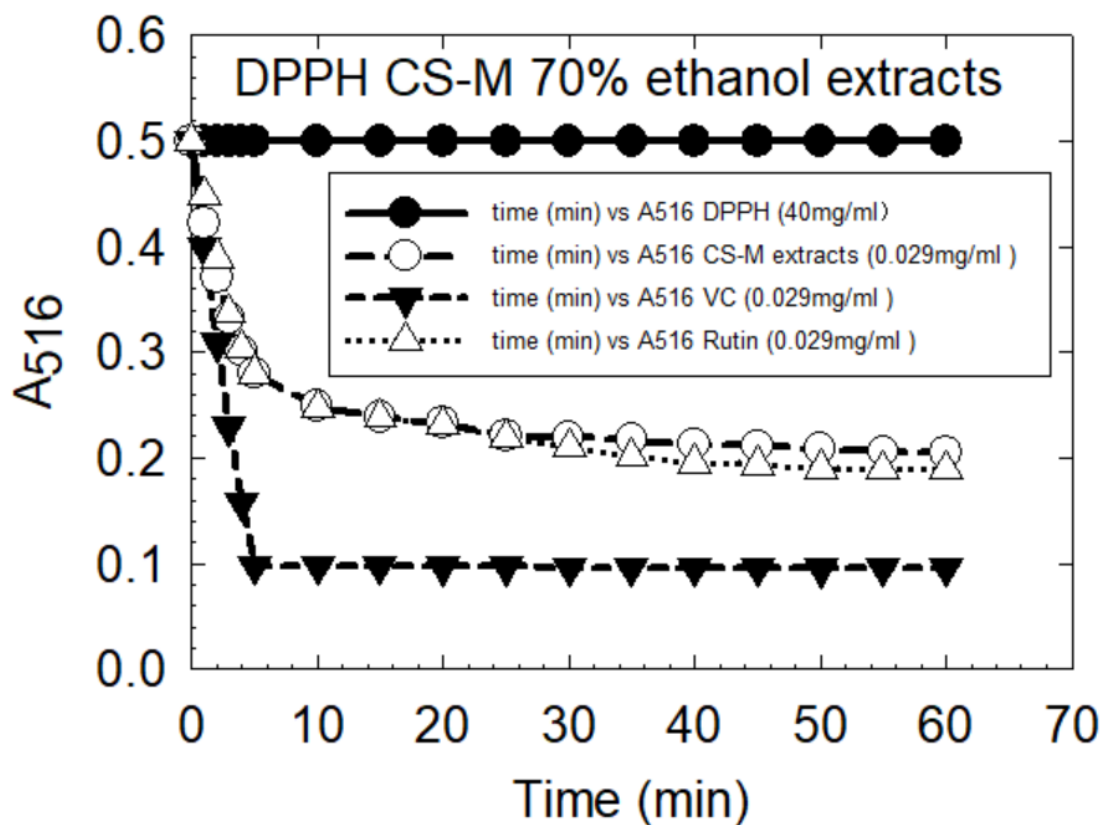
Figure 23. DPPH CS-M 70% ethanol extracts scavenging kinetics
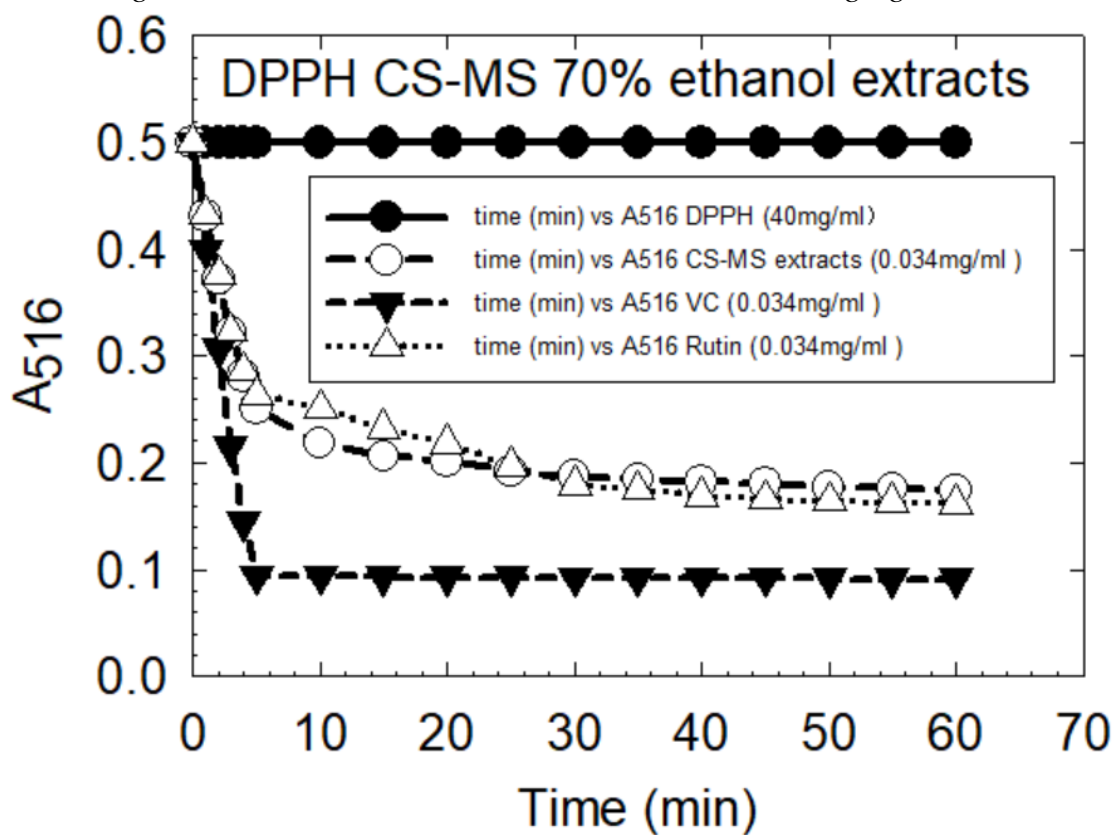
Figure 24. DPPH CS-MS 70% ethanol extracts scavenging kinetics

Table 1. The inhibition of the DPPH radical

Scavenger	Inhibition (%)
CS-S (0.22 mg/mL)	59.33 ±0.61
VC (0.22 mg/mL)	78.63 ±0.45
Rutin (0.22 mg/mL)	62.03 ±0.35
CS-M (0.29 mg/mL)	59.20 ±0.92
VC (0.29 mg/mL)	80.63 ±0.96
Rutin (0.29 mg/mL)	62.30 ±0.76
CS-MS (0.34 mg/mL)	65.20 ±0.90
VC (0.34 mg/mL)	81.63 ±0.67
Rutin (0.34 mg/mL)	67.30 ±1.08

3.1.3 ABTS radical scavenging activity measurement

As can be seen from Figure 25 and Table 2, along with the longer extraction time 90 min it showed a stronger capability of ABTS radical scavenging in each maturity stage CS extracts sample. The same pattern as in DPPH scavenging, the capability of different maturity stages CS ABTS scavenging rank from the strongest to the weakest was also CS-MS, CS-S and CS-M. Also all of the samples had an apparent decreasing trend in the beginning 5 min and then the trends became placid. It is noticeable that the ABTS radical scavenging capability was getting remarkably discriminatory according to the maturity stages especially the difference between the CS-S and CS-M compared with the DPPH radical scavenging measurement and analysis. Additionally, the vitamin C as the comparison group, showed a much stronger radical scavenging capability than the CS extracts samples.
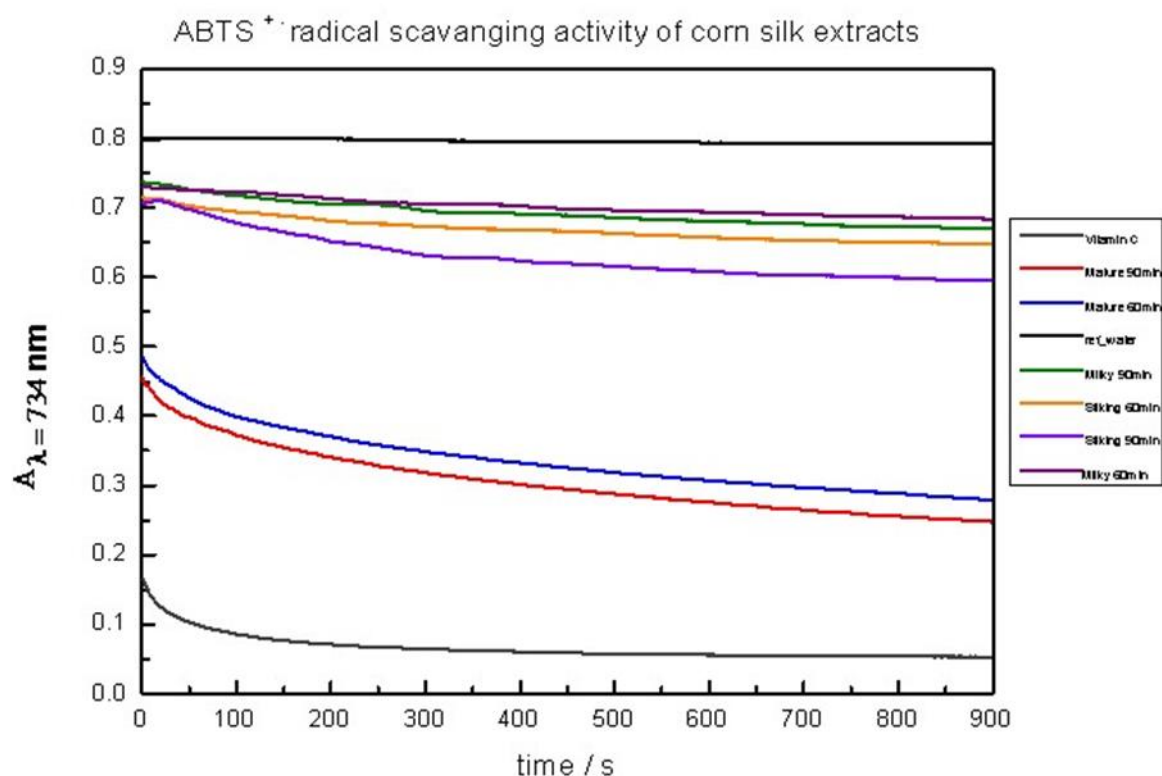
Figure 25. Different extracting times and maturity stages CS extracts ABTS scavenging kinetics

Table 2. The inhibition of the ABTS radical

Scavenger	Inhibition (%)
CS-S (60 min)	19.21 ±0.55
CS-S (90 min)	25.68 ±0.60
CS-M (60 min)	14.52 ±0.60
CS-M (90 min)	16.41 ±0.65
CS-MS (60 min)	65.46 ±0.72
CS-MS (90 min)	69.17 ±0.56
VC	93.28 ±0.45

3.1.4 Ferricion reducing anti-oxidant power and copper ion reductive capability

Table 3 and table 4 show the anti-oxidant capability of different maturity stages CS extracts in the reduction reaction with Fe^{3+} and Cu^{2+}. For both Fe^{3+} and Cu^{2+}, the different maturity stages CS extracts were capable to reduce the Fe^{3+} and Cu^{2+} by it anti-oxidant property. The among the three stages of CS, CS-MS extracts had a much stronger anti-oxidant effect than CS-S and CS-M, CS-M had the

weakest anti-oxidant capability, which is also consist with the result of EPR, DPPH and ABTS measurement. However, CS-S extracts showed a remarkably higher anti-oxidant effect than the CS-M to the Fe^{3+} compared with the similarities between CS-M and CS-S in the previous EPR, DPPH and ABTS assays.

Table 3. Ferricion reducing anti-oxidant power

CS extracts samples	Ferricion reducing power
CS-S	1.33 ± 0.32
CS-M	0.53 ± 0.11
CS-MS	2.63 ± 0.15

Table 4. Copper ion reductive capability

CS extracts samples	Copper ion reductive capability
CS-S	0.89 ± 0.09
CS-M	0.78 ± 0.09
CS-MS	1.21 ± 0.13

3.2 CS extracts bioactive ingredients, functional groups and molecuar chemical structures analysis and determination

3.2.1 NMR analysis

As can be seen from Figure 26- 30, typical polyphenols and flavonoids waveshapes had shown in the NMR analysis results and the CS-S, CS-M and CS-MS samples methanol extracts showed the very similar NMR chemicalshift vs. absorption intensity wave shapes, indicating the chemical structures of the functional ingredients from the CS-S, CS-M and CS-MS samples are very similar. However, the results of the NMR analysis was not clear enough to determine the specific functional ingredients from CS methanol extracts.
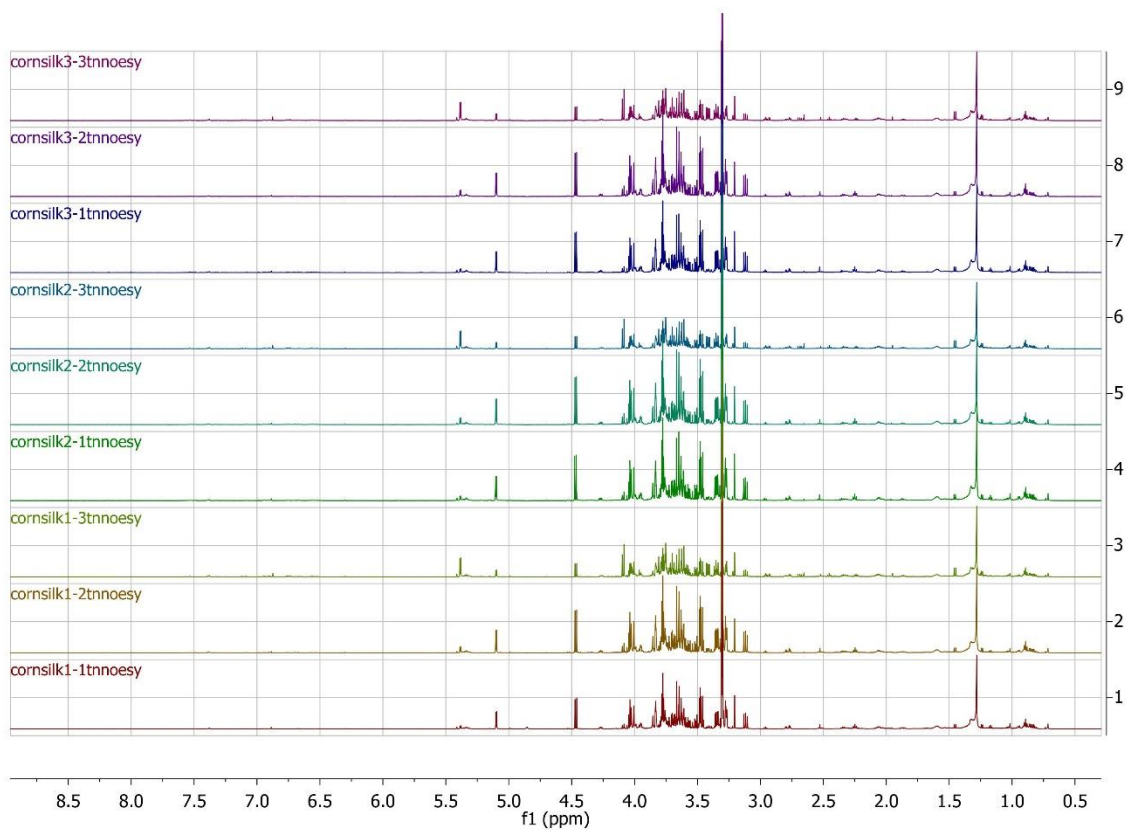
Figure 26. The CS methanol extracts NMR analysis results in the chemicalshift δ range from 0ppm to 9ppm, where cornsilk 1 is the CS-S sample extracts, cornsilk 2 is the CS-M sample extracts, cornsilk 3 is the CS-MS sample extracts.
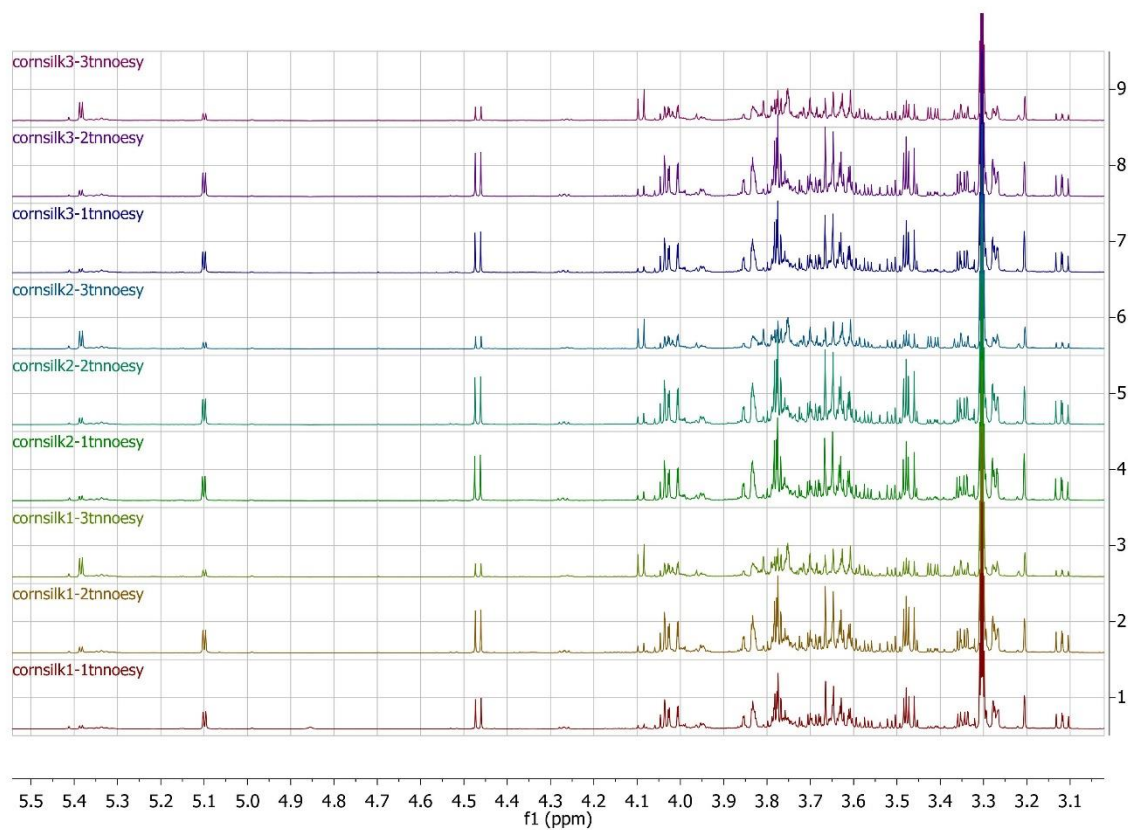
Figure 27. The CS methanol extracts NMR analysis results in the chemicalshift δ range from 3.1ppm to 5.5ppm, where cornsilk 1 is the CS-S sample extracts, cornsilk 2 is the CS-M sample extracts, cornsilk 3 is the CS-MS sample extracts.
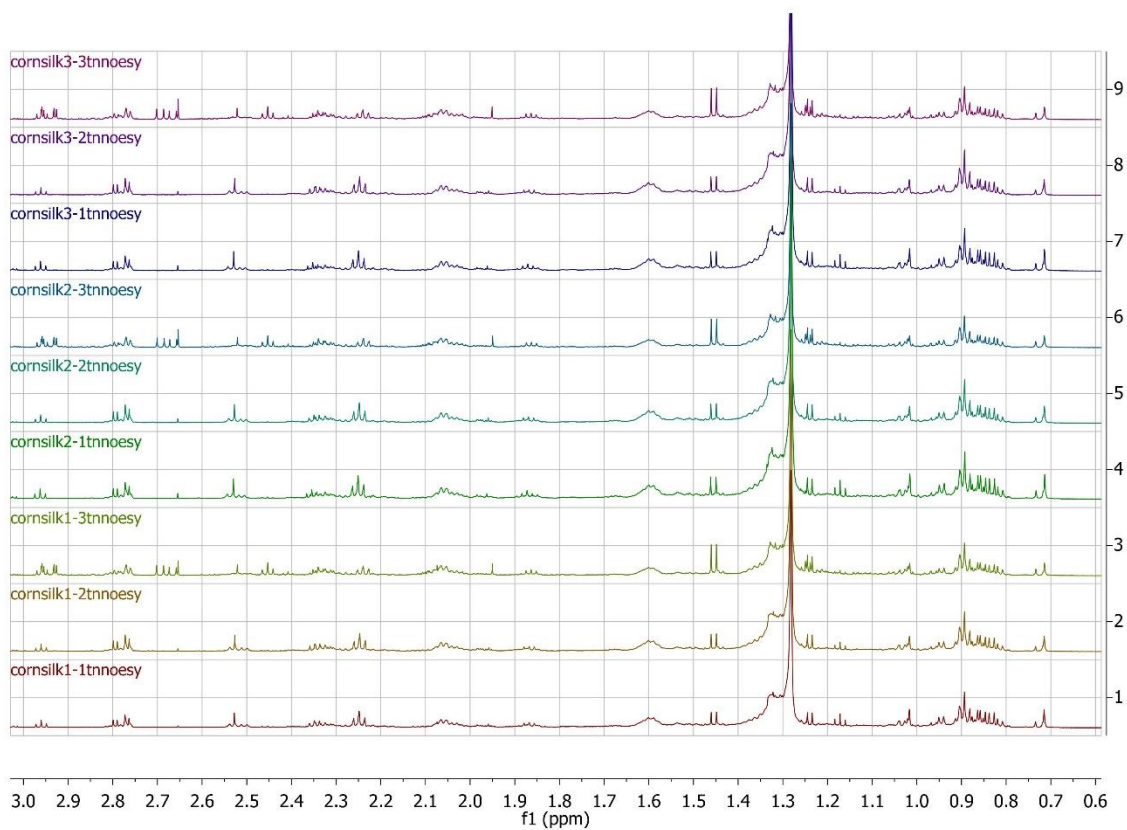
Figure 28. The CS methanol extracts NMR analysis results in the chemicalshift δ range from 0.6ppm to 3.0ppm, where cornsilk 1 is the CS-S sample extracts, cornsilk 2 is the CS-M sample extracts, cornsilk 3 is the CS-MS sample extracts.
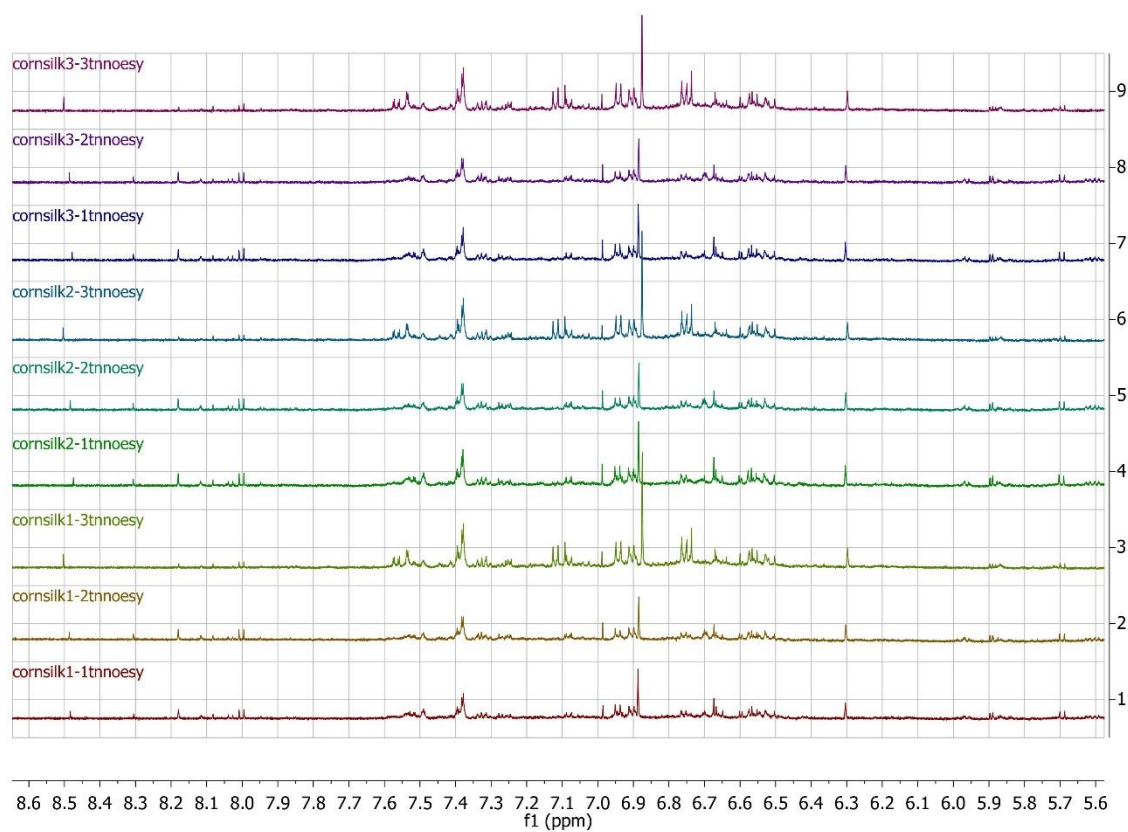
Figure 29. The CS methanol extracts NMR analysis results in the chemicalshift δ range from 5.6ppm to 8.6ppm, where cornsilk 1 is the CS-S sample extracts, cornsilk 2 is the CS-M sample extracts, cornsilk 3 is the CS-MS sample extracts.
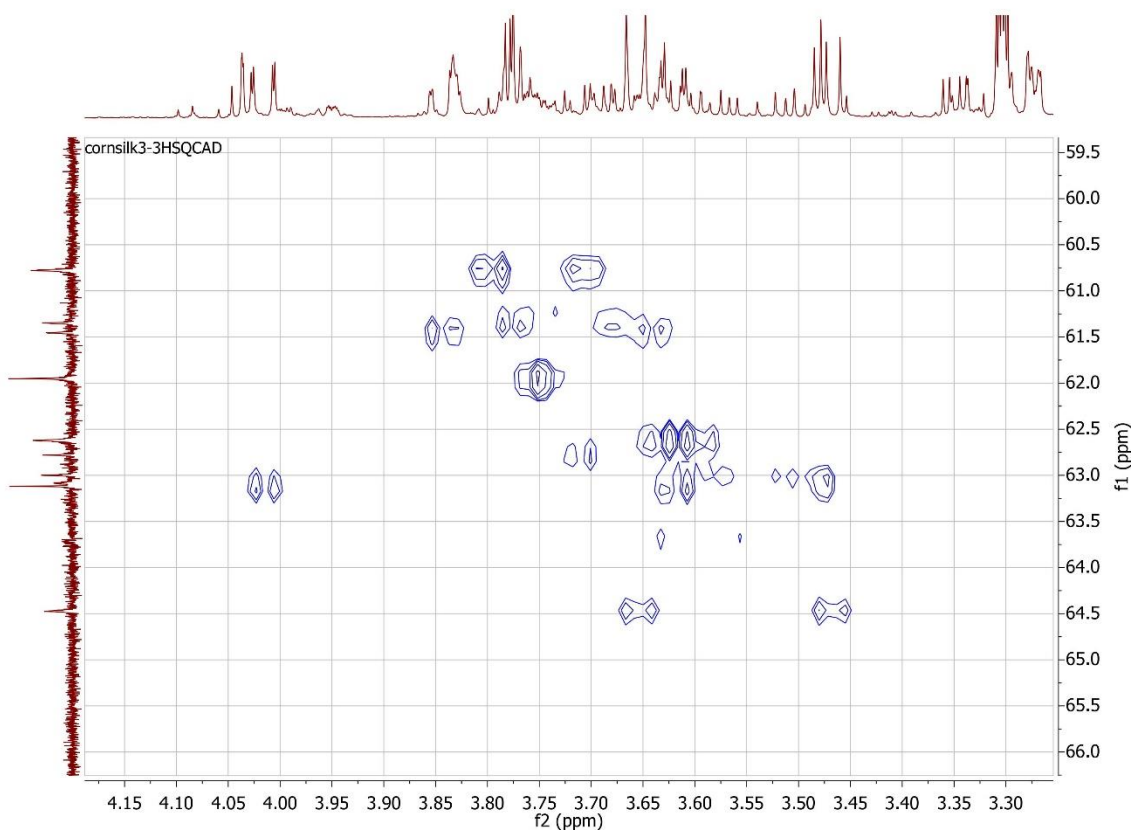
Figure 30. The CS methanol extracts NMR analysis results in the 2D-chemicalshift δ_1 range from 3.25ppm to 4.2ppm and δ_2 range from 66ppm to 59.5ppm, where cornsilk 3 is the CS-MS sample extracts.

3.2.2 FTIR analysis

Table 5 shows the results of FTIR analysis of the extracted CS flavonoids, polysaccharides and steroids, corresponding the result of the afterwards HPLC analysis.

Table 5. CS flavonoids, polysaccharides and steroids FTIR analysis

Functional ingredients	Peak wavenumber (cm^{-1})	Functional groups
Flavonoids	615	CO_2^-
	683	CO_2^-
	879	COH
	1050	NO_3^-
	1090	PO_4^{3-}
	1640	$C=C$

57

	2900	CH$_2$
	2980	CH$_3$
	3380	OH
Polysaccharides	609	CO$_2^-$
	681	CO$_2^-$
	1630	C=C
	3380	OH
Steroids	631	CO$_2^-$
	636	CO$_2^-$
	877	COH
	1040	NO$_3^-$
	1090	PO$_4^{3-}$
	1270	S=O, P=O, CH$_2$, C-N
	1340	NO$_3^-$, NO$_2$
	1390	CH$_3$
	1430	COH, NH$_4^+$,
	1460	CO$_3^{2-}$
	1490	NH$_3^+$
	1660	C=O
	2880	CH$_3$
	2950	CH$_3$
	2970	CH$_3$
	3350	OH

3.2.2 HPLC analysis

As can be seen from Figure 31- 33, the similar elution time vs. intesity curves have shown for CS-S, CS-M and CS-MS methanol extract samples in HPLC analysis in the 60°C， 70°C and 80°C extraction temperatures respectively, indicating the kinds of the determined functional ingredients from CS-S, CS-M and CS-MS in 60°C， 70°C and 80°C extraction temperatures are similar. According to the intesity peaks along with the elution time, the caffeic acid, chlorogenic acid, elagic acid, epicatechin, epigallocatechin, ferrulic acid, hydroxybenzoic_acid, kaempferol, protocatechuic etylester, protocatechuic_acid, rutin, sinapic acid, t-2-hydroxycin.acid_o-coum, trans - cinnamic acid, trans - p - coum acid, vanillic acid and their concentrations were determined, the results and the extraction temperature vs. concentration kinetics and the comparison among CS-S, CS-M and CS-MS samples are as shown from Figure 34 - 49. It is illustrated from Figure 34 - 49 that caffeic acid, epicatechin, ferrulic acid, protocatechuic etylester, protocatechuic_acid, rutin, trans - p - coum acid have the higheat extraction rate in the temperature of 70°C, the rest of the phenolic acids have the higheat extraction yield rate in the temperature of 80°C for the various heat sensitivities of the different phenolic acids. Almost all of the determined phenolic acids contents are significantly coralated to the maturity stages, which is the CS-MS has the highest extracted phenolic acids content, the CS-S has the lowest, except for rutin, which has the highest phenolic acids content for CS-M samples. Therefore, the extraction temperature has the significant influences to the menthol extraction rate of the CS phenolic acids and the maturity stage has the significant influences to the CS phenolic acids content.
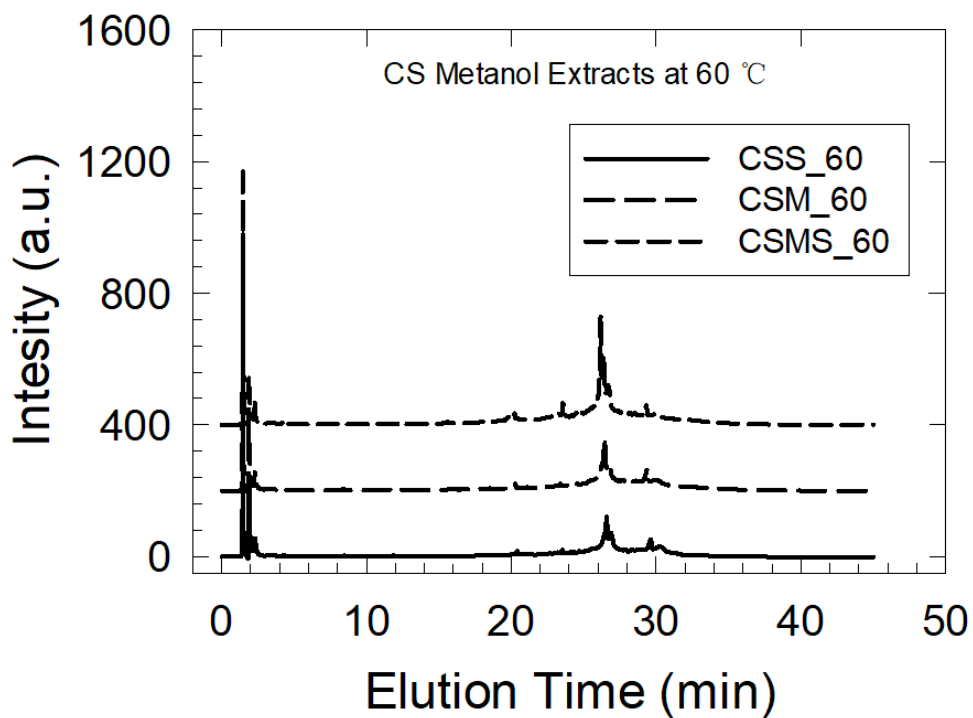
Figure 31. CS-S, CS-M, CS-MS 60°C methanol extracts HPLC analysis
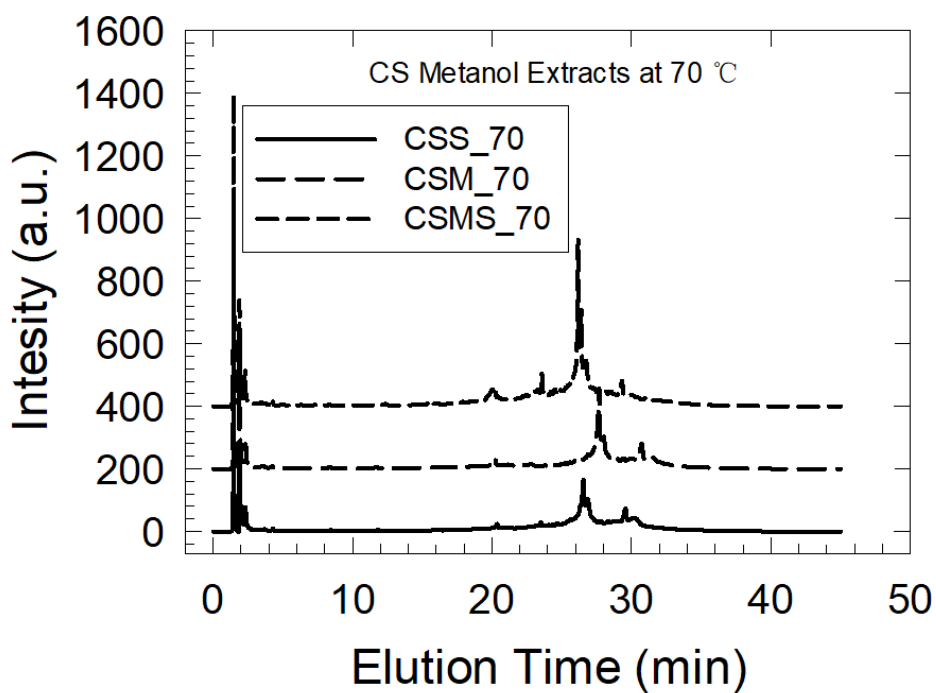
Figure 32. CS-S, CS-M, CS-MS 70°C methanol extracts HPLC analysis
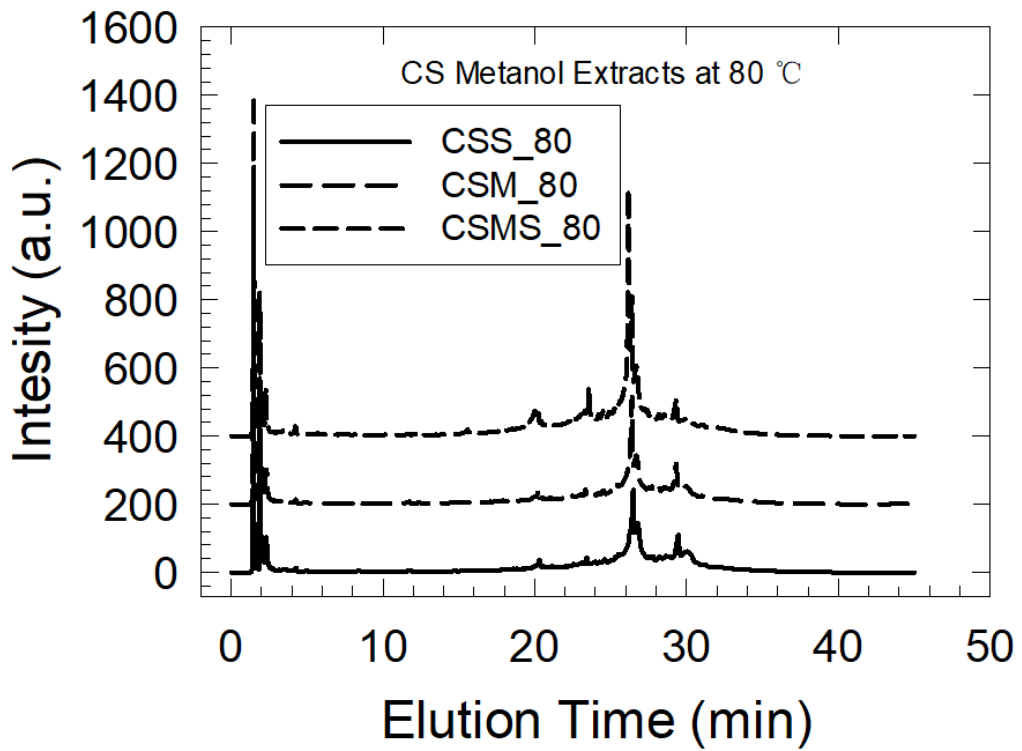
Figure 33. CS-S, CS-M, CS-MS 80℃ methanol extracts HPLC analysis
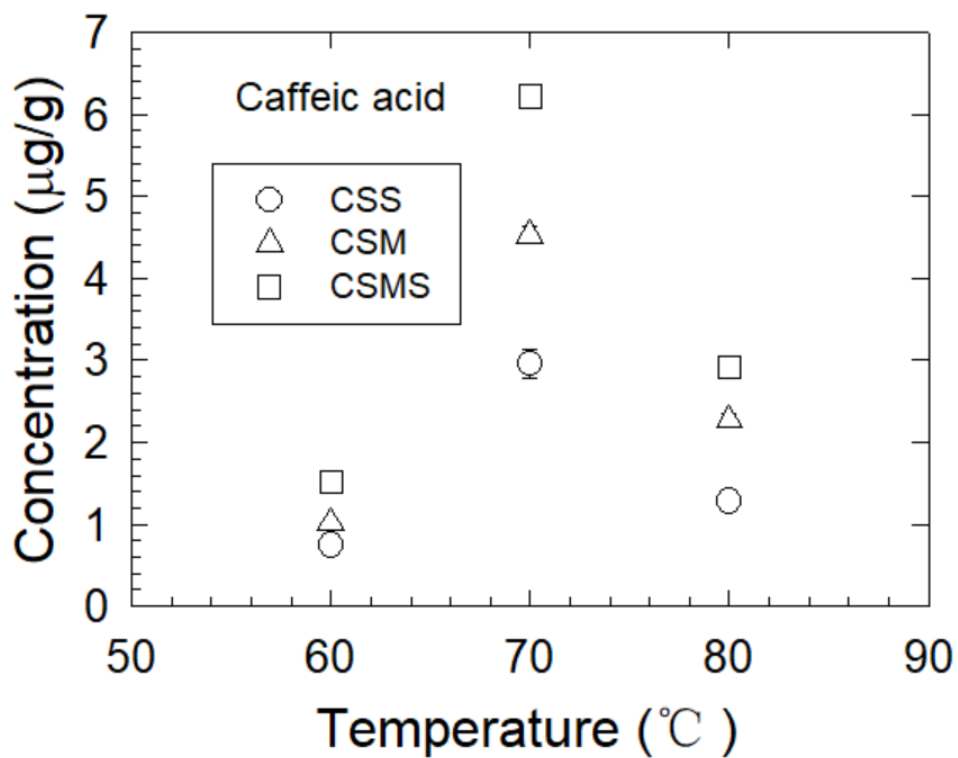
Figure 34. Temperature vs. concentration CS-S, CS-M, CS-MS caffeic acid methanol extraction kinetics in accordance with the HPLC analysis.
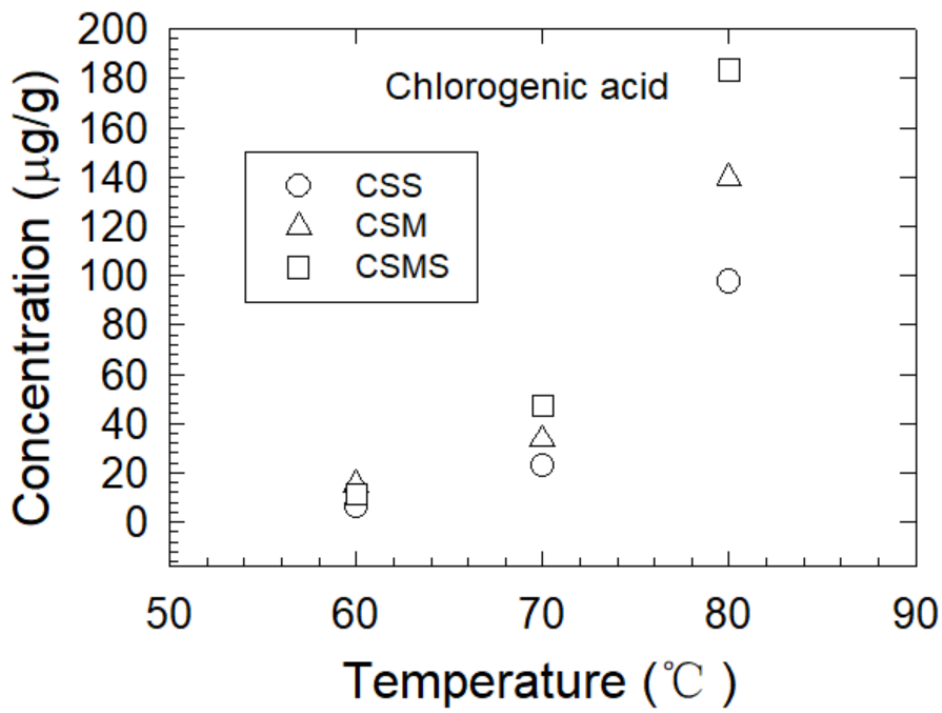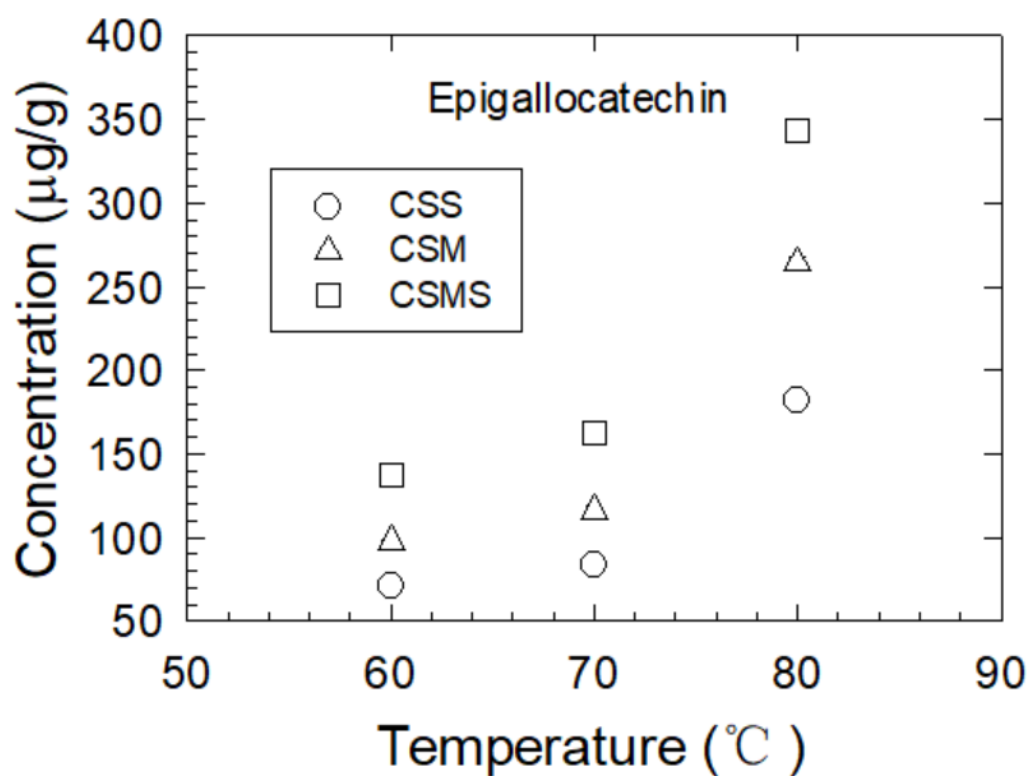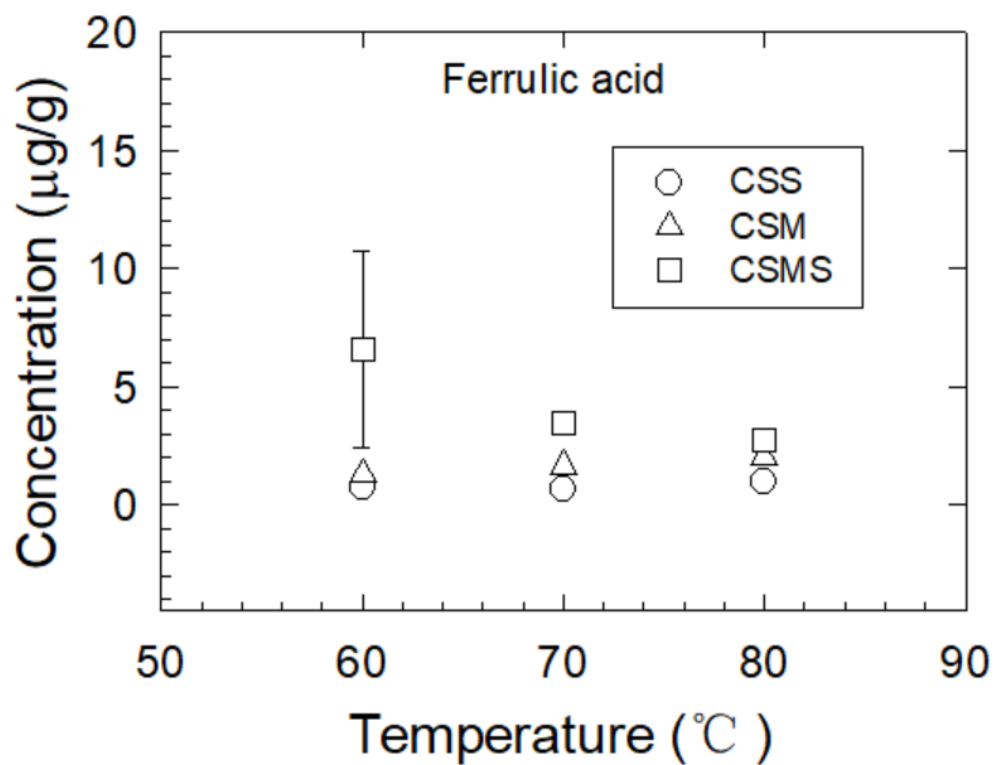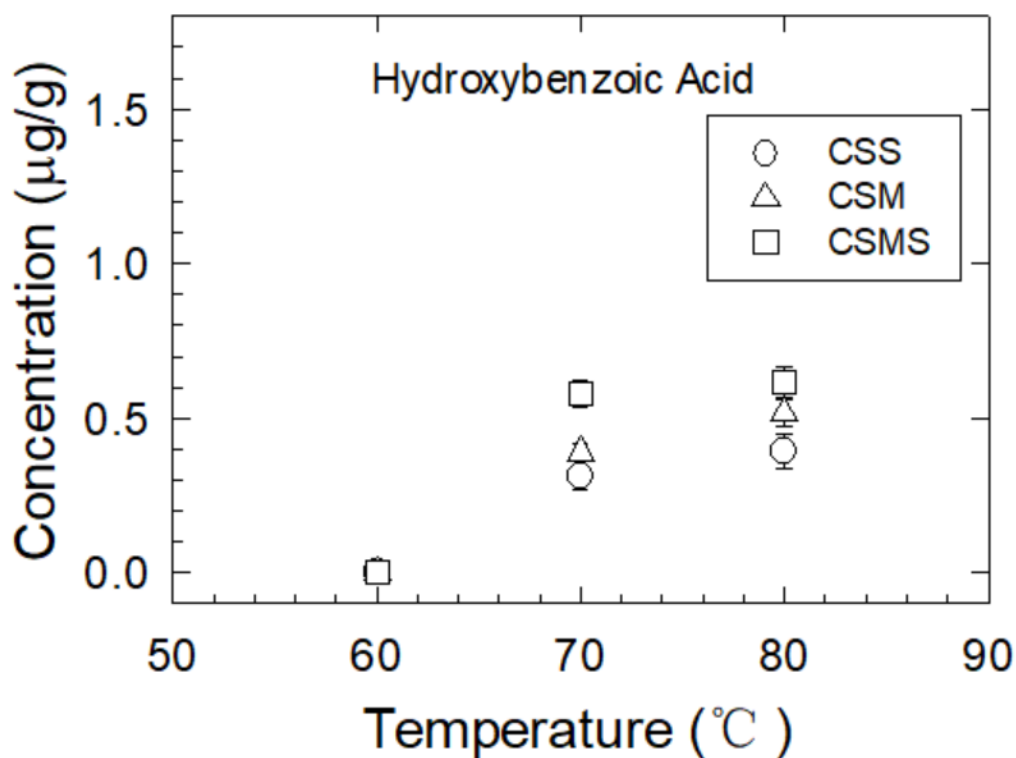
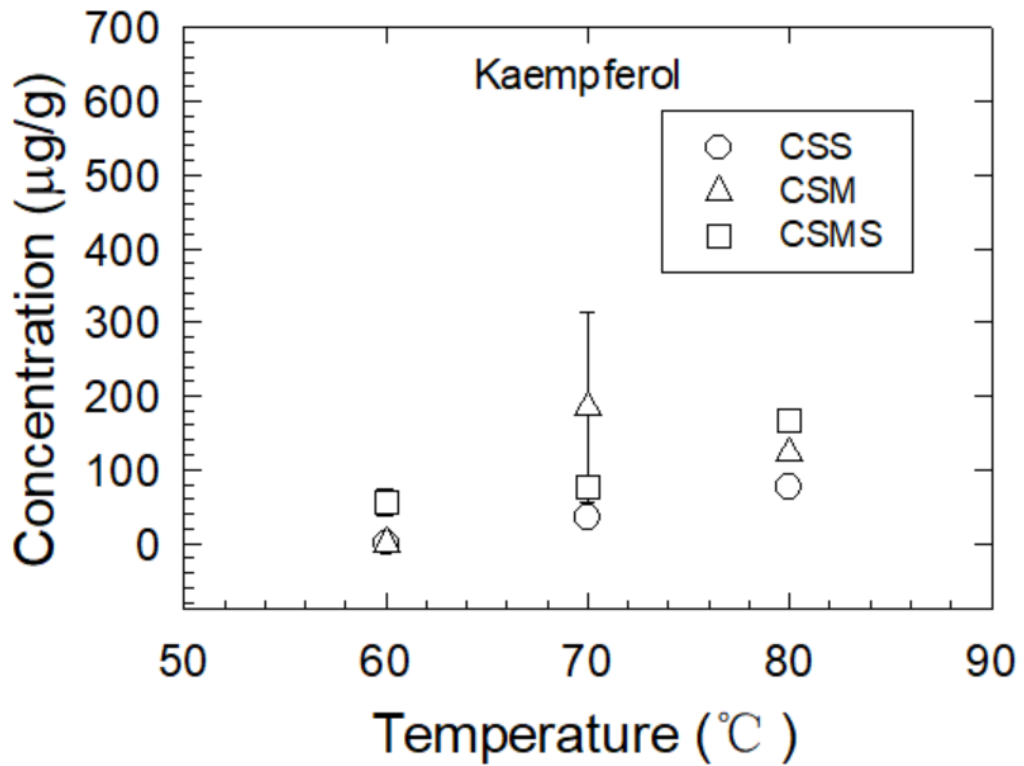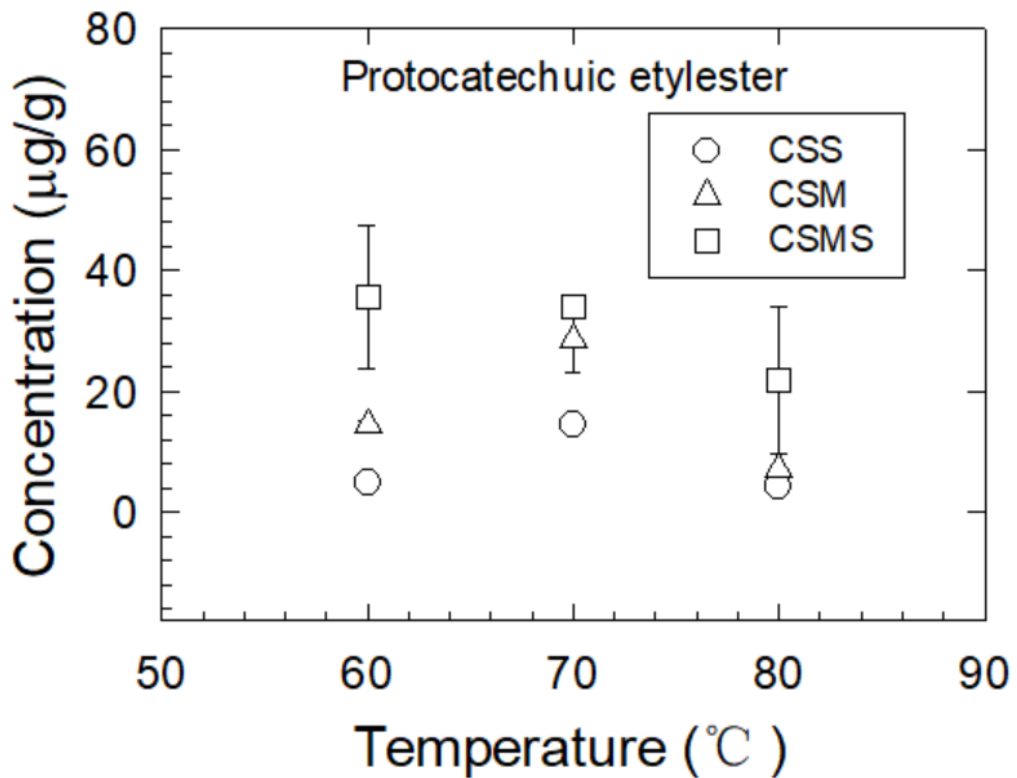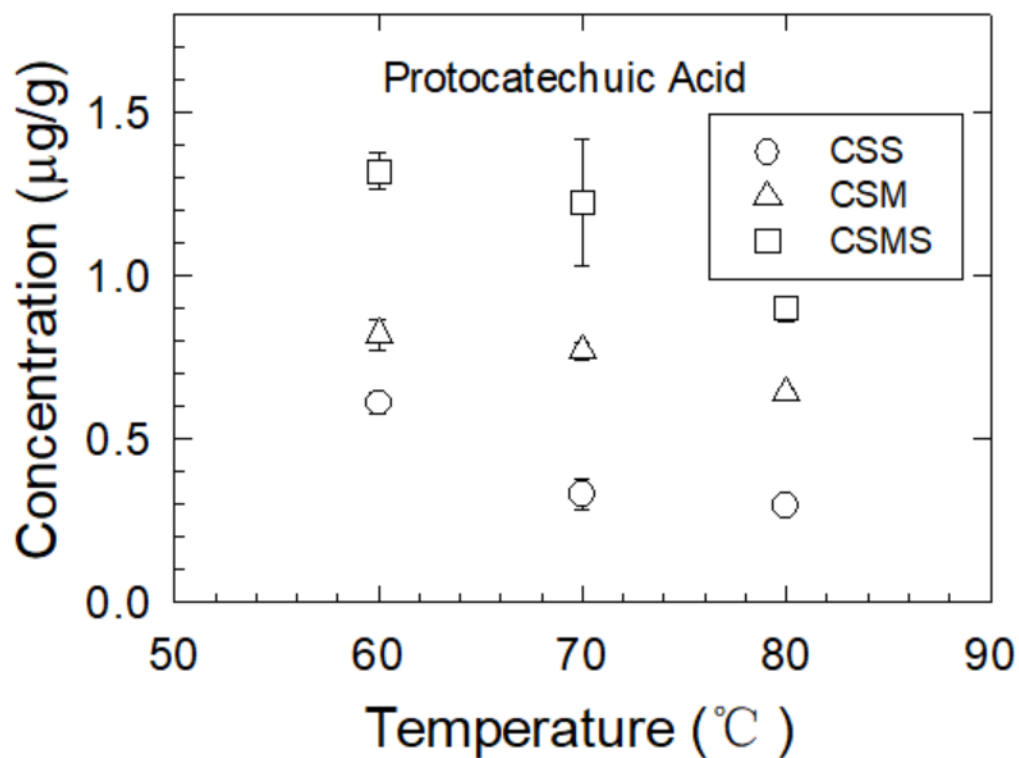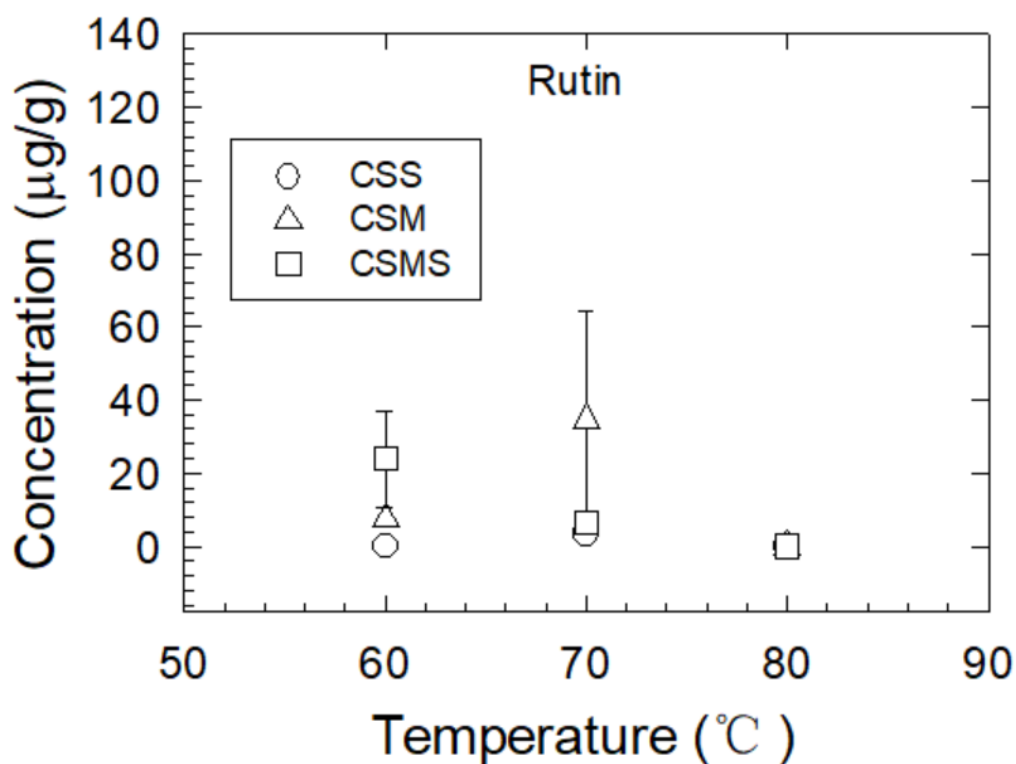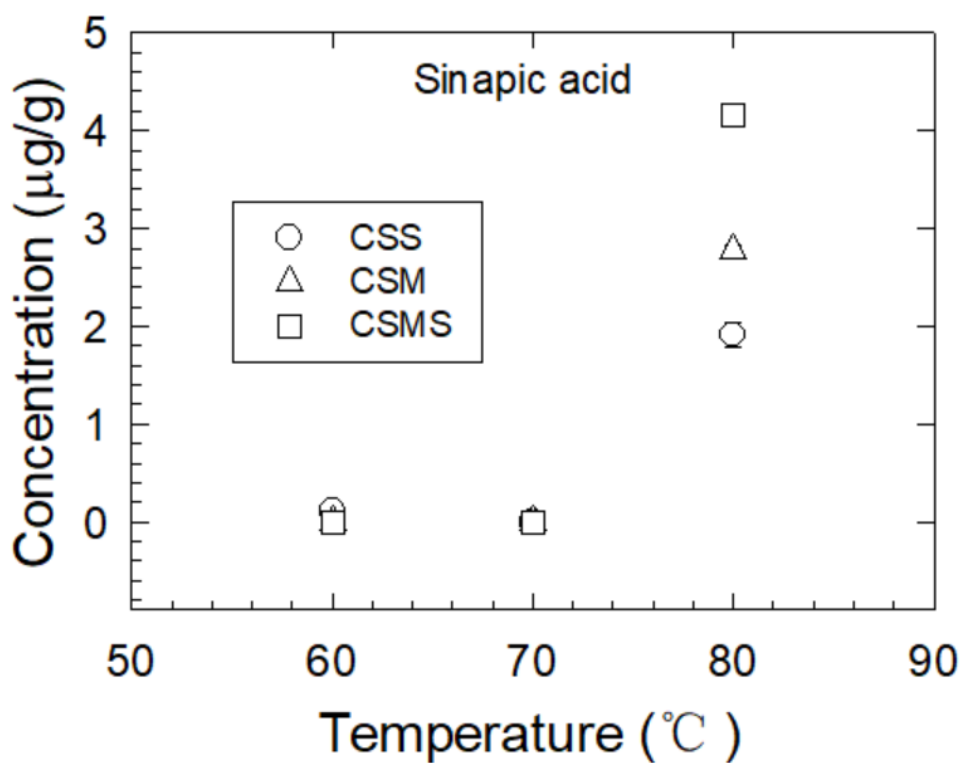*Figure 35. Temperature vs. concentration CS-S, CS-M, CS-MS chlorogenic acid methanol extraction kinetics in accordance with the HPLC analysis.*
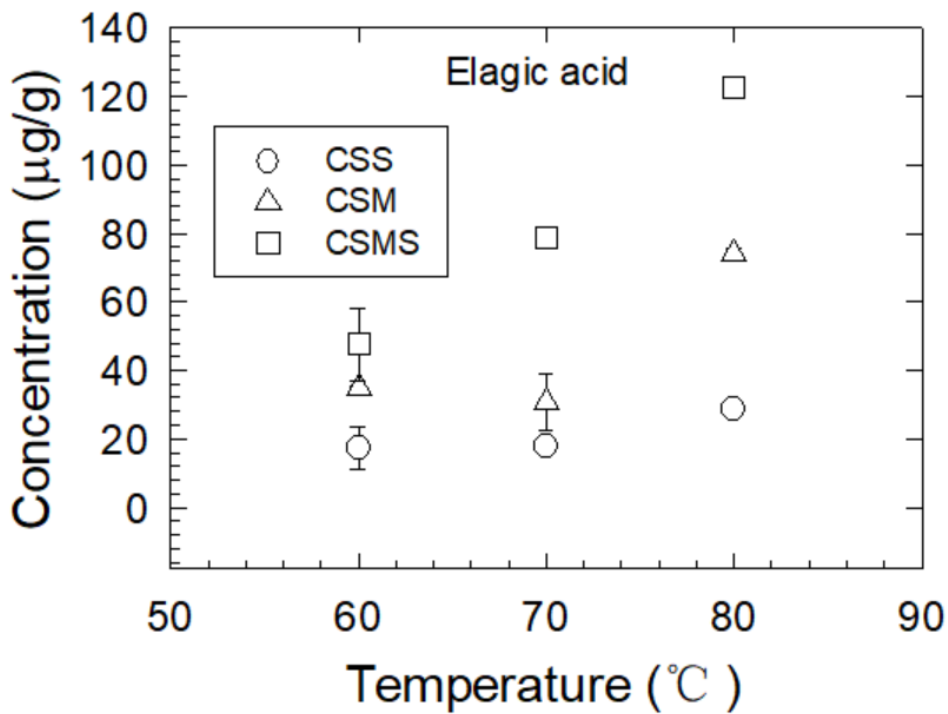
Figure 36. Temperature vs. concentration CS-S, CS-M, CS-MS elagic acid methanol extraction kinetics in accordance with the HPLC analysis.
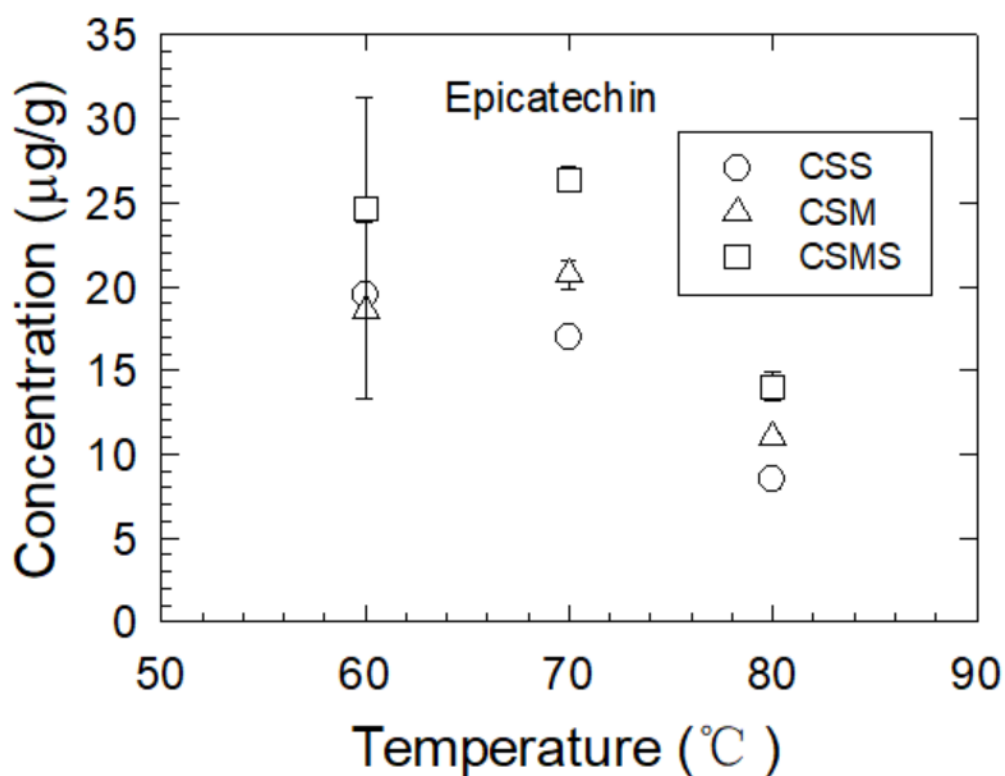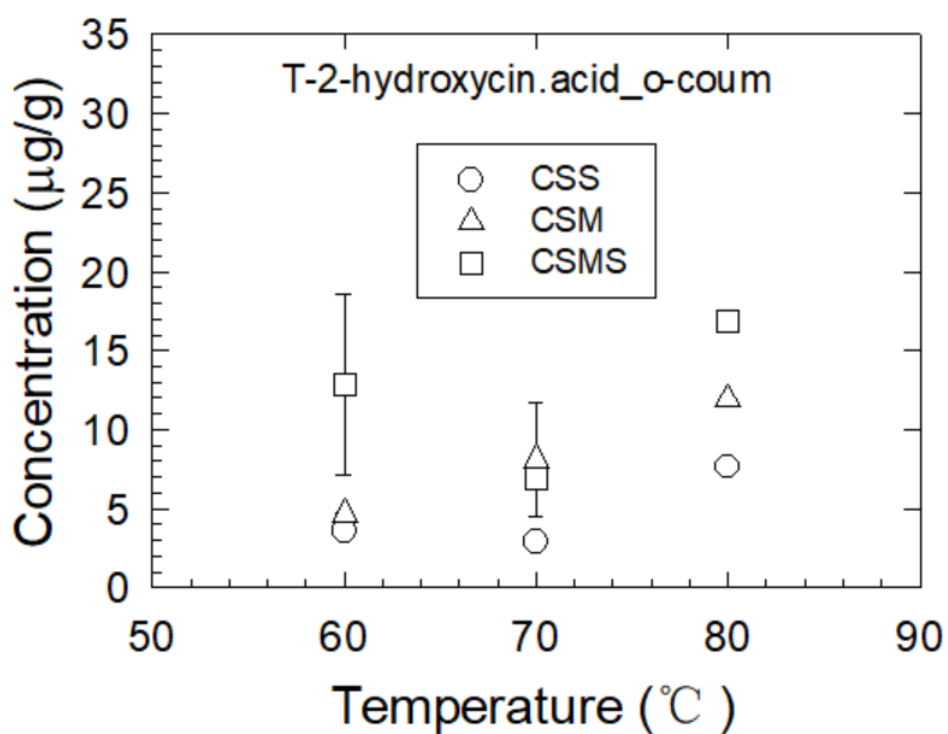
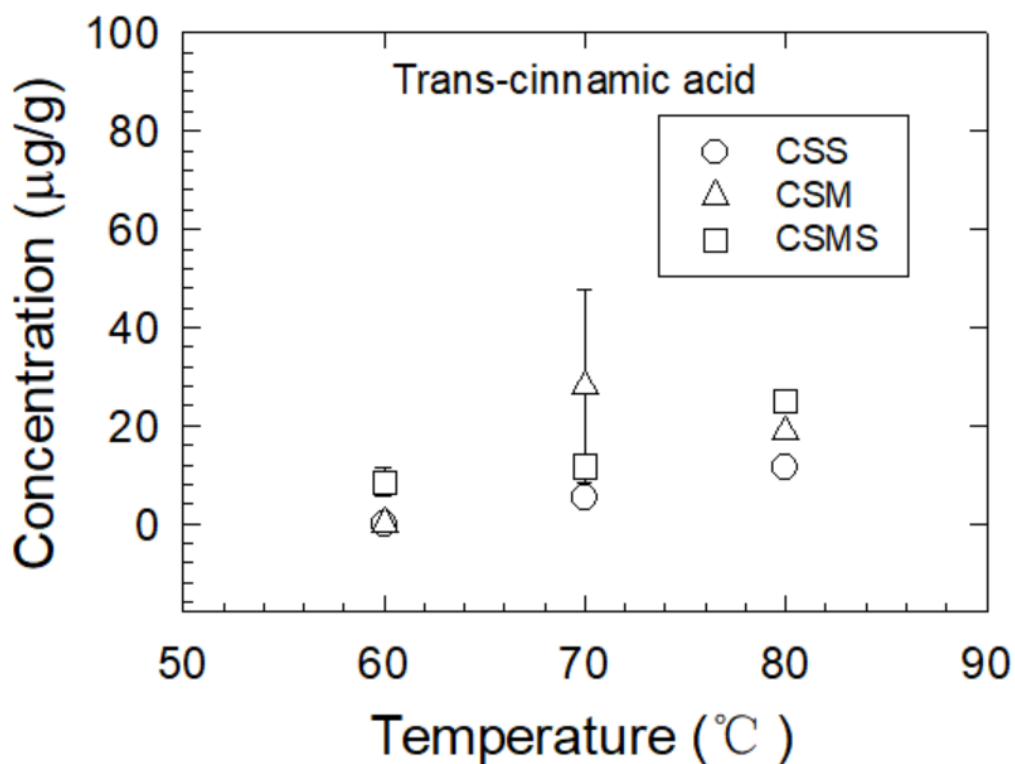*Figure 37. Temperature vs. concentration CS-S, CS-M, CS-MS epicatechin methanol extraction kinetics in accordance with the HPLC analysis.*

Figure 38. Temperature vs. concentration CS-S, CS-M, CS-MS epigallocatechin methanol extraction kinetics in accordance with the HPLC analysis.

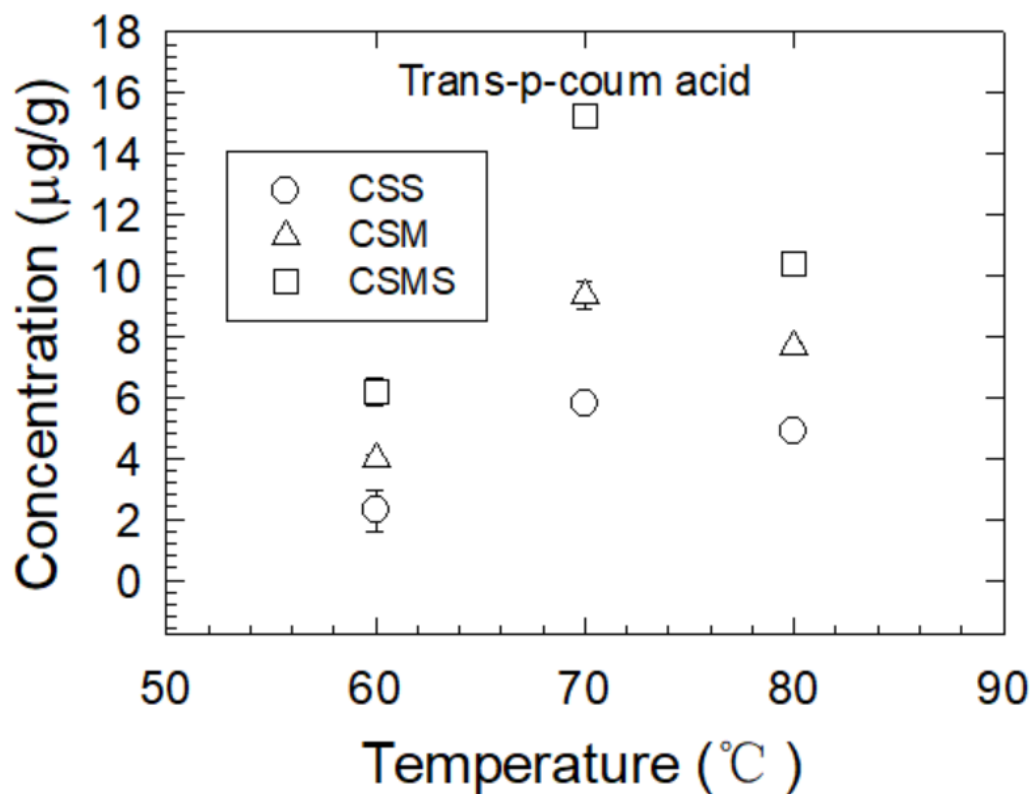*Figure 39. Temperature vs. concentration CS-S, CS-M, CS-MS ferrulic acid methanol extraction kinetics in accordance with the HPLC analysis.*

Figure 40. Temperature vs. concentration CS-S, CS-M, CS-MS hydroxybenzoic_acid methanol extraction kinetics in accordance with the HPLC analysis.

Figure 41. Temperature vs. concentration CS-S, CS-M, CS-MS kaempferol methanol extraction kinetics in accordance with the HPLC analysis.
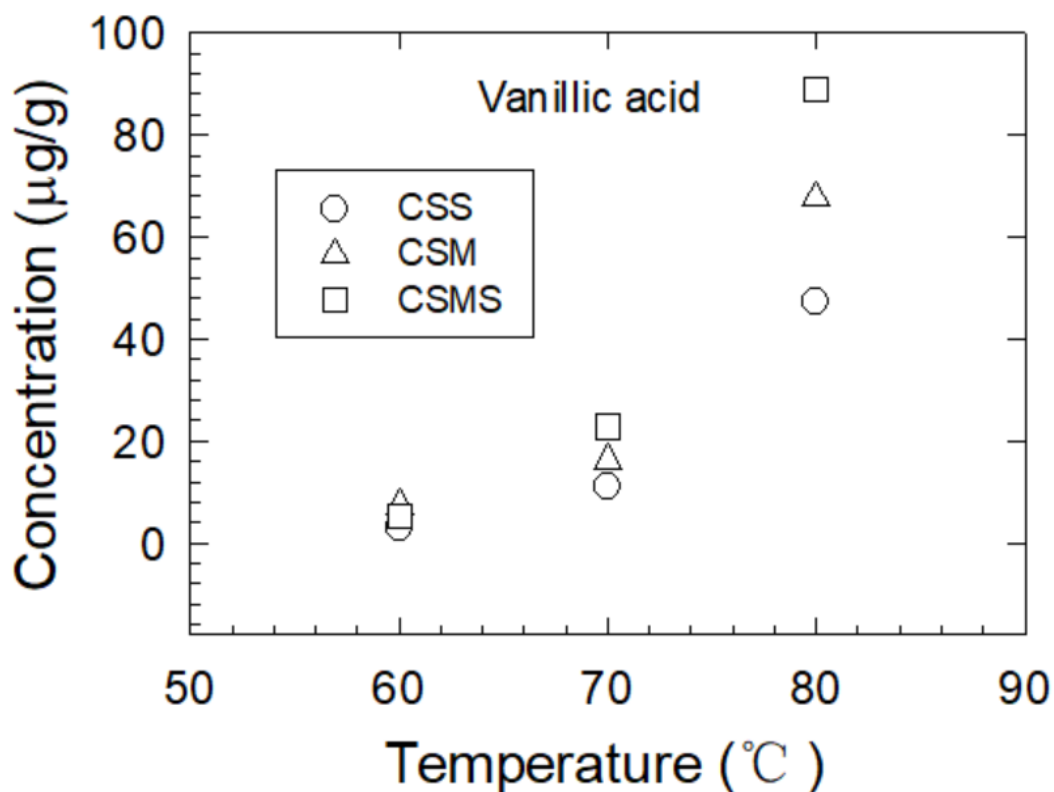

Figure 42. Temperature vs. concentration CS-S, CS-M, CS-MS protocatechuic etylester methanol extraction kinetics in accordance with the HPLC analysis.

Figure 43. Temperature vs. concentration CS-S, CS-M, CS-MS protocatechuic_acid methanol extraction kinetics in accordance with the HPLC analysis.

Figure 44. Temperature vs. concentration CS-S, CS-M, CS-MS rutin methanol extraction kinetics in accordance with the HPLC analysis.

66

Figure 45. Temperature vs. concentration CS-S, CS-M, CS-MS sinapic acid methanol extraction kinetics in accordance with the HPLC analysis.

Figure 46. Temperature vs. concentration CS-S, CS-M, CS-MS
t - 2 - hydroxycin.acid_o - coum methanol extraction kinetics in accordance with the HPLC analysis.

Figure 47. Temperature vs. concentration CS-S, CS-M, CS-MS trans-cinnamic acid methanol extraction kinetics in accordance with the HPLC analysis.

Figure 48. Temperature vs. concentration CS-S, CS-M, CS-MS trans-p-coum acid methanol extraction kinetics in accordance with the HPLC analysis.

Figure 49. Temperature vs. concentration CS-S, CS-M, CS-MS vanillic acid methanol extraction kinetics in accordance with the HPLC analysis.

3.3 Vitro Enzyme Inhibition Test

3.3.1 Thrombin inhibition activity test

Figure 50 shows the similar trends of thrombin inhibition activity kinetics for CS flavonoids, polysaccharides and steroids, the inhibition rates are all positively coorelated to the reaction time, where the polysaccharides have the highest thrombin inhibition activity than the CS polysaccharides and steroids extracts, meanwhile, the steroids have the lowest. It is notable that from 0 – 1 min, the inhibition rate increased sheerly and after 1 min, the trend became subdued for all of the CS flavonoids, steroids and polysaccharides samples. The result indicates the CS polysaccharides have the best effect of anti-coagulation among the three CS extracts and CS steroids have the worst.
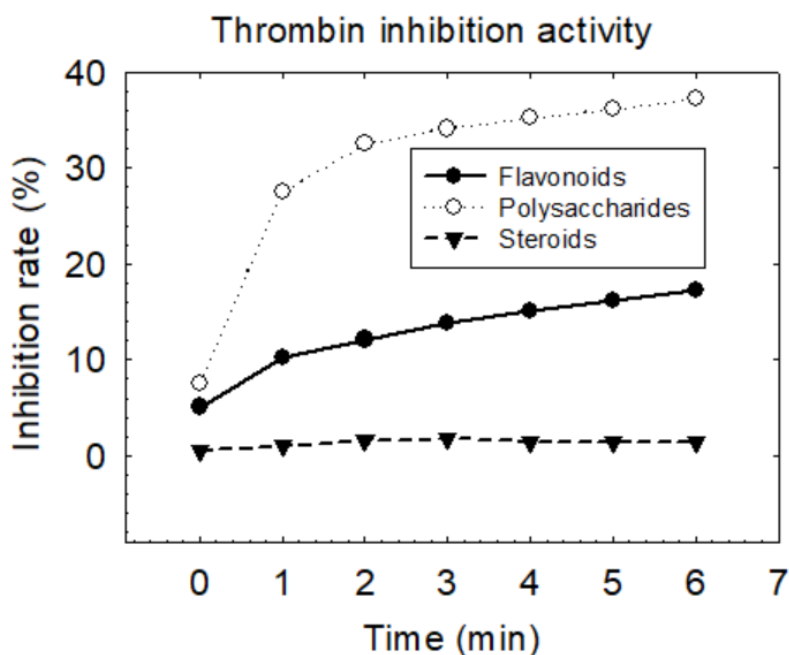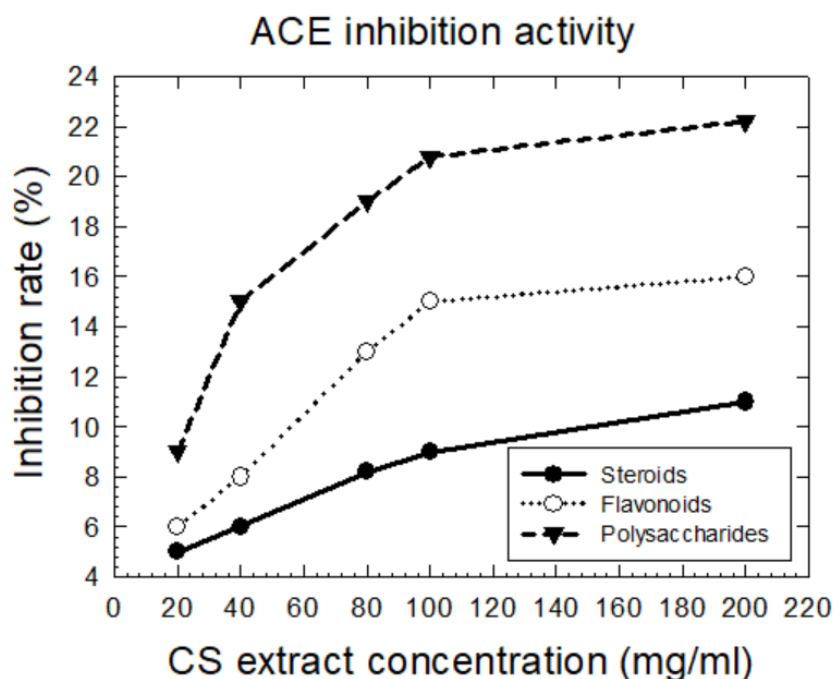
Figure 50. CS flavonoids, polysaccharides and steroids thrombin inhibition activity kinetics

3.3.2 ACE inhibition activity test

Figure 51 shows the similar trends of ACE inhibition activity kinetics for CS flavonoids, polysaccharides and steroids, the inhibition rates are all positively coorelated to the CS extract concentrations, where the polysaccharides have the highest ACE inhibition activity than the CS polysaccharides and steroids extracts, meanwhile, the steroids have the lowest. It is notable that from 20 – 100 mg/mL CS extract concentration, the inhibition rate increased sheerly and after 100 mg/mL, the trend became subdued for all of the CS flavonoids, steroids and polysaccharides samples. The result indicates the CS polysaccharides have the best effect of anti- hypertension among the three CS extracts and CS steroids have the worest.
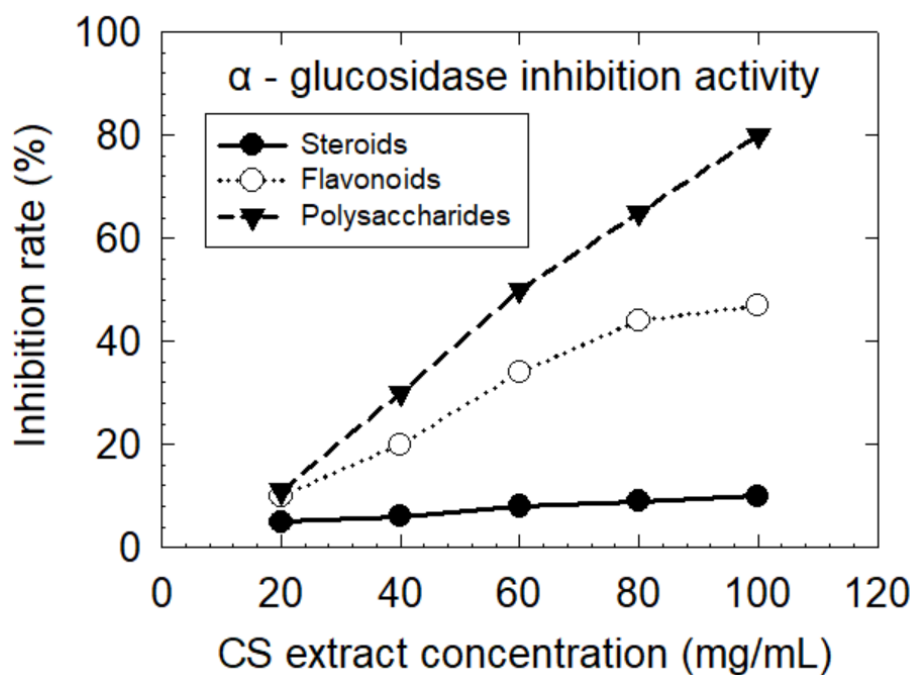
Figure 51. CS flavonoids, polysaccharides and steroids ACE inhibition activity kinetics

3.3.3 α- glucosidase inhibition activity test

Figure 52 shows the similar trends of α- glucosidase inhibition activity kinetics for CS flavonoids, polysaccharides and steroids, the inhibition rates are all positively coorelated to the CS extract concentrations, where the polysaccharides have the highest α- glucosidase inhibition activity than the CS polysaccharides and steroids extracts, meanwhile, the steroids have the lowest. It is notable that from 20 – 80 mg/mL CS extract concentration, the inhibition rate increased sheerly and after 80 mg/mL, the trend became subdued for the CS flavonoids sample. The result indicates the CS polysaccharides have the best effect of anti - diabetes among the three CS extracts and CS steroids have the worest.
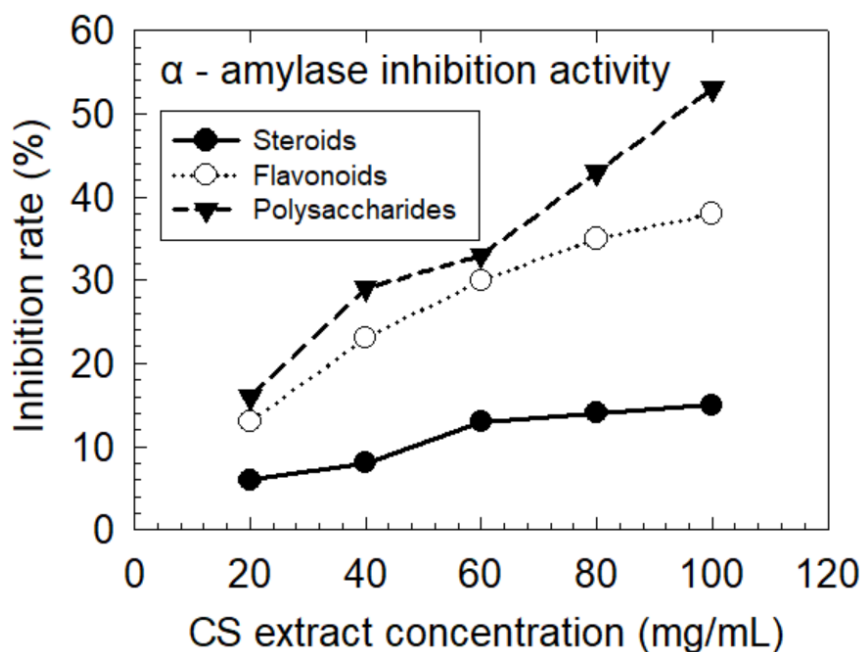
71

Figure 52. CS flavonoids, polysaccharides and steroids α- glucosidase inhibition activity kinetics

3.4.4 α- amylase inhibition activity test

Figure 53 shows the similar trends of α- amylase inhibition activity kinetics for CS flavonoids, polysaccharides and steroids, the inhibition rates are all positively coorelated to the CS extract concentrations, where the polysaccharides have the highest α- amylase inhibition activity than the CS polysaccharides and steroids extracts, meanwhile, the steroids have the lowest. The result indicates the CS polysaccharides have the best effect of anti - diabetes among the three CS extracts and CS steroids have the worest.

Figure 53. CS flavonoids, polysaccharides and steroids α- amylase inhibition activity kinetics

3.4.5 XOD inhibition activity test

Figure 54 shows the similar trends of XOD inhibition activity kinetics for CS flavonoids, polysaccharides and steroids, the inhibition rates are all positively coorelated to the CS extract concentrations, where the flavonoids have the highest XOD inhibition activity than the CS polysaccharides and steroids extracts, meanwhile, the steroids have the lowest. The result indicates the CS flavonoids have the best effect of anti - gout among the three CS extracts and CS steroids have the worest.
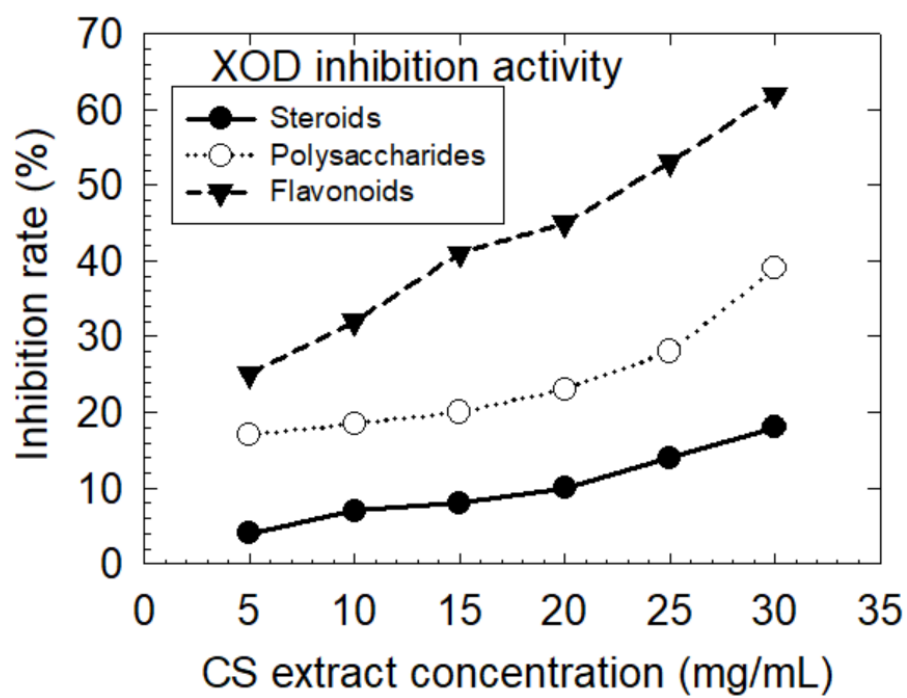
Figure 54. CS flavonoids, polysaccharides and steroids XOD inhibition activity kinetics

CONCLUSION

The current work researched about the three different maturity stages (silking stage, milky stage and mature stage) corn silk fiber and powder physicochemical properties and corn silk extracts biochemical properties, applied the technologies of UV-VIS, HPLC, NMR, FTIR and Fluorescence excitation−emission mapping to extract, determine the corn silk flavonoids, polysaccharides and steroids and optimized the extraction methods, the phenolic acids such as caffeic acid, chlorogenic acid, elagic acid, epicatechin, epigallocatechin, ferrulic acid, hydroxybenzoic_acid, kaempferol, protocatechuic etylester, protocatechuic_acid, rutin, sinapic acid, t-2-hydroxycin.acid_o-coum, trans - cinnamic acid, trans - p - coum acid, vanillic acid and their concentrations were determined. It was applied the technologies of TG/DTA and SEM to analyze and research the corn silk fiber and powder thermol properties and microstructures, applied the technologies of EPR, DPPH and ABTS free - radicals scavenging capability test, ferricion and copper ion anti - oxident capability test and vitro enzyme inhibition activity test including the enzymes of α - glucosidase and α - amylase (anti - diabetes), thrombin (anti - coagulation), angiotensin converting enzyme (ACE) (anti - hypertension) and xanthine oxidase (XOD) (anti-gout) to analyze the corn silk extracts biochemical properties, the results show that the CS maturity is significantly corrected to the radical scavenging capability, where the CS-MS extracts have the strongest radical scavenging capability, then CS-S medium, CS - M the weakest, furthermore, the CS polysaccharides have the best anti-diabetes, anti-coagulation and anti-hypertension effect, CS flavonoids have the best anti-gout effect, meanwhile, the CS steroids showed the worst effect for all of the anti-diabetes, anti-coagulation, anti-hypertension and anti-gout vitro enzymatic inhibition tests.

It can assume that the above research will play an irreplaceable role in analyzing the physicochemical and biochemical properties of botanic materials in the areas of food production, pharmacy, veterinary, animal feed and healthcare.

BENEFITS OF THE OBTAINED RESULTS FOR THE STUDY SUBJECT FOOD TECHNOLOGY

Based on the above mentioned results of the study performed one can expect the following benefits for the study subject as follows:

1. There were obtained extraction kinetics data of medically valuable substances, such as flavonoids, polysaccharides and plant steroids suitable as the starting parameters for the optimization of the extraction procedures in semi-pilot scale production units.
2. There was confirmed high radical scavenger activity of all above mentioned extracted substances by means of Electron Paramagnetic Resonance and DPPA and ABTS radical inhibition experiments.
3. There were confirmed high inhibition activities of extracted substances from the corn silk material in vitro to the enzymes such as α - glucosidase and α - amylase (anti - diabetes), thrombin (anti - coagulation), angiotensin converting enzyme (ACE) (anti - hypertension) and xanthine oxidase (XOD) (anti-gout) thus indicating its positive health effect.
4. There were determined 16 phenolic substances such as α - glucosidase and α - amylase (anti - diabetes), thrombin (anti - coagulation), angiotensin converting enzyme (ACE) (anti - hypertension) and xanthine oxidase (XOD) (anti-gout) in extracts and their extraction kinetics were quantified.
5. Obtained data represent complex study of both nutrition as well as pharmaceutical industry interesting substances suitable for application in special food products.

REFERENCES

Angelovicová, M., & Semivanová, M. (2013). The effect of iodine in production of broiler chickens and selected quality indicators of breast muscles. *Potravinarstvo, 7*(1), 111-119. doi:10.5219/297

Bakirtzi, C., Triantafyllidou, K., & Makris, D. P. (2016). Novel lactic acid-based natural deep eutectic solvents: Efficiency in the ultrasound-assisted extraction of antioxidant polyphenols from common native greek medicinal plants. *Journal of Applied Research on Medicinal and Aromatic Plants, 3*(3), 120-127. doi:http://dx.doi.org/10.1016/j.jarmap.2016.03.003

Bhattacharya, M., Srivastav, P. P., & Mishra, H. N. (2014). Optimization of process variables for supercritical fluid extraction of ergothioneine and polyphenols from pleurotus ostreatus and correlation to free-radical scavenging activity. *The Journal of Supercritical Fluids, 95*, 51-59. doi:http://dx.doi.org/10.1016/j.supflu.2014.07.031

C., S. K., M., S., & K., R. (2016). Microwave-assisted extraction of polysaccharides from cyphomandra betacea and its biological activities. *International Journal of Biological Macromolecules, 92*, 682-693. doi:http://dx.doi.org/10.1016/j.ijbiomac.2016.07.062

Chen, S., Chen, H., Tian, J., Wang, J., Wang, Y., & Xing, L. (2014). Enzymolysis-ultrasonic assisted extraction, chemical characteristics and bioactivities of polysaccharides from corn silk. *Carbohydrate Polymers, 101*, 332-341. doi:http://dx.doi.org/10.1016/j.carbpol.2013.09.046

Chen, S., Chen, H., Tian, J., Wang, Y., Xing, L., & Wang, J. (2013). Chemical modification, antioxidant and α-amylase inhibitory activities of corn silk polysaccharides. *Carbohydrate Polymers, 98*(1), 428-437. doi:http://dx.doi.org/10.1016/j.carbpol.2013.06.011

Choi, D. J., Kim, S., Choi, J. W., & Park, Y. I. (2014). Neuroprotective effects of corn silk maysin via inhibition of H2O2-induced apoptotic cell death in SK-N-MC cells. *Life Sciences, 109*(1), 57-64. doi:http://dx.doi.org/10.1016/j.lfs.2014.05.020

Dankowska, A. (2016). In Downey G. (Ed.), *5 - advances in fluorescence emission spectroscopy for food authenticity testing* Woodhead Publishing. doi:https://doi.org/10.1016/B978-0-08-100220-9.00005-9

Deng, C., Huang, T., Jiang, Z., Lv, X., Liu, L., Chen, J., & Du, G. (2019). In Singh S. P., Pandey A., Du G. and Kumar S.(Eds.), *Chapter 7 - enzyme engineering and industrial bioprocess* Elsevier. doi:https://doi.org/10.1016/B978-0-444-64085-7.00007-1

Ebrahimzadeh, M. A., Pourmorad, F., & Hafezi, S. (2008). Antioxidant activities of iranian corn silk. *Turkish Journal of Biology, 32*(1), 43-49.

Firdaous, L., Fertin, B., Khelissa, O., Dhainaut, M., Nedjar, N., Chataigné, G., . . . Dhulster, P. (2017). Adsorptive removal of polyphenols from an alfalfa white proteins concentrate: Adsorbent screening, adsorption kinetics and

equilibrium study. *Separation and Purification Technology, 178*, 29-39. doi:http://dx.doi.org/10.1016/j.seppur.2017.01.009

Hasanudin, K., Hashim, P., & Mustafa, S. (2012). Corn silk (stigma maydis) in healthcare: A phytochemical and pharmacological review. *Molecules, 17*(8), 9697-9715. doi:10.3390/molecules17089697

Hossain, M. B., Tiwari, B. K., Gangopadhyay, N., O'Donnell, C. P., Brunton, N. P., & Rai, D. K. (2014). *Ultrasonic extraction of steroidal alkaloids from potato peel waste* doi:https://doi.org/10.1016/j.ultsonch.2014.01.023

Ivanišová, E., Rajtar, M., Francáková, H., Tokár, M., Dráb, Š, Kluz, M., & Kacániová, M. (2017). Characterization of bioactive compounds from monascus purpureus fermented different cereal substrates. *Potravinarstvo Slovak Journal of Food Sciences, 11*(1), 183-189. doi:10.5219/722

Jing, S., wang, S., Li, Q., Zheng, L., Yue, L., Fan, S., & Tao, G. (2016). Dynamic high pressure microfluidization-assisted extraction and bioactivities of cyperus esculentus (C. esculentus L.) leaves flavonoids. *Food Chemistry, 192*, 319-327. doi:http://dx.doi.org/10.1016/j.foodchem.2015.06.097

Kafle, B. P. (2020). In Kafle B. P. (Ed.), *Chapter 5 - application of UV–VIS spectrophotometry for chemical analysis* Elsevier. doi:https://doi.org/10.1016/B978-0-12-814866-2.00005-1

Kato-Schwartz, C. G., Corrêa, R. C. G., de Souza Lima, D., de Sá-Nakanishi, A. B., de Almeida Gonçalves, G., Seixas, F. A. V., . . . Peralta, R. M. (2020). *Potential anti-diabetic properties of merlot grape pomace extract: An in vitro, in silico and in vivo study of α-amylase and α-glucosidase inhibition* doi:https://doi.org/10.1016/j.foodres.2020.109462

Ko, M., Kwon, H., & Chung, M. (2016). Pilot-scale subcritical water extraction of flavonoids from satsuma mandarin (citrus unshiu markovich) peel. *Innovative Food Science & Emerging Technologies, 38, Part A*, 175-181. doi:http://dx.doi.org/10.1016/j.ifset.2016.10.008

Krejzová, E., Bittová, M., Krácmar, S., Vojtíšková, P., Kubán, V., & Golian, J. (2017). Effect of thermal treatment on rutin content in selected buckwheat products using calcium as an internal tracer. *Potravinarstvo Slovak Journal of Food Sciences, 11*(1), 679-684. doi:10.5219/853

Kuchtová, V., Minarovicová, L., Kohajdová, Z., & Karovicová, J. (2016). Effect of wheat and corn germs addition on the physical properties and sensory qualityof crackers. *Potravinarstvo, 10*(1), 543-549. doi:10.5219/598

Larina, L. I. (2019). *Organosilicon azoles: Structure, silylotropy and NMR spectroscopy* Academic Press. doi:https://doi.org/10.1016/bs.aihch.2019.08.001

Lee, J., Lee, S., Kim, S., Choi, J. W., Seo, J. Y., Choi, D. J., & Park, Y. I. (2014). Corn silk maysin induces apoptotic cell death in PC-3 prostate cancer cells via mitochondria-dependent pathway. *Life Sciences, 119*(1–2), 47-55. doi:http://dx.doi.org/10.1016/j.lfs.2014.10.012

Li, Y., Kang, X., Li, Q., Shi, C., Lian, Y., Yuan, E., . . . Ren, J. (2018). *Anti-hyperuricemic peptides derived from bonito hydrolysates based on in vivo*

hyperuricemic model and in vitro xanthine oxidase inhibitory activity doi:https://doi.org/10.1016/j.peptides.2018.08.001

Liu, J., Lin, S., Wang, Z., Wang, C., Wang, E., Zhang, Y., & Liu, J. (2011). Supercritical fluid extraction of flavonoids from maydis stigma and its nitrite-scavenging ability. *Food and Bioproducts Processing, 89*(4), 333-339. doi:http://dx.doi.org/10.1016/j.fbp.2010.08.004

Liu, J., Wang, C., Wang, Z., Zhang, C., Lu, S., & Liu, J. (2011). The antioxidant and free-radical scavenging activities of extract and fractions from corn silk (zea mays L.) and related flavone glycosides. *Food Chemistry, 126*(1), 261-269. doi:http://dx.doi.org/10.1016/j.foodchem.2010.11.014

Liu, Q., Lv, C., Yang, Y., He, F., & Ling, L. (2005). *Study on the pyrolysis of wood-derived rayon fiber by thermogravimetry–mass spectrometry* doi:https://doi.org/10.1016/j.molstruc.2004.01.016

Lozano-Sánchez, J., Borrás-Linares, I., Sass-Kiss, A., & Segura-Carretero, A. (2018). In Sun D. (Ed.), *Chapter 13 - chromatographic technique: High-performance liquid chromatography (HPLC)* Academic Press. doi:https://doi.org/10.1016/B978-0-12-814264-6.00013-X

Macanga, J., Popelka, P., Koréneková, B., Maskalová, I., Klempová, T., Feckaninová, A., . . . Marcincák, S. (2017). Effect of feeding of prefermented bioproduct containing gamma-linolenic acid and beta-carotene on selected parameters of broiler chicken meat quality. *Potravinarstvo Slovak Journal of Food Sciences, 11*(1), 466-471. doi:10.5219/781

Mahmoudi, M., & Ehteshami, S. (2010). *P.2.d.002 antidepressant activity of iranian corn silk* doi:https://doi.org/10.1016/S0924-977X(10)70556-3 "

Maksimović, Z. A., & Kovačević, N. (2003). Preliminary assay on the antioxidative activity of maydis stigma extracts. *Fitoterapia, 74*(1–2), 144-147. doi:http://dx.doi.org/10.1016/S0367-326X(02)00311-8

Maksimović, Z., Malenčić, Đ, & Kovačević, N. (2005a). Polyphenol contents and antioxidant activity of maydis stigma extracts. *Bioresource Technology, 96*(8), 873-877. doi:http://dx.doi.org/10.1016/j.biortech.2004.09.006

Maksimović, Z., Malenčić, Đ, & Kovačević, N. (2005b). Polyphenol contents and antioxidant activity of maydis stigma extracts. *Bioresource Technology, 96*(8), 873-877. doi:http://dx.doi.org/10.1016/j.biortech.2004.09.006

Marques, G. S., Leão, W. F., Lyra, M. A. M., Peixoto, M. S., Monteiro, R. P. M., Rolim, L. A., . . . Soares, L. A. L. (2013). *Comparative evaluation of UV/VIS and HPLC analytical methodologies applied for quantification of flavonoids from leaves of bauhinia forficata* doi:https://doi.org/10.1590/S0102-695X2012005000143

Masek, A., Chrzescijanska, E., Latos, M., Zaborski, M., & Podsedek, A. (2017). Antioxidant and antiradical properties of green tea extract compounds. *International Journal of Electrochemical Science, 12*(7), 6600-6610. doi:10.20964/2017.07.06

Michalová, V., & Tancinová, D. (2017). Growth of microorganisms in the pre-fermentation tanks in the production of ethanol. *Potravinarstvo Slovak Journal of Food Sciences, 11*(1), 529-534. doi:10.5219/771

Mohamed, M. A., Jaafar, J., Ismail, A. F., Othman, M. H. D., & Rahman, M. A. (2017). In Hilal N., Ismail A. F., Matsuura T. and Oatley-Radcliffe D.(Eds.), *Chapter 1 - fourier transform infrared (FTIR) spectroscopy* Elsevier. doi:https://doi.org/10.1016/B978-0-444-63776-5.00001-2

Mohsen, S. M., & Ammar, A. S. M. (2009). Total phenolic contents and antioxidant activity of corn tassel extracts. *Food Chemistry, 112*(3), 595-598. doi:http://dx.doi.org/10.1016/j.foodchem.2008.06.014

Mukasyan, A. S. (2017). In Borovinskaya I. P., Gromov A. A., Levashov E. A., Maksimov Y. M., Mukasyan A. S. and Rogachev A. S.(Eds.), *DTA/TGA-based methods*. Amsterdam: Elsevier. doi:https://doi.org/10.1016/B978-0-12-804173-4.00040-5

Peng, K., Zhang, S., & Zhou, H. (2016). Toxicological evaluation of the flavonoid-rich extract from maydis stigma: Subchronic toxicity and genotoxicity studies in mice. *Journal of Ethnopharmacology, 192*, 161-169. doi:http://dx.doi.org/10.1016/j.jep.2016.07.012

Périno, S., Pierson, J. T., Ruiz, K., Cravotto, G., & Chemat, F. (2016). Laboratory to pilot scale: Microwave extraction for polyphenols lettuce. *Food Chemistry, 204*, 108-114. doi:http://dx.doi.org/10.1016/j.foodchem.2016.02.088

Prakash Maran, J., Manikandan, S., Thirugnanasambandham, K., Vigna Nivetha, C., & Dinesh, R. (2013). Box–Behnken design based statistical modeling for ultrasound-assisted extraction of corn silk polysaccharide. *Carbohydrate Polymers, 92*(1), 604-611. doi:http://dx.doi.org/10.1016/j.carbpol.2012.09.020

Prakash Maran, J., Sivakumar, V., Sridhar, R., & Prince Immanuel, V. (2013). Development of model for mechanical properties of tapioca starch based edible films. *Industrial Crops and Products, 42*, 159-168. doi:http://dx.doi.org/10.1016/j.indcrop.2012.05.011

Prasad, A. S. (2016). Iron oxide nanoparticles synthesized by controlled bio-precipitation using leaf extract of garlic vine (mansoa alliacea). *Materials Science in Semiconductor Processing, 53*, 79-83. doi:http://dx.doi.org/10.1016/j.mssp.2016.06.009

Rafsanjany, N., Sendker, J., Lechtenberg, M., Petereit, F., Scharf, B., & Hensel, A. (2015). Traditionally used medicinal plants against uncomplicated urinary tract infections: Are unusual, flavan-4-ol- and derhamnosylmaysin derivatives responsible for the antiadhesive activity of extracts obtained from stigmata of zea mays L. against uropathogenic E. coli and benzethonium chloride as frequent contaminant faking potential antibacterial activities? *Fitoterapia, 105*, 246-253. doi:http://dx.doi.org/10.1016/j.fitote.2015.07.014

Rahman, N. A., & Wan Rosli, W. I. (2014a). Nutritional compositions and antioxidative capacity of the silk obtained from immature and mature corn.

Journal of King Saud University - Science, 26(2), 119-127. doi:http://dx.doi.org/10.1016/j.jksus.2013.11.002

Rahman, N. A., & Wan Rosli, W. I. (2014b). Nutritional compositions and antioxidative capacity of the silk obtained from immature and mature corn. *Journal of King Saud University - Science, 26*(2), 119-127. doi:http://dx.doi.org/10.1016/j.jksus.2013.11.002

Reddy, V. P. (2020). In Reddy V. P. (Ed.), *3 - free-radical reactions in the synthesis of organofluorine compounds* Elsevier. doi:https://doi.org/10.1016/B978-0-12-813286-9.00003-1

Sabiu, S., O'Neill, F. H., & Ashafa, A. O. T. (2016). Kinetics of α-amylase and α-glucosidase inhibitory potential of zea mays linnaeus (poaceae), stigma maydis aqueous extract: An in vitro assessment. *Journal of Ethnopharmacology, 183*, 1-8. doi:http://dx.doi.org/10.1016/j.jep.2016.02.024

Sarepoua, E., Tangwongchai, R., Suriharn, B., & Lertrat, K. (2015). Influence of variety and harvest maturity on phytochemical content in corn silk. *Food Chemistry, 169*, 424-429. doi:http://dx.doi.org/10.1016/j.foodchem.2014.07.136

Sawicki, T., Martinez-Villaluenga, C., Frias, J., Wiczkowski, W., Peñas, E., Bączek, N., & Zieliński, H. (2019). *The effect of processing and in vitro digestion on the betalain profile and ACE inhibition activity of red beetroot products* doi:https://doi.org/10.1016/j.jff.2019.01.053

Shan, B., Xie, J., Zhu, J., & Peng, Y. (2012). Ethanol modified supercritical carbon dioxide extraction of flavonoids from momordica charantia L. and its antioxidant activity. *Food and Bioproducts Processing, 90*(3), 579-587. doi:http://dx.doi.org/10.1016/j.fbp.2011.09.004

Štenclová, H., Karásek, F., Štastník, O., Zeman, L., Mrkvicová, E., & Pavlata, L. (2016). The effect of reduced zinc levels on performance parameters of broiler chickens. *Potravinarstvo, 10*(1), 272-275. doi:10.5219/580

Süli, J., Hamarová, I., & Sobeková, A. (2017). Possible consequences of the sucrose replacement by a fructose-glucose syrup. *Potravinarstvo Slovak Journal of Food Sciences, 11*(1), 425-430. doi:10.5219/772

Vranješ, M., Popović, B. M., Štajner, D., Ivetić, V., Mandić, A., & Vranješ, D. (2016). Effects of bearberry, parsley and corn silk extracts on diuresis, electrolytes composition, antioxidant capacity and histopathological features in mice kidneys. *Journal of Functional Foods, 21*, 272-282. doi:http://dx.doi.org/10.1016/j.jff.2015.12.016

Wang, R., Wu, G., Du, L., Shao, J., Liu, F., Yang, Z., . . . Wei, Y. (2016). Semi-bionic extraction of compound turmeric protects against dextran sulfate sodium-induced acute enteritis in rats. *Journal of Ethnopharmacology, 190*, 288-300. doi:http://dx.doi.org/10.1016/j.jep.2016.05.054

Wei, M., Yang, Y., Chiu, H., & Hong, S. (2013). Development of a hyphenated procedure of heat-reflux and ultrasound-assisted extraction followed by RP-HPLC separation for the determination of three flavonoids content in scutellaria

barbata D. don. *Journal of Chromatography B, 940*, 126-134. doi:http://dx.doi.org/10.1016/j.jchromb.2013.09.015

Weiz, G., Braun, L., Lopez, R., de Mar á, P. D., & Breccia, J. D. (2016). Enzymatic deglycosylation of flavonoids in deep eutectic solvents-aqueous mixtures: Paving the way for sustainable flavonoid chemistry. *Journal of Molecular Catalysis B: Enzymatic, 130*, 70-73. doi:http://dx.doi.org/10.1016/j.molcatb.2016.04.010

Whelihan, M. F., Kiankhooy, A., & Brummel-Ziedins, K. E. (2014). *Thrombin generation and fibrin clot formation under hypothermic conditions: An in vitro evaluation of tissue factor initiated whole blood coagulation* doi:https://doi.org/10.1016/j.jcrc.2013.10.010

Will, M. (2020). In Will M. (Ed.), *Chapter 2 - history of SEMS* Gulf Professional Publishing. doi:https://doi.org/10.1016/B978-0-12-820040-7.00002-8

Wu, Q., Pan, N., Deng, K., & Pan, D. (2008). *Thermogravimetry–mass spectrometry on the pyrolysis process of lyocell fibers with and without catalyst* doi:https://doi.org/10.1016/j.carbpol.2007.08.005

Xie, X., Zhu, D., Zhang, W., Huai, W., Wang, K., Huang, X., . . . Fan, H. (2017). Microwave-assisted aqueous two-phase extraction coupled with high performance liquid chromatography for simultaneous extraction and determination of four flavonoids in crotalaria sessiliflora L. *Industrial Crops and Products, 95*, 632-642. doi:http://dx.doi.org/10.1016/j.indcrop.2016.11.032

Yamasaki, H., & Grace, S. C. (1998). *EPR detection of phytophenoxyl radicals stabilized by zinc ions: Evidence for the redox coupling of plant phenolics with ascorbate in the H2O2-peroxidase system* doi:https://doi.org/10.1016/S0014-5793(98)00048-9

Yang, J., Li, X., Xue, Y., Wang, N., & Liu, W. (2014). Anti-hepatoma activity and mechanism of corn silk polysaccharides in H22 tumor-bearing mice. *International Journal of Biological Macromolecules, 64*, 276-280. doi:http://dx.doi.org/10.1016/j.ijbiomac.2013.11.033

Yang, R., Geng, L., Lu, H., & Fan, X. (2017). Ultrasound-synergized electrostatic field extraction of total flavonoids from hemerocallis citrina baroni. *Ultrasonics Sonochemistry, 34*, 571-579. doi:http://dx.doi.org/10.1016/j.ultsonch.2016.06.037

Yin, X., You, Q., & Jiang, Z. (2011). Optimization of enzyme assisted extraction of polysaccharides from tricholoma matsutake by response surface methodology. *Carbohydrate Polymers, 86*(3), 1358-1364. doi:http://dx.doi.org/10.1016/j.carbpol.2011.06.053

Zhang, L., & Wang, M. (2017). Optimization of deep eutectic solvent-based ultrasound-assisted extraction of polysaccharides from dioscorea opposita thunb. *International Journal of Biological Macromolecules, 95*, 675-681. doi:http://dx.doi.org/10.1016/j.ijbiomac.2016.11.096

Zhang, Y., Shan, X., & Gao, X. (2011). Development of a molecularly imprinted membrane for selective separation of flavonoids. *Separation and Purification Technology, 76*(3), 337-344. doi:http://dx.doi.org/10.1016/j.seppur.2010.10.024

Zhao, W., Yin, Y., Yu, Z., Liu, J., & Chen, F. (2012). Comparison of anti-diabetic effects of polysaccharides from corn silk on normal and hyperglycemia rats. *International Journal of Biological Macromolecules, 50*(4), 1133-1137. doi:http://dx.doi.org/10.1016/j.ijbiomac.2012.02.004

Zhao, W., Yu, Z., Liu, J., Yu, Y., Yin, Y., Lina, S., & Chen, F. (2011). Optimized extraction of polysaccharides from corn silk by pulsed electric field and response surface quadratic design. *Journal of the Science of Food and Agriculture, 91*(12), 2201-2209. doi:10.1002/jsfa.4440

Zhou, T., Xiao, X., Li, G., & Cai, Z. (2011). Study of polyethylene glycol as a green solvent in the microwave-assisted extraction of flavone and coumarin compounds from medicinal plants. *Journal of Chromatography A, 1218*(23), 3608-3615. doi:http://dx.doi.org/10.1016/j.chroma.2011.04.031

Zhu, C., & Liu, X. (2013). Optimization of extraction process of crude polysaccharides from pomegranate peel by response surface methodology. *Carbohydrate Polymers, 92*(2), 1197-1202. doi:http://dx.doi.org/10.1016/j.carbpol.2012.10.073

Žilić, S., Janković, M., Basić, Z., Vančetović, J., & Maksimović, V. (2016). Antioxidant activity, phenolic profile, chlorophyll and mineral matter content of corn silk (zea mays L): Comparison with medicinal herbs. *Journal of Cereal Science, 69*, 363-370. doi:http://dx.doi.org/10.1016/j.jcs.2016.05.003

Złotek, U., Mikulska, S., Nagajek, M., & Świeca, M. (2016). The effect of different solvents and number of extraction steps on the polyphenol content and antioxidant capacity of basil leaves (ocimum basilicum L.) extracts. *Saudi Journal of Biological Sciences, 23*(5), 628-633. doi:http://dx.doi.org/10.1016/j.sjbs.2015.08.002

LIST OF PICTURES

LIST OF TABLES

LIST OF SYMBOLS AND ABBREVIATIONS

%	percent
°C	centigrade
D	detector
e_i	error
g	gram
k	the number of independent parameters
S	light source
X_i	variable
X_j	variable
Y	response
β_0	model intercept coefficient
β_{ij}	the second-order terms
β_j	interaction coefficients of linear
β_{jj}	quadrantic
μM	millimole
ml	milliliter
ABTS	2, 2'-azino-bis(3-ethylbenzothiazoline-6-sulfonic acid)
ACE	angiotensin converting enzyme
ADP	adenosine diphosphate
BBD	box-behnken design
CAT	catalase from micrococcus lysodeiktic
CS	corn silk
CSBIE	corn silk bioactive ingredients extraction
CSF	corn silk flavonoids
CSM	corn silk milky stage
CSMS	corn silk mature stage
CSP	corn silk polysaccharides
CSS	corn silk silking stage

DCS	dry mass of corn silk
DMSO	dimethyl sulfoxide
DNA	deoxyribonucleic acid
DPPH	1,1-diphenyl-2-picrylhydrazyl
DTA	differential thermal analysis
EPR	electron paramagnetic resonance
FTIR	fourier transform infrared spectrometer
GAE	gallic acid equivalents
HCl	hydrochloric acid
H_2O_2	hydrogen peroxide
HO2-	hydrogen peroxide radicals
HPLC	high performance liquid chromatography
H_2SO_4	sulfuric acid
MPa	mega pascal
MTT	thiazolyl blue tetrazolium bromide
mRNA	messenger ribonucleic acid
NMR	nuclear magnetic resonance
PBS	phosphate buffer
RCO-	acyl radicals
RE	rutin equivalents
RO-	alkoxy radicals
RO2-	peroxyalkyl radicals
Sa	sample
SEM	scanning electron microscope
SOD	superoxide dismutase
TAC	total anthocyanin
TFC	total flavonoids
TG	thermogravimetric analysis
TPC	total phenolic
UV-VIS	ultraviolet and visible spectrophotometry

XOD   xanthine oxidase

LIST OF PUBLICATIONS

Year of publication 2019

Jimp

SALEK, R. N., VAŠINA, M., LAPČÍK, L., ČERNÍKOVÁ, M., LORENCOVÁ, E., LI, P., BUŇKA, F. Evaluation of various emulsifying salts addition on selected properties of processed cheese sauce with the use of mechanical vibration damping and rheological methods. LWT-Food Science and Technology. 2019, 107, 178-184.

Jscop

LI, P., LAPČÍK, L., LAPČÍKOVÁ, B., KALYTCHUK, S. Physico-chemical study of steroids from different matureness corn silk material. Potravinárstvo: Slovak Journal of Food Sciences. 2019, 13 (1), 658-664.

Year of publication 2018

Jimp

LI, P., LAPČÍK, L. Výzkum funkčních složek kukuřičného hedvábí. Chemické listy. 2018, 112 (2), 93-97.

Jscop

LI, P., LAPČÍK, L., LAPČÍKOVÁ, B., KALYTCHUK, S. Physico-chemical study of flavonoids from different matureness corn silk material. Potravinárstvo: Slovak Journal of Food Sciences. 2018, 12, 347-354.

Year of publication 2017

Jscop

VALENTA, T., LAPČÍKOVÁ, B., LAPČÍK, L., LI, P. The effect of conformational transition of gelatin-polysaccharide polyelectrolyte complex on its functional properties. Potravinárstvo Slovak Journal of Food Sciences. 2017, 11, 587-596.

LAPČÍK, L., LAPČÍKOVÁ, B., ŽIŽKOVÁ, H., LI, P., VOJTEKOVÁ, V. Effect of cocoa fat content on wetting and surface energy of chocolate. Potravinárstvo: Slovak Journal of Food Sciences. 2017, 11, 410-416.

OVERVIEW OF ACTIVITIES DURING STUDY

Participation in international conferences

XIV. VEDECKÁ KONFERENCIA S MEDZINÁRODNOU ÚČASŤOU, BEZPEČNOSŤ A KONTROLA ‚POTRAV Ń, 30. – 31. marec 2017, Piešťany, Slovensk árepublika

XV. SCIENTIFIC CONFERENCE WITH INTERNATIONAL PARTICIPATION, FOOD SAFETY AND CONTROL, www.bezpecnostpotravin.sk, March 22 – 23, 2018, Piešťany, Slovakia

XVI. SCIENTIFIC CONFERENCE WITH INTERNATIONAL PARTICIPATION, FOOD SAFETY AND CONTROL, www.bezpecnostpotravin.sk, March 28 – 29, 2019, Piešťany, Slovakia

**Projects within the Internal Grant Agency of the Czech Republic ,
TBU (co - researcher)**

IGA2017

IGA2018

IGA2019

IGA2020

Abroad study experience

Institute of Catalysis and Surface Chemistry, Cracow, Poland. Tutor: Prof. P. Warszynsky. (1/9/2019 – 30/9/2019)

Slovak Technical University in Bratislava. Tutor: Prof. M. Valko, DSC. (1/10/2019 – 6/1/2020)

CURRICULUM VITAE

Personal data

Name: Li Peng

Gender: Male

Date of birth: 07/07/1985

Phone: +420776348335

E-mail: li@utb.cz

Address: NAM.T.G.MASARYKA 1281 MSI room number 220B, Zlin 760 01, Czechia

Education

Shaanxi Normal University Sept.2007-Jul.2010

Major: Agricultural Products Processing and Storage Engineering

Degree: Master of Agriculture

Shaanxi Normal University Sept.2003-Jul.2007

Major: Food Science&Engineering

Degree: Bachelor of Science

Tomas Bata Universisty in Zlin Sept.2016-

Major: Food Technology

Degree: PhD

Language skills

Chinese: Native

English: C2 (with 120 hour TESOL Certificate Course, Certificate Number: 100-190013)

Czech: Beginner

Computer skills

MS Office (Word, Excel, PowerPoint)

SigmaPlot (Systat Software, USA)

Work experience

Jul.2010-Jul.2016 Tianjin Ruijing Metabolic Disease Hospital, China

Position: Nutritionist

Li Peng

The study of functional ingredients from corn silk

Doctoral thesis